UNIVERSITÉ DE MONTRÉAL

NONLINEAR FINITE ELEMENT ANALYSIS OF THE HUMAN TIBIOFEMORAL JOINT IN AXIAL ROTATION

ADEL BENHAJ JILANI
DÉPARTEMENT DE GÉNIE MÉCANIQUE
ÉCOLE POLYTECHNIQUE DE MONTRÉAL

MÉMOIRE PRÉSENTÉ EN VUE DE L'OBTENTION
DU DIPLÔME DE MAÎTRISE ÈS SCIENCES APPLIQUÉES
(GÉNIE MÉCANIQUE)
MAI 1996

UNIVERSITÉ DE MONTRÉAL

ÉCOLE POLYTECHNIQUE DE MONTRÉAL

Ce mémoire intitulé:

NONLINEAR FINITE ELEMENT ANALYSIS OF THE HUMAN TIBIOFEMORAL JOINT IN AXIAL ROTATION

présenté par: BENHAJ JILANI Adel

en vue de l'obtention du diplôme de: Maîtrise ès sciences appliquées

a été dûment accepté par le jury d'examen constitué de:

M. CHAABAN Ahmad, Ph.D., président

M. DAMMAK Maher, Ph.D., membre

M. SHIRAZI-ADL Aboulfazl, Ph.D., membre et directeur de recherche

To my mother,

my father,

my brother,

and my sisters,

whose love and

support I cherish

ACKNOWLEDGEMENTS

It is a great pleasure to acknowledge the assistance and guidance given to me by *Prof. Aboulfazl S. Shirazi-Adl*, my advisor, one whose contributions and ideas to this study are deeply appreciated. Thanks are also due to the other members of my graduate commitee, *Prof. Ahmad Chaaban* and *Dr. Maher Dammak*, for their interest in my research and the council and guidance given. The author wishes to express his gratitude to *Mr. Mohamed Z. Bendjaballah* for his assistance throughout the research work.

RÉSUMÉ

Dans cette étude, un modèle réaliste tridimensionnel d'éléments finis du genou humain incluant le fémur, le tibia, la rotule, leurs différentes couches de cartilage, les ménisques ainsi que les principaux ligaments est utilisé comme base pour des analyses nonlinéaires par éléments finis considerant un chargement en torsion interne et externe sur le fémur allant jusqu'à 10 N-m. Dans ce modèle, les ménisques sont représentés par un matériau composite d'une matrice solide renforcée par des fibres de collagène dans les directions radiale et circonferencielle alors que l'articulation qui s'opère entre les différentes couches de cartilage ainsi qu'entre les couches de cartilage et les ménisques, et l'enroulement du ligament collatéral interne autour du bord tibial proximal sont modelisés par un algorithme général de contact sans friction avec grands déplacements. Afin de valider le modèle, la charge appliquée au système ainsi que les conditions aux rives ont été choisies de manière à simuler les essais expérimentaux trouvés dans la littérature. Le tibia étant fixé, le fémur fût libéré dans toutes les directions de translation avec la rotation en flexion-extension fixée alors que la rotation en varus-valgus a été fixée pour quelques analyses et libérée pour d'autres.

Le modèle a été utilisé dans la détermination des roles respectifs des principaux ligaments lors d'un chargement en torsion interne et externe respectivement avec et sans force de compression initiale et ce par l'analyse et comparaison de la réponse en rotation axiale du joint femoro-tibial ainsi que les forces résultantes détectées dans les différents ligaments suivant une séquence de sectionnement de quelques ligaments. Nos résultats montrent clairement qu'avec la rotation en varus-valgus fixée, les ligaments collatéraux sont les principaux resistants à la torsion interne; alors qu'en

rotation externe seule le collatéral latéral joue un rôle majeur. De plus, les croisés sont interdépendants lors d'un chargement en rotation externe alors que le PCL (ligament croisé postérieur) est apparu complètement laché lors de la rotation interne. La fixation de la rotation en varus-valgus pour le modèle intact induit des changements dans la distribution des tensions dans les différents ligaments seulement en torsion externe. La charge de compression initiale de 1000N a causé une réduction drastique dans la laxité rotatoire durant l'application de moments de torsion allant jusqu'a ± 0,5 N-m accompagnée d'une diminution remarquable dans les tensions des ligaments, à l'exception de celle du ACL (ligament croisé antérieur).

Le modèle d' éléments finis nous a permis également de déterminer les régions de contact ainsi que les forces de contact transmises à partir des différentes zones potentielles à savoir les contacts fémur/tibia, fémur/ménisque et ménisque/tibia pour les plateaux médial et latéral durant l'application croissante du moment de torsion au joint femoro-tibial. Les résultats ont montré que lors de l'application du moment de torsion interne, le ménisque latéral est plus sollicité; en effet, la charge axiale supportée par ce ménisque était supérieure à celle supportée par le ménisque médial alors que durant l'application d'un moment externe c'est le ménisque médial qui devient plus sollicité. L'analyse de ces mêmes régions et forces de contact ainsi que des contraintes aux centroïdes des éléments formant les couches de cartilage articulaire montre que lors de la rotation interne, la zone du cartilage tibiale recouverte par le ménisque a été principalement chargée dans la région centrale près du bord du plateau latéral alors que la zone non recouverte a été chargée plutôt postérieurement sur la partie médiale de l'épine tibiale. Similairement, lors du chargement en torsion externe, le chargement maximal a été obtenu près de l'épine tibiale médiale pour la partie du cartilage non recouverte de ménisque, et postérieurement près de la zone d'insertion méniscale sur le plateau latéral.

Les résultats de cette étude concordent d'une manière globale avec les études expérimentales présentées dans la littérature, décrivant la cinématique du joint femorotibial ainsi que le rôle des différents ligaments lors de la rotation axiale du fémur ou du tibia. Il est important de souligner à ce niveau que le modèle qui est entre nos mains est le seul modèle en 3-D dans la littérature qui, basé sur une géométrie réelle et précise, regroupe tous les constituants importants d' un genou à savoir: fémur, tibia, rotule, ménisques et ligaments. Les modèles analytiques précédents manquent de rigueur quant à la modélisation de quelques aspects mécaniques nécessaires pour l'accomplissement d'analyses élastostatiques et nonlinéaires d'un modèle de genou. Ce modèle offre donc des avantages par rapport aux modèles existants parmi lesquels: la discrétisation en éléments finis qui tient compte des surfaces articulaires nécessaires pour l'analyse nonlinéaire de contact, la nature composite (non-homogène) du ménisque et l'enroulement du ligament collatéral interne autour du bord tibial proximal.

Les résultats obtenus lors de cette étude sont d'un grand apport car ils nous permettent de mieux comprendre la biomécanique du joint femoro-tibial et plus particulièrement la fonction de chaque ligament quand le genou subit des charges de torsion axiale. Ces connaissances seront sans doute très bénéfiques et recherchées dans d'autres disciplines liées à cette étude comme les études des prothèses du genou ou prothèses ligamentaires ou encore dans le domaine de la prévention et traitement des maladies et malaises du genou.

ABSTRACT

Being a multi-compartmental structure, located between the body's two largest lever-arms, and sustaining high forces, the knee is prone to injuries and chronic diseases such as dislocation, arthiritis, ligamentous rupture, and meniscal tear. In many cases, prompt and effective treatment can prevent the development of serious instability and arthiritis. A proper understanding of the knee joint biomechanics significantly improves the prevention and treatment of knee joint disorders and injuries. Furthermore, total knee arthroplasty and prosthetic ligament replacement are two examples that can directly benefit from such knowledge.

In this research, a realistic three-dimensional model of the entire human knee joint including femur, tibia, patella, cartilage layers, menisci, and joint ligaments along with a nonlinear finite element package program were used to investigate the response of the tibiofemoral joint, neglecting the patellofemoral joint, at full extension under internal-external torques of up to 10 N-m applied to the femur. The menisci were represented as a non-homogeneous composite of a solid matrix reinforced by radial and circumferential collagen fibres. The articulation of cartilage layers with each other as well as with intervening menisci and the wrapping of the medial collateral ligament with the tibia were treated as general large displacement frictionless contact problems. Analyses were carried out with the tibia fixed while the femur was free to translate in the proximal-distal, medial-lateral, and anterior-posterior directions; the internal-external rotation was left free, the varus-valgus rotation was either fixed or free while flexion-extension rotation was maintained fixed throughout the study. The influences of selective sectioning of some ligaments and axial compression as a preload on the joint response in axial rotation were also investigated.

By analyzing and comparing patterns of change in the femoral axial rotation as well as in the total resultant ligament forces upon selective sectioning of particular ligaments, our results showed that at full flexion with the coupled varus-valgus rotation fixed, both collateral ligaments were the major restraints to internal rotation; however, only the lateral collateral ligament played a major role in resisting external torque. The cruciate ligaments were found to be interdependent (sectioning of one caused a large drop in the tensile force of the other) during external rotation and that the posterior cruciate ligament was completely lax during internal rotation. Setting the varus-valgus free produced some major changes in the ligaments tensile forces only during external rotation. The compressive preload of 1000 N caused a major reduction in the rotary laxity during applied torque of ± 0.5 N-m and some decreases in all ligaments tensile forces with the exception of the tensile force in the anterior cruciate ligament. During internal rotation, the covered cartilage was loaded primarily in the region located centrally and laterally at the lateral plateau; however, the uncovered cartilage was primarily loaded in the region located posteriorly and laterally at the medial plateau. During external rotation, the uncovered cartilage was mainly loaded in the region located near the medial tibial spine; however, the covered cartilage was mainly loaded in the region located posteriorly and medially at the lateral plateau. In general, the predictions of the present study were found to be in a reasonable agreement with the experimental results available in the literature.

The knowledge gained in the course of this research is expected to enhance our understanding of biomechanics of the tibiofemoral joint, particularly the function of the ligaments in axial rotation. This will then be beneficial in the total knee arthroplasty, prosthetic ligament replacement as well as in the treatment and prevention of knee ligament injuries.

CONDENSÉ

Le genou humain est une structure multi-compartimentale qui supporte des efforts assez élevés pouvant atteindre cinq fois le poids du corps qui sont souvent, quand elles sont combinées, la cause de plusieurs malaises comme la dislocation osseuse, l'arthrite, rupture des ligaments et des ménisques.

Dans plusieurs cas un traitement précoce et efficace peut s'averer suffisant pour freiner le développement de l'arthrite et améliorer la stabilité du genou. Une comprehension detaillée de la biomécanique du genou augmente notre aptitude à prevenir les désordres du genou et nous aide à prescrire des traitements plus adequats et efficaces. Des domaines comme la conception de prothèses articulaires du genou et ligamentaires sont deux exemples qui tirent profit de cette connaisance.

Le genou se compose de deux articulations fonctionnelles principales: la première, fémorotibiale, entre fémur et tibia, de type double condylien et la deuxième fémopatellaire, entre rotule et fémur, de type throchléen. L'ensemble des surfaces articulaires, par le biais desquelles s'établissent les différents contacts, ne sont pas tout à fait congruentes, de ce fait, le mouvement relatif du tibia par rapport au fémur lors d'une simple flexion du genou est très complexe, il peut être représenté par un mouvement à six degrés de liberté dans l'espace. Ainsi, le tibia glisse postérieurement sur le fémur dans un mouvement long s'accompagnant progressivement d'une rotation interne dans le plan horizontal.

En tout, sept régions de contact sont recensées: entre ménisques et cartilage tibial, cartilage fémoral et entre cartilage fémoral et cartilage tibial, pour les côtés médial

et latéral, respectivement, enfin le dernier contact est établi entre cartilage fémoral et cartilage rotulien quand le mouvement de flexion s'amorce. Il est à noter que lors de cette flexion l'activité musculaire au niveau des quadriceps est notable, des efforts additionnels, variables en direction et amplitude, sont appliqués par le biais du tendon rotulien à la rotule. Ces articulations ont donc pour principales tâches de permettre une grande mobilité de la jambe par rapport à la cuisse, de supporter des charges très élevées et brusques, de les orienter, et de les redistribuer uniformément sur les surfaces de manière à assurer la stabililé de la structure, sans pour autant charger excessivement l'une ou l'autre des ces composantes.

Dans des conditions normales, ménisqües et cartilages sont fortement hydratés, cette particularité dicte à ces deux composantes leurs plus importants comportements mécaniques, soient une résistance en compression et perméabilité relativement faibles. Ces comportements leurs procurent une grande capacité à absorber les chocs et répartir les charges qu'ils reçoivent uniformément sur une plus grande région de contact afin d'y réduire les contraintes.

En plus, des muscles qui sont des structures biologiques actives, les ligaments, des structures dites passives, participent à la stabilisation de l'articulation et au contrôle des déplacements en flexion, ainsi que lors d'autres mouvements combinés. De plus ces ligaments présentent des comportements différents lors de la flexion du fémur et l'application des chargements couplés.

Les études expérimentales menées dans le domaine de la biomécanique du genou humain sont très nombreuses et touchent plusieurs axes de recherche. On retrouve entre autres des recherches qui s'intéressent à la quantification des surfaces de contact et des pressions de contact dans le but de mieux comprendre le mécanisme de transfert

de charges à travers le joint et de pouvoir ainsi prédire les zones de cartilages à haut risque de développer des dégénerescences du cartilage ou l'esions méniscales. Beaucoup d'autres recherches s'intéressent au comportement de la structure ligamentaire lors des chargements en élaborant des montages permettant la mesure des déformations et des efforts dans les ligaments pour en évaluer le degré de laxité et ses conséquences sur la performance globale du genou.

Durant les deux dernières décennies, des études basées sur des modélisations mathématiques des contacts fémorotibial et fémopatellaire ont enregistré des progrés dans le domaine de l'analyse numérique et des techniques informatiques. Des modèles, au départ simplifiés, sont apparus dans le but de simuler aussi bien le comportement dynamique que statique du genou. Ils considèrent par exemple une approche 2-D, dans un plan sagittal, du contact fémopatellaire ou bien une approche 3-D décrivant les surfaces de contact articulaires par des polynômes de troisième et quatrième degré tout en supposant un contact rigide entre elles. D'autres modèles n'ont pas pris en considération les géométries des surfaces articulaires, leurs intérêts s'orientaient principalement à définir la contribution du système ligamentaire à la rigidité totale du genou. Des approches plus réalistes qui ont marqué cette tendance ont tenu compte cette fois des géométries complexes des surfaces articulaires, des contacts rigides ou déformables ainsi du comportement non linéaire des ligaments, néanmoins la plupart de ces approches faites sur le contact fémorotibial n'incluant pas les ménisques et modélisent s'il ya lieu, le cartilage par une couche d'épaisseur uniforme. On trouve aussi des modèles biphasiques qui, bien que basées sur une géométrie axisymétrique des ménisques, supposent un comportement anisotropique pour la phase solide du tissu.

Dans cette étude, un modèle réaliste tridimensionnel d'éléments finis du genou humain incluant le fémur, le tibia, la rotule, leurs différentes couches de cartilage, les ménisques ainsi que les principaux ligaments est utilisé comme base pour des analyses non-linéaires par éléments finis considerant un chargement en torsion interne et externe sur le fémur allant jusqu'à 10 N-m.

Dans ce modèle, les ménisques sont représentés par un matériau composite d'une matrice solide renforcée par des fibres de collagène dans les directions radiales et circonferencielles alors que l'articulation qui s'opère entre les différentes couches de cartilage ainsi qu'entre les couches de cartilage et les ménisques, et l'enroulement du ligament collatéral interne autour du bord tibial proximal sont modelisés par un algorithme général de contact sans friction avec grands déplacements.

Afin de valider le modèle, la charge appliquée au système ainsi que les conditions aux rives ont été choisies de manière à simuler les essais expérimentaux trouvés dans la littérature. Le tibia étant fixé, le fémur fût libéré dans toutes les directions de translation avec la rotation en flexion-extension fixée alors que la rotation en varus-valgus a été fixée pour quelques analyses et libérée pour d'autres.

Dans chapitre 2 on décrit la méthode utilisée pour modéliser le problème du contact à grands déplacements et déformations. Lors, d'une analyse non-liéaire, deux portions de surfaces initialement en contact peuvent se séparer et revenir en contact à nouveau. Pour chaque pas de charge, le programme utilisé sert à identifier les zones de contact et à quantifier les forces de contact qui y seront transmises. Une courbe exprimant la contrainte en fonction de la pénétration est requise pour chacun des types de contact existant à savoir: cartilage-cartilage ou bien ménisque-cartilage. Pour chaque noeud qui pénètre une facette cible, un ressort sera généré et auquel sera associé

une rigidité obtenue de la courbe sus-mentionnée. Une génération automatique d'un maillage en éléments finis est faite. On a opté pour des éléments solides à 8 noeuds pour les différents cartilages, 81 éléments pour le cartilage tibial, 244 éléments pour le cartilage fémoral et 49 éléments pour le cartilage patellaire. Les ménisques sont modélisés par un matériau composite, soit une matrice très peu compressible forcée de fibres de collagène dans les directions radiale et circonférentielles. Des éléments solides 8 noeuds sont choisis pour modéliser la matrice solide avec un nombre total de 424 éléments tandisque 1212 éléments uniaxiaux ont été nécessaires pour modéliser les fibres de collagène. Les structures osseuses: tibia, fémur et rotule, sont considérés lors des analyses comme trois corps rigides, représentés chacun, par un noeud primaire qui est le centre de masse de la structure osseuse. Ce choix est parfaitement justifié vu la rigidité beaucoup plus élévée de l'os devant celle des autres tissus mous en présence.

Au chapitre 3, on utilise le présent modèle pour déterminer les rôles respectifs des principaux ligaments lors d'un chargement en torsion interne et externe respectivement avec et sans force de compression initiale et ce par l'analyse et comparaison de la réponse en rotation axiale du joint femoro-tibial ainsi que les forces résultantes détectées dans les différents ligaments suivant une séquence de sectionnement de quelques ligaments. Les résultats obtenus dans ce chapitre montrent clairement qu'avec la rotation en varus-valgus fixée, les ligaments collatéraux sont les principaux resistants de la torsion interne; alors qu'en rotation externe seule le collatéral latéral joue un rôle majeur. Lors d'un chargement en rotation externe nos résultats montrent clairement que les croisés sont interdépendant, cependant, le PCL est apparu complètement laché lors de la rotation interne. La fixation de la rotation en varus-valgus pour le modèle intact induit des changements dans la distribution des tensions dans les différents ligaments seulement en torsion externe. La charge de compression initiale

de 1000N cause une réduction drastique dans la laxité rotatoire durant l'application de moments de torsion allant jusqu'a $\pm$ 0.5 N-m accompagnée d'une diminution remarquable dans les tensions des ligaments à l'exception de celle du ACL. Le modèle d'éléments finis permet également de déterminer les régions de contact ainsi que les forces de contact transmises à partir des différentes zones potentielles à savoir les contacts fémur/tibia, fémur/ménisque et ménisque/tibia pour les plateaux médial et latéral durant l'application croissante du moment de torsion au joint femoro-tibial. Les résultats montrent que lors de l'application du moment de torsion interne, le ménisque latéral est plus sollicité; en effet, la charge axiale supportée par ce ménisque est supérieure à celle supportée par le ménisque medial alors que durant l'application d'une torsion externe c'est le ménisque medial qui devient plus sollicité. L'analyse de ces mêmes régions et forces de contact ainsi que des contraintes aux centroïdes des éléments formant les couches de cartilage articulaire montre que lors de la rotation interne la zone du cartilage tibiale recouverte par le ménisque est principalement chargée dans la région centrale près du bord du plateau latéral alors la zone non recouverte est chargée plutôt postérieurement sur la partie médiale de l'épine tibiale. Similairement, lors du chargement en torsion externe, le chargement maximal est obtenu près de l'épine tibiale médiale pour la partie du cartilage non recouverte de ménisque, et postérieurement près de la zone d'insertion méniscale sur le plateau latéral.

Le chapitre 4 présente en détail la discussion des résultats obtenus. Les résultats de cette étude concordent d'une manière globale avec les études expérimentales présentées dans la littérature, décrivant la cinématique du joint femoro-tibial ainsi que le rôle des différents ligaments lors de la rotation axiale du fémur ou du tibia. Le modèle qui est entre nos mains est le seul modèle en 3-D dans la littérature qui, basé

sur une géométrie réelle et précise, regroupe tous les constituants importants d'un genou à savoir: fémur, tibia, rotule, ménisques et ligaments. Les modèles analytiques précédents manquent de rigueur quant à la modélisation de quelques aspects mécaniques nécessaires pour l'accomplissement d'analyses élastostatiques et nonlinéaires d'un modèle de genou. Ce modèle offre donc des avantages par rapport aux modèles existants parmi lesquels: la discrétisation en éléments finis qui tient compte des surfaces articulaires nécessaires pour l'analyse nonlinéaire de contact, la nature composite (non-homogène) du ménisque et l'enroulement du ligament collatéral interne autour du bord tibial proximal. À cause de l'articulation multi-compartimentale qui s'opère dans ce modèle, un algorithme de contact plus performant sur le plan de convergence qui tolère un certain niveau de pénétration a été utilisé pour accomplir l'analyse nonlinéaire. Le niveau de raffinement du maillage même s'il paraît être adéquat pour cette analyse peut être amélioré sur les surfaces du cartilage articulaire pour mieux modéliser le contact mais il faut s'attendre dans ce cas à des temps d'exécution beaucoup plus importants. Cependant, le modèle présenté est applicable aux chargements quasi-statique à court terme et ne considère que la réponse élastostatique du système, en négligeant sa réponse transitoire, sa viscoélasticité et les mouvements de fluide qui s'y opèrent. De plus, les propriétés de matériaux de tous les tissus ainsi que les déformations initiales dans les différents ligaments ont été choisies dans la littérature et un changement aussi minime que ce soit dans ces paramètres ou bien dans la géométrie du joint peut affecter les résultats obtenus mais on s'attend à ce que les conclusions de ce travail demeurent valides. L'absence des capsules ligamentaires dans cette étude et les différentes conditions aux rives (Tibia fixé et fémur chargé) peut également affecter les résultats.

Au chapitre 5, les conclusions de ce travail ainsi que des travaux futurs suggérés sont présentés. Les résultats obtenus lors de cette étude sont d'un grand apport car ils

nous permettent de mieux comprendre la biomécanique du joint femoro-tibial et plus particulièrement la fonction de chaque ligament quand le genou subit des charges de torsion axiale. Ces connaissances seront sans doute trés bénéfiques et recherchées dans d'autres disciplines liées à cette étude comme les études des prothèses du genou ou prothèses ligamentaires ou encore dans le domaine de la prévention et traitement des maladies et malaises du genou.

TABLE OF CONTENTS

LIST OF TABLES

LIST OF FIGURES

NOMENCLATURE

aACL	anterior bundle of the anterior cruciate ligament
aLCL	anterior bundle of the lateral collateral ligament
aMCL	anterior bundle of the medial collateral ligament
aPCL	anterior bundle of the posterior cruciate ligament
ACL	anterior cruciate ligament
α	collagen fibre volume fraction content
D_{ij}	components of rate of deformation tensor
δv_i	virtual velocity components
E	Young's modulus of elasticity
E_M	estimated elastic modulus of the matrix
E_F^{SEC}	strain-dependent non-linear elastic secant modulus of the meniscus
E_T^{SEC}	strain-dependent non-linear elastic secant modulus of collagen fibres
E_{ijkl}^{τ}	components of incremental moduli relating τ_{ij}^{∇} to D_{kl}
ϵ	engineering strain
ϵ_1	non-linear strain level parameter for the ligaments
F_i	components of body forces
iMCL	inferior bundle of the medial collateral ligament
K	ligament stiffness

L	lateral
LCL	lateral collateral ligament
LMSG	liquid metal strain gauge
M	medial
MCL	medial collateral ligament
n_i	components of the unit normal to the surface
ν	Poisson's ratio
pACL	posterior bundle of the anterior cruciate ligament
pLCL	posterior bundle of the lateral collateral ligament
pMCL	posterior bundle of the medial collateral ligament
pPCL	posterior bundle of the posterior cruciate ligament
P	posterior
PCL	posterior cruciate ligament
PLB	posterolateral bundle
sLCL	superior bundle of the lateral collateral ligament
s_{ij}	components of nominal stress tensor
$\dot{s}_{ij}$	material rate of s_{ij}
S_T	the part of the reference surface on which tractions are prescribed
σ	engineering stress
σ_{ij}	components of true stress tensor
TY	varus-valgus rotation

T_i components of traction forces

τ_{ij} components of Kirchhoff stress tensor

τ_{ij}^{∇} co-rotational rate of τ_{ij}

v_i components of velocities

$v_{i,j}$ components of velocity gradients

CHAPTER I

INTRODUCTION

The knee is the largest and one of the most complex joints in the human body. It is particularly prone to injuries and arthiritis. Some of the popular activities such as skiing, football and running are responsible for thousands of knee injuries each year. Severe injuries to the knee may result in tears of any or all the ligaments. In addition, many forms of arthiritis affect the knee joint much more frequently than other joints. Fortunately, new techniques and early diagnosis as well as more sophisticated rehabilitation practices have enabled physicians to treat injuries much more effectively. In many cases, prompt and effective treatment can prevent the development of serious instability and arthiritis. Hence, a proper understanding of knee joint biomechanics significantly improves the prevention and treatment of knee joint disorders and injuries. Moreover, total knee arthroplasty and prosthetic ligament replacement are two examples that can directly benefit from such knowledge.

1.1 Biomechanics of the knee joint

It is not the author's intention to present all aspects of the knee joint biomechanics, but to introduce those parts that are referred to often in this work. Information that is beyond the scope of this chapter with regard to the function of ligaments, bony geometry, articular cartilage, menisci, and the musculature is readily available in the literature (Gray, 1973; Kapandji, 1970). This chapter briefly reviews the biomechanics of the knee joint directly related to this research.

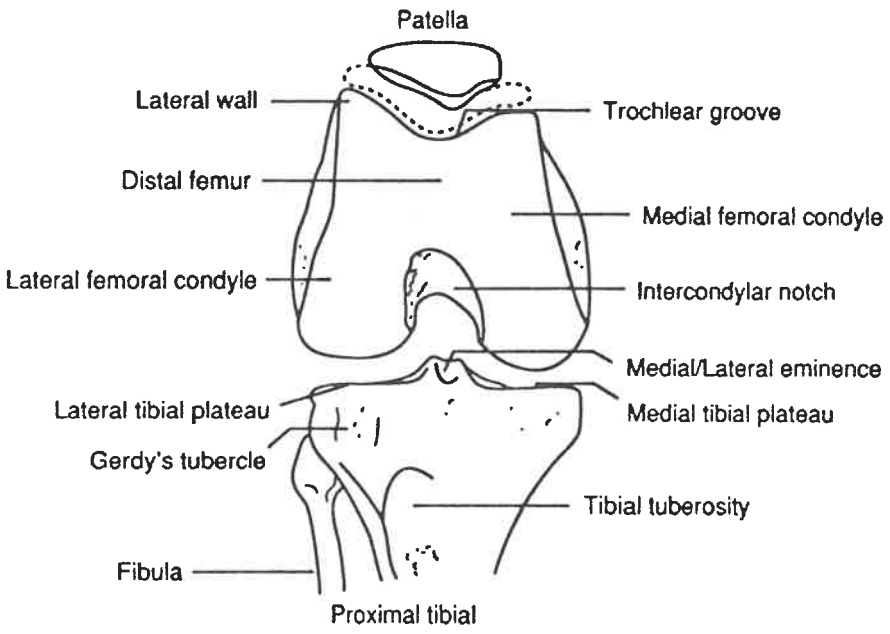

Figure 1.1: Osseous components of a right knee. (After Insall, 1984)

The knee consists of two condylar joints, representing the medial and lateral tibiofemoral articulations, and a sellar joint between the patella and trochlear groove of the femur (Figure 1.1) (Insall, 1984). The tibiofemoral and patellofemoral joints are contained within a single synovial cavity. The tibiofemoral joint relies on muscular, meniscal, and ligamentous support to maintain biomechanical and anatomical integrity (Figures 1.2- 1.6). The knee joint transmits loads, participates in motion, aids in conservation of momentum, and provides a force couple for activities involving the leg (Kapandji, 1970). From the mechanical point of view, the knee is a compromise that sets out to reconcile two of the joint almost mutually exclusive requirements, great stability and mobility (Frankel and Nordin, 1980).

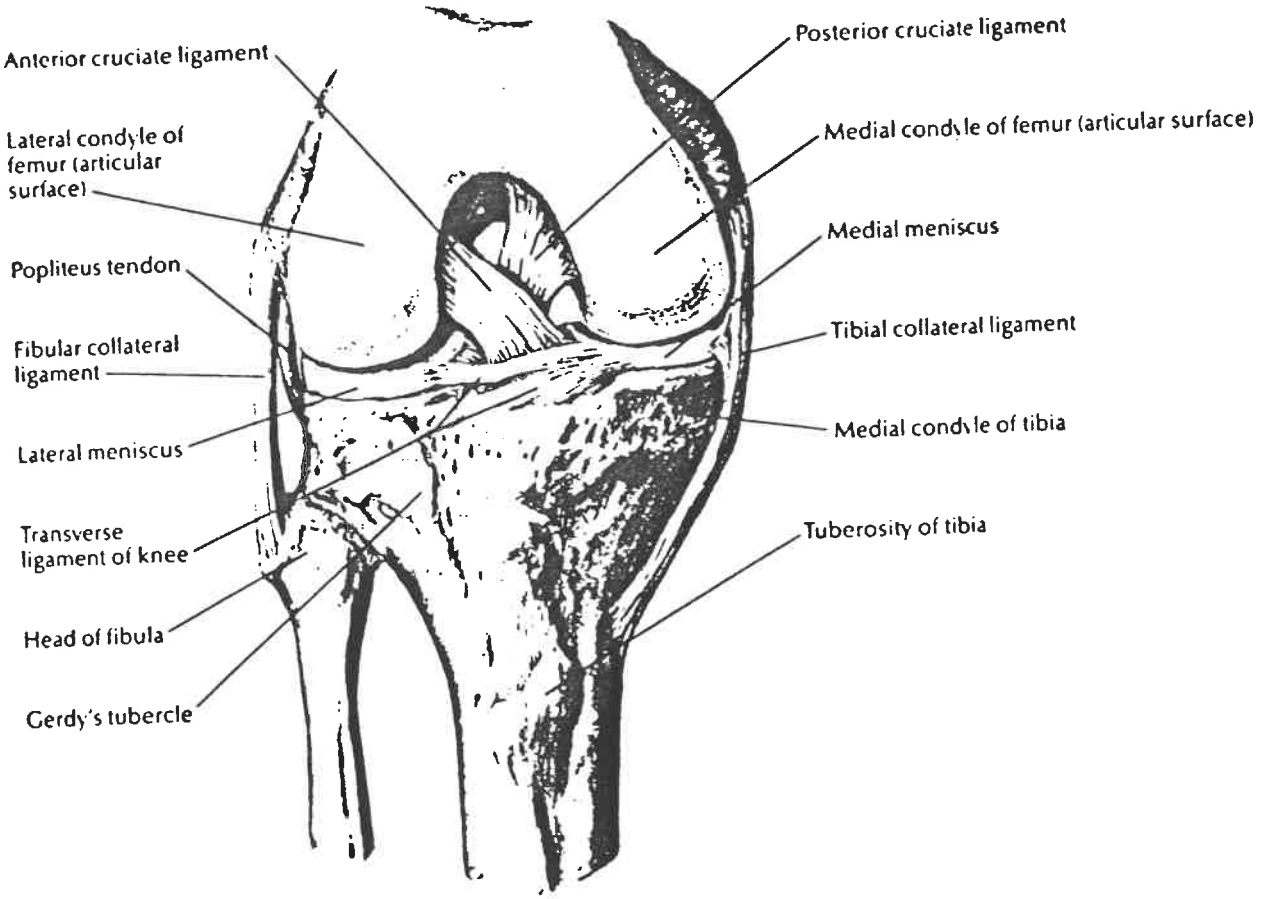

Figure 1.2: Cruciate and Collateral Ligaments of a flexed right knee: anterior view. (After Netter, 1991)

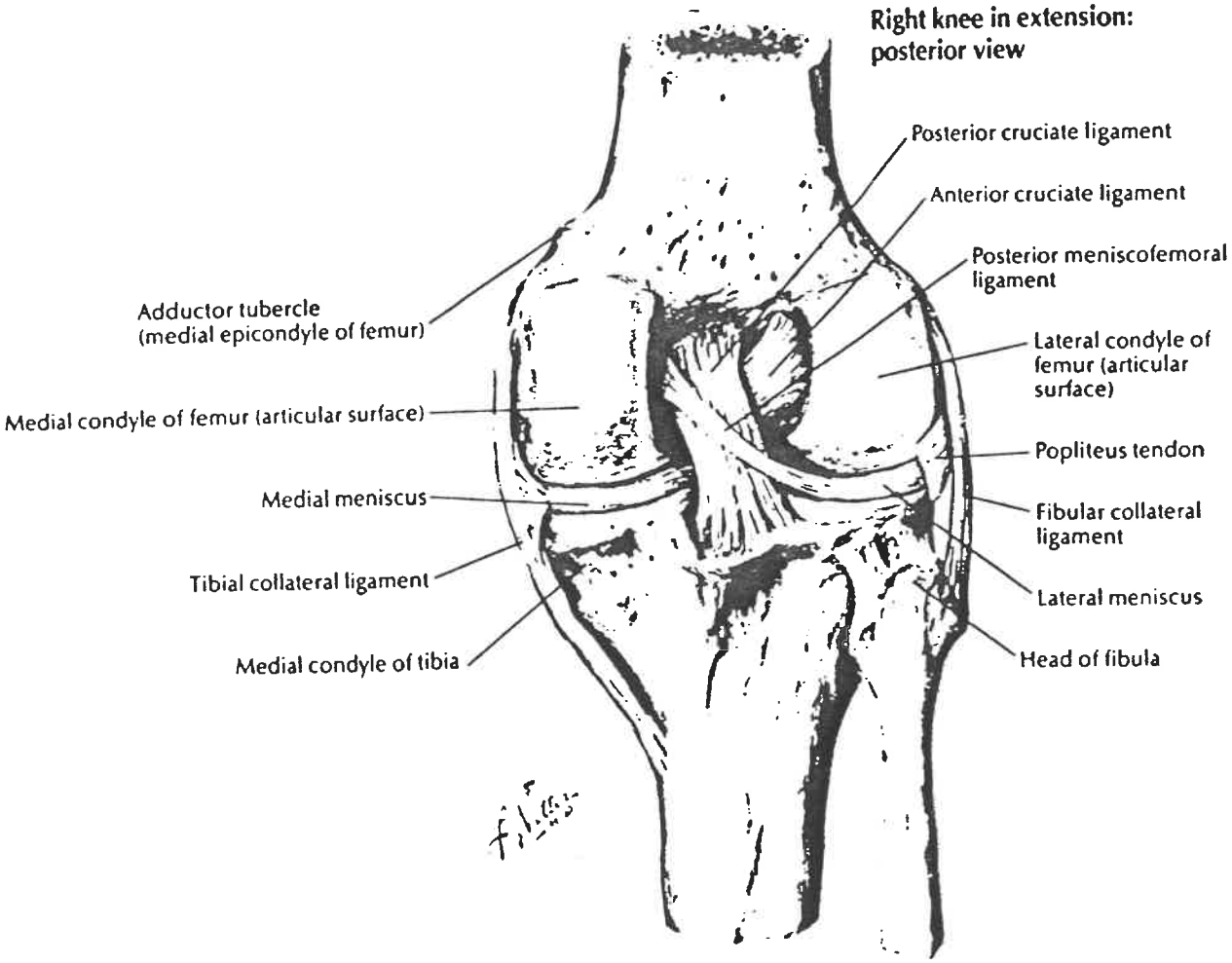

Figure 1.3: Cruciate and Collateral Ligaments of an extended right knee: posterior view. (After Netter, 1991)

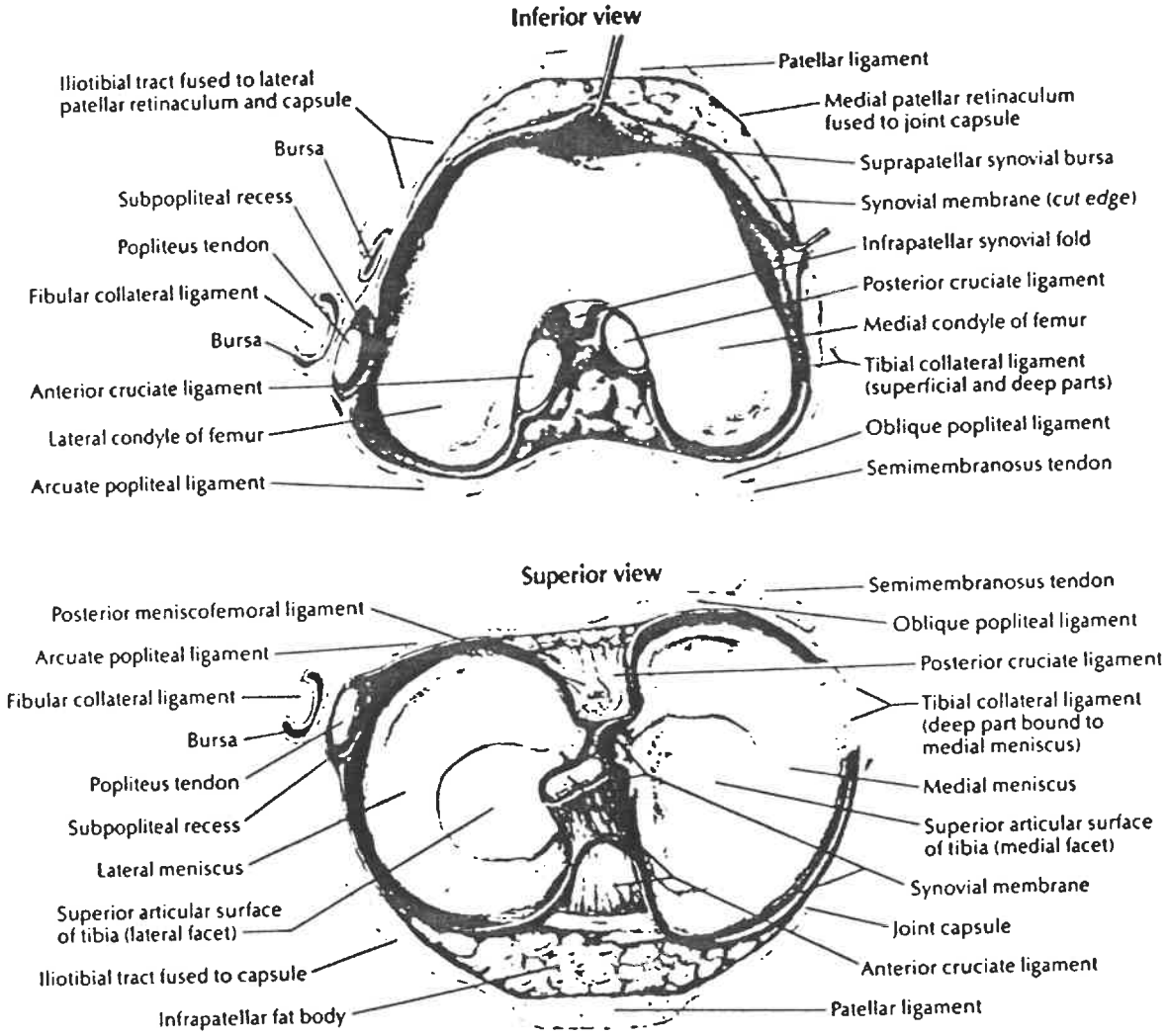

Figure 1.4: Inferior and superior views of the interior of a right knee. (After Netter, 1991)

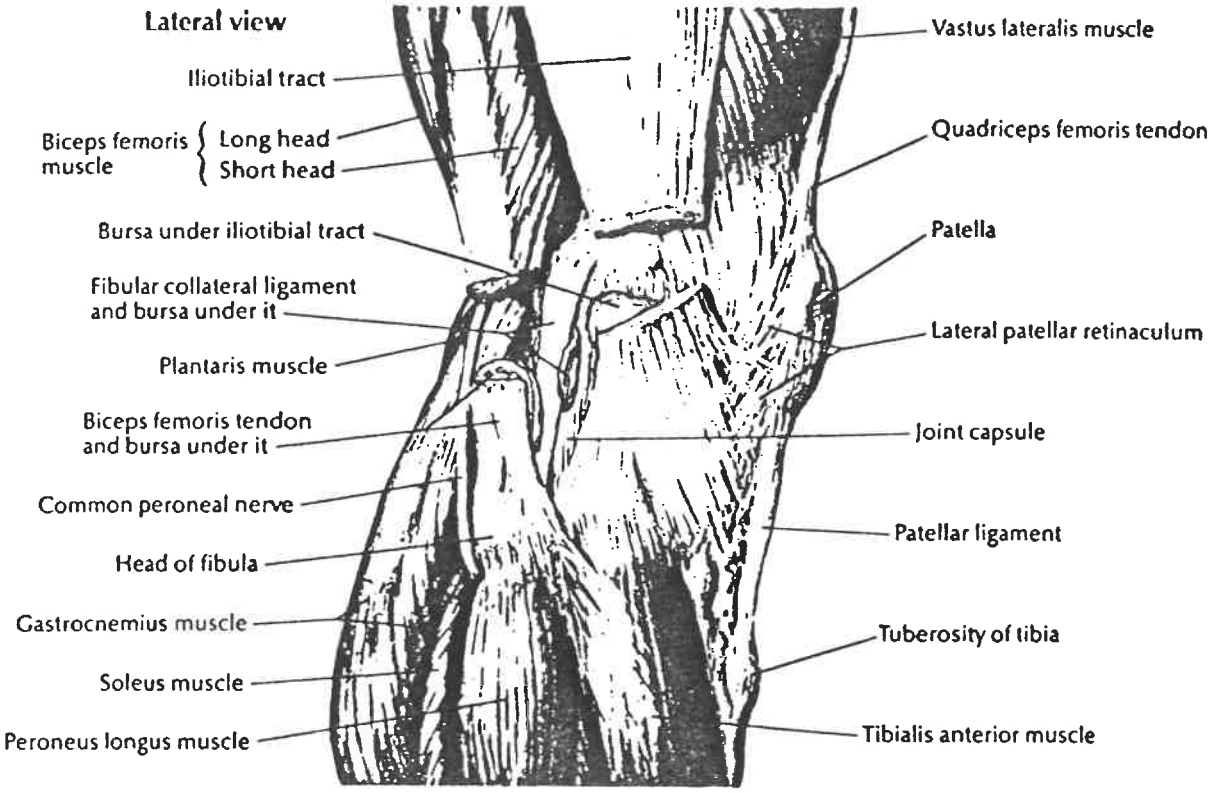

Figure 1.5: Lateral view of a right knee. (After Netter, 1991)

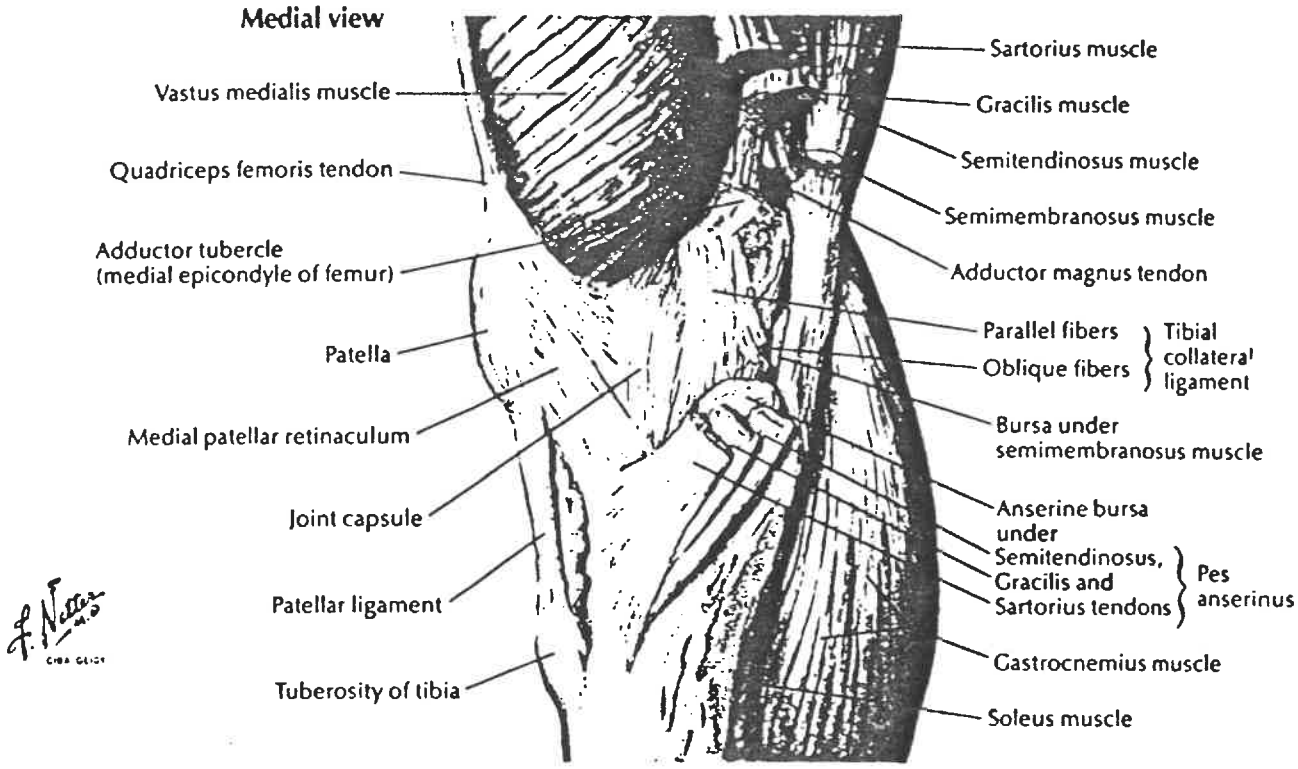

Figure 1.6: Medial view of a right knee. (After Netter, 1991)

The traditional description of the tibiofemoral joint is that of a modified hinge joint with two degrees of freedom. These movements include flexion and extension around the mediolateral axis, and rotation around a longitudinal axis. However, more recent analyses indicate that the tibiofemoral joint has six degrees of freedom, three rotational and three translational, occurring around three anatomic axes (Figure 1.7) (Goodfellow and O'Connor, 1978). Anatomical axes are vertical (or longitudinal), transverse and anteroposterior. All joint motions may be described in a three-axis system (Markolf et al., 1976). Each axis defines one rotation and one translation. Flexion-extension is the rotation around the transverse axis; medial-lateral tibial translation shares the same axis. Anterior and posterior translation, or drawer, of the tibia occurs along the anteroposterior axis; the rotation along this axis is abduction and adduction of the tibia. Varus-valgus stability is a measure of rotation around this axis. Internal and external tibial rotation occurs around a longitudinal axis. Compression and distraction of the joint is the translation along the same axis. A description of the kinematic movement of the tibiofemoral joint is based, in large part, on an analysis of the osseous anatomy and indicates that the joint movements are coupled in a precise and predictable pattern. Knee flexion and extension comprises a complex series of motions occurring between the femur and the tibia.

Far from being a simple hinge-type joint, rolling, sliding, and axial rotation occur simultaneously during different portions of the knee's normal range of motion. Comparison of the weight bearing surfaces of the femoral and tibial condyles reveals the femoral surface to be significantly larger than that of the tibia (Müller, 1983). In addition to this combination of rolling and sliding, axial rotation also occurs between the femur and the tibia, especially as the knee nears extension. This rotation is called the *screw-home mechanism* (Grood et al., 1984) or *automatic rotation* (Müller, 1983).

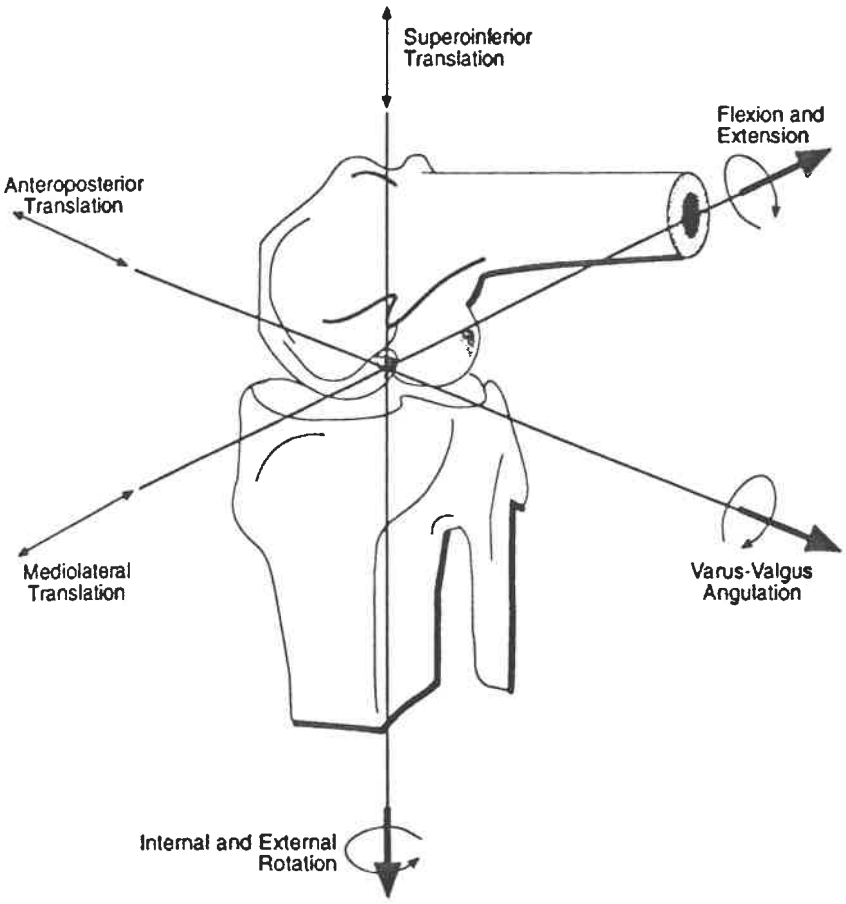

Figure 1.7: Six degrees of freedom of the tibiofemoral joint. (After Goodfellow and O'Connor, 1978)

Examination of the femoral-tibial joint reveals its division into slightly different medial and lateral condyles. The two femoral condyles are asymmetric in shape with the medial femoral condyle longer and narrower than the lateral femoral condyle. Hence, during extension, the medial condyle tends to spin, whereas the lateral condyle has a greater degree of roll and slide. This results in internal femoral rotation, or relative external rotation of the tibia. Automatic rotation is guided by tension developed in the anterior (ACL) and posterior (PCL) cruciate ligaments (Figures 1.8- 1.9) (Girgis et al., 1975; Kapandji, 1970; Müller, 1983). Superimposed on this rotation is anterior translation of the tibia. During flexion, the opposite motions occur between the femur and tibia. Flexion is associated with internal rotation of the tibia, posterior translation of the tibia, and inferior glide of the patella. During flexion, rotation of the tibia is initiated by the popliteus muscle (Markolf et al., 1976; Reider et al., 1981) and continues as allowed by the geometry of the joint surfaces.

Active tibial rotation differs from automatic rotation in that it is caused by muscular effort instead of passive elements. During voluntary rotation, the axis of rotation passes through the medial compartment, not the center of the tibia because more spin and less translation occurs between the medial condyle and plateau as compared with the lateral compartment. During external rotation of the tibia, the lateral tibial plateau slides posteriorly. The opposite kinematics occur with internal tibial rotation. If the cruciate ligaments are damaged, the axis of rotation is displaced within the medial compartment and may become located out of the joint entirely. This results in abnormal and excessive motions between the articular surfaces (Noyes et al., 1983).

The menisci (Figure 1.4) perform two mechanical functions. First, they act to maintain the joint space by serving as shock absorbers when compressive forces are placed on the knee (Grood et al., 1984). Second, they improve the congruency of the joint.

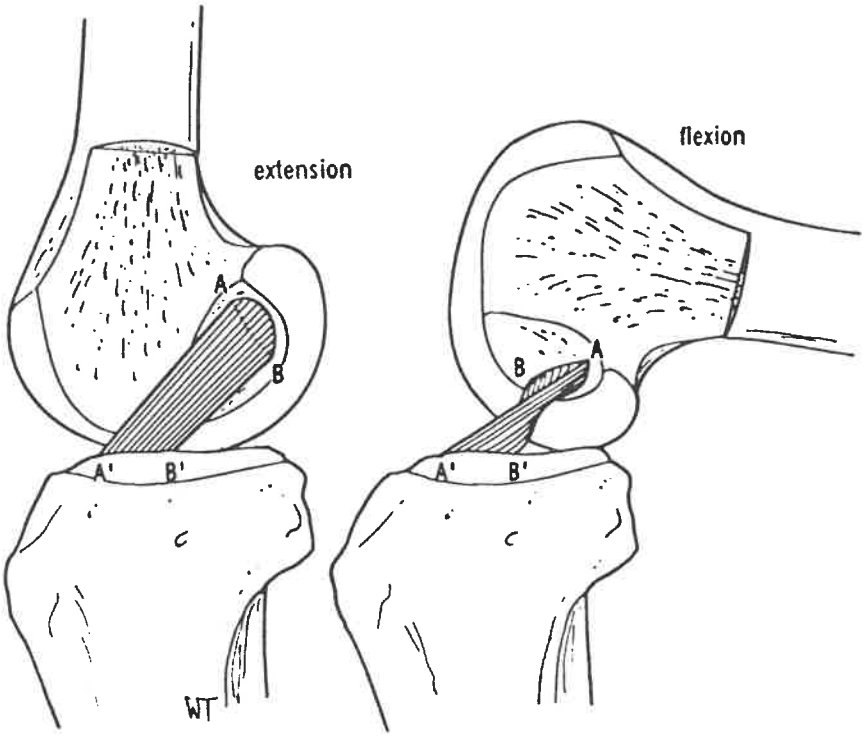

The Posterolateral band (B-B') of the ACL is taut in extension. In flexion, the anteromedial band (A-A') is taut and the posterolateral band (B-B') is relaxed.

Figure 1.8: Anterior cruciate ligament biomechanics. (After Girgis et al., 1975)

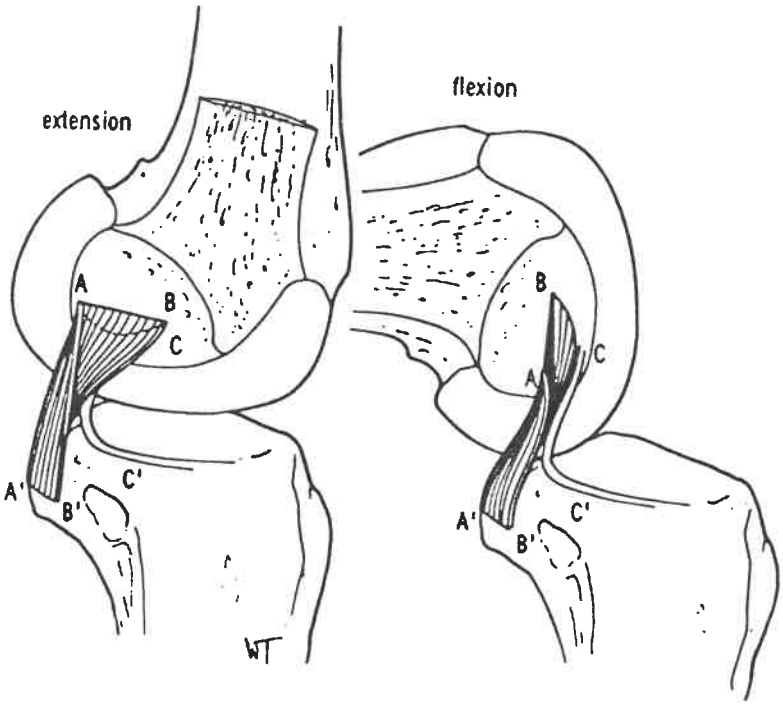

In flexion the bulk of the PCL is taut (A-A'). In extension it is relaxed (A-A').

Figure 1.9: Posterior cruciate ligament biomechanics. (After Girgis et al., 1975)

Because the tibial plateaus are slightly convex, the placement of the meniscus in the medial and lateral compartments provides a concave surface for articulation with the femoral condyles. This increased congruency improves joint stability (Maquet and Pelzer, 1977; Walker and Erkman, 1975), and decreases contact stresses on the articular surfaces of the knee (Grood et al., 1984; Maquet and Pelzer, 1977; Walker and Erkman, 1975). The menisci move during flexion, extension and rotation of the knee. The medial meniscus has more extensive capsular and ligamentous attachments, therefore, its motion is less than that of the lateral meniscus. During extension, the menisci are pulled forward. This is accomplished by the meniscopatellar ligaments, which transmit tension generated by contraction of the quadriceps muscle group. External rotation of the tibia on the femur causes the medial meniscus to move posteriorly while the lateral meniscus moves anteriorly. The reverse occurs with internal tibial rotation (Kapandji, 1970). These meniscal motions occur due to the passive tension generated in the meniscopatellar ligaments and due to geometric restraint of the femoral condyles (Kapandji, 1970). In total seven contact regions are present in the knee joint. the meniscus/tibial cartilage, femoral cartilage/meniscus and femoral cartilage/tibial cartilage contact regions at both lateral and medial compartments, in addition to femoral cartilage/patellar cartilage as knee flexion progresses.

The musculature surrounding the knee functions to move the joint throughout its range of motion, often with great strength and power. The knee muscles also protect the knee by providing dynamic joint stability in support of the passive static stabilization system. A third function of the thigh/knee muscles is the control of the weight-bearing forces generated during athletic activities of daily living to reduce the stress placed on the load-bearing joint surfaces, menisci, and ligaments. Muscle, ligamentous, and other soft tissue restraints limit range of motion of the knee. Active

flexion ranges from 125^o to 140^o, depending on the amount of hip flexion (Kapandji, 1970). Active tibial rotation reaches a maximum of 20^o to 25^o of internal rotation and 40^o of external rotation (Kapandji, 1970). Voluntary tibial rotation does not occur with the knee extended due to positioning of the tibial spines within femoral condyles and the angle of insertion of hamstrings (Kapandji, 1970). Axial rotation reaches its maximal range between 45^o and 90^o of knee flexion (Kapandji, 1970).

Because motion occurs in three dimensions, the ligaments of the knee must function to protect the knee in all three planes. The four major ligaments of the knee, the anterior cruciate (ACL), posterior cruciate (PCL), medial collateral (tibial collateral or MCL), and lateral collateral (fibular collateral or LCL), provide the primary ligament restraining force to resist abnormal motion. Biochemically, the ligaments of the knee are composed primarily of Type-I collagen, with variable amounts of elastin and reticulin. The collagen that makes up the ligaments is grouped into bundles with characteristic sinusoidal waviness that allows the ligament to elongate or shorten slightly in an accordion-like fashion to adapt to external stresses. Ligaments are viscoelastic materials and their nonlinear time- and history dependent properties have been described in the literature (Lin et al., 1987; Woo et al., 1981; Woo et al., 1982). Similar to other soft tissues, the mechanical properties of the ligaments are dependent on age and sex. Noyes and Grood (1976) compared the mechanical properties of human cadaveric ACL from younger and older human donors. They showed that the force carried by the ACL decreased markedly with increasing age. The ACLs failed at an average 1730 N for the younger humans (16-26 years) and only at 734 N for the older group (48-83 years). Selected material properties, such as elastic modulus and strain energy density, were shown to significantly decline with increasing age (Noyes and Grood, 1976). Studies comparing the tensile behavior of the ACL and MCL

from both animal and human cadaveric models gave conflicting results. Newton et al. (1990) reported that the modulus of the normal rabbit MCL was nearly twice that of the ACL. This in contrast to a study of human knee ligaments by Butler et al. (1986), in which differences between the mechanical properties of the ACL, PCL, MCL, and LCL could not be demonstrated. A review of the function of the ligaments of the knee in axial rotation is given in a later section.

The knee joint must provide not only a wide range of motion, but also a sufficient structural stability to transmit large loads from the femur to the tibia. These two tasks impose an enormous mechanical burden on the knee joint. Yet throughout a life span of many decades and millions of loading cycles, the knee joint shows little or no evidence of wear (Lipshitz and Glimcher, 1979; Mow and Mak, 1986). A major reason for this is the presence of the almost frictionless articular cartilage bearing surface (with a coefficient of less than 0.01) (Dowson, 1981; Malcolm, 1976; Mow and Mak, 1986; Unsworth and Dowson, 1975). The extraordinarily low wear rate and friction coefficient result from the unique composition, structure, and material properties of the cartilage tissues that enable them to bear and distribute the very large loads of articulation at the knee (Paul, 1976). In general, at the patellar surface, cartilage thickness ranges from 1 to 5 mm, whereas that at the femoral groove is generally less than 2 mm. Over the femoral condyles and tibial plateau, cartilage thickness ranges from 1 to 3 mm (Mow et al., 1990). The ability of the cartilage and menisci to undergo and withstand large deformations is dictated by their viscoelasticity, toughness, and resiliency which are in turn affected by the composition and molecular organization of the tissues. These tissues are mainly composed of collagen, proteoglycans, and elastin fibers (Black, 1988; Ewing, 1989; Frankel and Nordin, 1980). The predominant collagen is type I, which accounts for more than 90 % of the

total collagen content. Depending on their proportions and orientations, these three elements define the mechanical properties of the tissues. Similar to the cartilage, the meniscus is a hydrated tissue. Water content contributes more than 70 % of its total weight (Mow et al., 1990). In terms of the compressive behavior of the meniscus, the composition of the tissue suggests that it should be considered a biphasic composite material consisting of a porous-permeable solid phase (Collagen and proteoglycans) and a fluid phase (water and dissolved electrolytes). The deformational behavior of the meniscus is that of a fluid-filled, porous-permeable, fiber reinforced composite solid matrix (Mow et al., 1992). Creep in cartilage and meniscus is caused by a constant loading that forces the flow and perhaps exudation of interstitial fluid into the joint space until equilibrium is reached. Equally important is the phenomenon of stress relaxation that occurs when the tissue is subjected to the action of a constant deformation. Although the initial stress on the tissue may be high, fluid redistribution within the tissue allows stress relaxation to occur with time (Mow et al., 1984).

Because of its exposed position in the limb, great functional demands are placed upon the knee by weight-bearing forces during day to day activities such as walking, running and jumping. Postak et al. (1992) reported that the axial compressive, axial torque, anterior-posterior shear, and medial-lateral shear loads can attain 6 to 7 times body-weight, 150 lb-in (i.e., 17 N-m), 2 to 3 times body-weight, and 1 to 1.5 times body-weight, respectively. Moreover, Chen and Black (1980) reported that the ACL is routinely exposed to loads that vary from 70 N while ascending stairs, to 210 N with level walking, to 485 N while descending an incline, and to 630 N while jogging. This appears to leave significant reserve for ACL protection with routine activities, however, loads during aggressive athletic activities are yet unmeasured and are certain to be significantly greater. Hence, being a two-compartment structure,

located between the body's two largest lever arms, and sustaining high forces, even with a poor degree of interlocking of the articular surfaces, the knee is susceptible to injuries and chronic diseases such as dislocation, arthiritis, ligamentous rupture, and meniscal tear. There is a vast amount of clinical literature that discusses these injuries and diseases with regard to etiology, pathomechanics, and operative procedures.

Arthroplasty which is the partial or total replacement of the knee by a prosthesis due to arthiritis (degeneration of the articular cartilage) is required in many cases to relieve severe pain which has not responded to conservative medical management. Although the surgical procedure for surface replacement prostheses may sacrifice the ACL, PCL, or both, it provides motion and stability to the knee, and corrects disabling deformity. Approximately 200,000 total knee replacements are performed each year in the United States (Niwa et al., 1992).

With the increasing number of ligament injury cases, most commonly ACL injuries, there is a considerable research that is being conducted to reconstruct the ligaments or to replace them with ligament prostheses. Artificial ligaments are used for two reasons. The first reason is to stabilize the knee while an own ligament or a transferred ligament gains enough strength to support the knee. The second reason is to completely replace an irreparably torn ligament. In this latter case, an artificial ligament is used as a last resort, when one's own supporting structures have failed. Artificial ligaments are of two types: synthetic and biological. They are also divided into two classifications based on their adaptation to the body: biodegradable and permanent. The different materials currently being tested include Dacron, polypropylene, bovine tendon and carbon fibers.

Meniscal tears in athletes are relatively common and may occur as an isolated injury or in combination with injury to other structures. Controversy exists over whether total or partial meniscectomy, excision of damaged meniscus, should be performed. However, with the better understanding of the important role of the menisci in providing stability of the knee, this drastic practice is less frequently used nowadays (Duval, 1989; Hainault, 1974; Niwa et al., 1992).

1.2 Literature review

This review section is divided into two parts: experimental and analytical studies. The first part deals with the previous experimental works involving the gross load-displacement characteristics in axial torque, the biomechanical role of the primary ligaments of the human knee in axial rotation, the techniques used to determine the contact areas and stresses at the tibiofemoral joint and the meniscal load-bearing characteristics. In the second part, a condensed review of the analytical models developed for the analysis of the biomechanics of the tibiofemoral joint.

1.2.1 Experimental studies

1.2.1.1 Gross response and biomechanical role of primary ligaments

Historically, suspected ligamentous injury has been evaluated by the investigation of the gross relative displacement of the tibiofemoral joint under the application of a specified load to the knee. Brantigan and Voshell (1941) measured the angular rotation of knee-joint specimens by applying a torque of 15 Kgf-cm (i.e., 1.5 N-m).

At full extension practically no rotation occurred, but at 90^o of flexion axial rotation ranged from 6^o to 24^o. Rotations at intermediate flexion angles were not given. Their research has been guided by the needs of clinical diagnosis. Their goal was to show the relationship between ligamentous structures and changes in knee joint displacement during clinical laxity tests when these ligaments are transected. *Laxity* is usually used as the opposite sense to stiffness and is defined as the total amount of displacement under specified loading. Although this methodology has been helpful in interpreting clinical diagnostic tests, it did not answer many questions regarding the function of the ligaments. This is partly due to the limitations of their test method. Indeed, their technique depended on the order of ligament cutting and the relative magnitudes of the changes in knee stability induced by a ligamentous deficit were difficult to quantify. *Instability* is defined to be the state of the knee associated with ligamentous deficiency. Hence, the complexity of the function and of interaction between muscles, ligaments, menisci, tendons, and other joint soft tissues complicates the interpretation of clinical tests used to assess their integrity. The importance of proper interpretation of these clinical tests and the increased interest in the surgical reconstruction of knees with ligament deficiencies has led to much study of the kinematics of normal and injured knees and to the development of several techniques and devices to measure the knee motion more precisely. Plane radiography before and after the application of forces (Frankel and Burstein, 1971; Kennedy and Fowler, 1971; Torzilli et al., 1981), along with mechanical systems (Edixhoven et al., 1987; Markolf et al., 1978) have been used *in vivo*. In some of these studies (Edixhoven et al., 1987; Torzilli et al., 1981) axial rotation of the tibia was unconstrained and measured during assessment of anterior drawer (knee flexed at 90^o) and Lachman (knee flexed at 15^o) tests, but most of these studies constrained the joint and measured motions in only one direction. Systems to measure the complete *in vivo* motion of the knee have been developed (Markolf et

al., 1978; Markolf, 1985; Oliver and Coughlin, 1987; Shiavi et al., 1987; Sydney et al., 1987), but the variations, in part, due to anatomical and physiological differences, the level of relaxation of the subject, positioning of the measurement devices, and movement of the devices to the bone or of soft tissue relative to the bone have made the interpretation of the results difficult.

The literature shows that the most detailed knowledge of knee joint motion during clinical examinations has been obtained from *in vitro* tests on cadaveric specimens which involve direct measurement of bone motion and allows controlled alterations, such as sectioning of selected structures, to be carried out in the same specimen for direct comparison. Moreover, *in vitro* tests provide indication of ligament function during the absence of muscular activity which might be expected to occur during a traumatic mechanism of injury where the external load occurs too rapidly for muscles to react, with the ligaments providing the only constraint.

Wang and Walker (1974) designed an apparatus (rotary laxity rig and an automatic Instron loading machine) to measure continuously the tibial torque rotation response of 27 cadaver knees tested at 25° of flexion. The bones were cut about 15 cm above and below the joint, and the capsule, quadriceps tendon, and ligamentous structures were preserved. In this study, the tibia was held so that it could move only by rotating about its long axis and the femur was fixed at 25° flexion angle. The rotary torque was imposed at the tibia by applying a force with a moment arm. Their results of the *primary laxity*, defined as the rotation for a low torque of ± 5 Kgf-cm (± 0.5 N-m), and the *secondary laxity* defined as the additional rotation at the extremes of motion at the maximum torque applied, demonstrated a wide variation of laxity occurring in knee joints with no obvious correlation with age, sex, race or body build. The average values of the primary laxity, the internal secondary laxity, and

the external secondary laxity when applying ± 50 Kgf-cm (5 N-m) were reported to be 18.6°, 6.96° and 7.87°, respectively. They also studied the effect of meniscectomy on axial rotary laxity and concluded that the menisci played a part in controlling laxity, particularly primary laxity. Moreover, they reported that sectioning of the cruciate ligaments (ACL and PCL) resulted in an increase in primary laxity that ranged from 10 to 30 per cent, with an average increase of 23 per cent. Sectioning of the collateral ligaments (LCL and MCL), however, resulted in an increase in primary laxity that ranged from 35 to 73 per cent, with an average increase of 49 per cent. Their studies on the effect of axial loading on laxity concluded that 100 Kgf axial load reduced the primary laxity to 20 per cent of that at zero load. In this method, although the relative load-transmitting roles of the ligaments in resisting the axial torque is determined, the tensions generated in the individual ligaments, and hence their specific mechanical responses, cannot be established. In another work, Wang et al. (1973) studied the effect of flexion and internal and external tibial rotation on the length patterns of the major ligaments of the knee. This approach involved determination of the length change of ligaments from measurements of the changes in distance between attachement sites. However, the results of length change are usually expressed as relative to those measured corresponding to a reference state, e.g., 0° flexion, of the joint. Since the state of *slackness* or *pretension* in the ligaments in the reference state is not amenable to measurements, the results cannot directly be interpreted in terms of ligament tension.

Markolf et al. (1976) measured torsional stabilities (stiffness and laxity) of 35 normal cadaver intact knees (ages ranged from 53 to 73 years) at 0°, 10°, 20°, 45°, 90° and 135° flexion angles using specially designed apparatus in conjunction with manual examination. The muscles and soft tissues were resected to within 12 cm of the joint line

and the capsule and ligamentous structures were preserved. The femur was clamped and served as the fixed reference to the torsion tests. Torque levels of approximately 8 N-m were applied manually to the tibia using an instrumented handle. Internal and external tibial rotations were measured by a rotary potentiometer aligned with the long axis of the tibia. All rotation results were recorded with the tibia in a position of neutral varus-valgus angulation. Because the responses of all knees to all modes of loading were nonlinear, reflecting increasing stiffness with load, they substituted a nonlinear response curve with a tri-linear variation and defined the slopes of linear segments as *stiffnesses* (one neutral or midrange stiffness and two terminal stiffnesses) and the horizontal distance between breakpoints as *laxity*. They studied the contributions of the supporting structures such as ligaments, capsule, and menisci, with respect to the torsional stability, by comparing the results obtained subsequent to the removal of a component with those of the intact joint. Their findings after sectioning of the medial collateral ligament indicated that it is the most important structure limiting rotary laxity. External tibial rotation terminal stiffness was not affected significantly by any of the sectioning procedures, while internal tibial rotation stiffness was reduced to 50 to 70 per cent of the intact value at full extension when the medial collateral was sectioned alone or in combination with the posterior capsule. Although, this method gave the relative load-transmitting roles of the ligaments through their sequential sectioning in terms of the increase in axial rotation of the tibia, the tensions generated in the individual ligaments, and hence their specific mechanical functions, could not be established.

Piziali et al. (1977) developed an experimental system to measure the coupled, nonlinear load-displacement behavior of the *in-vitro* knee joint. Rastegar et al. (1979) used this system to study the effects of fixed axes of rotation on the torsional load

displacement characteristics of one *in vitro* human knee where the axis of rotation is shifted up to 4.5 cm medial-laterally, and anterior-posteriorly. Using the *stiffness method*, selected displacements (axial rotation in this case) of the joint are imposed and changes in the forces and moments required to create those displacements are recorded. Piziali et al. (1980) utilized the foregoing experimental system to determine the contribution of the cruciate ligaments to torsional load-displacement characteristics and the effect of the condylar interference on torsional loads of one cadaveric human (23 year-old male) knee at full extension. Using the stiffness method, they modeled the knee by a 12×12 beam stiffness matrix. The axial rotation was applied across the joint and the resulting forces and moments at each end of the joint were measured using six-degree-of-freedom dynamometers attached to the tibia and the femur. They concluded that the contribution of condylar contact to torsional loads were negligible and the cruciate ligaments did not interfere with each other during external tibial rotation and supported negligible loads. However, for internal tibial rotation, they found out that the cruciates carried a considerable portion of the torsional load as they wind around each other. For these studies, all applied rotations were about a single axis which was centered medial-laterally and anterior-posteriorly. Through use of the same technique, Seering et al. (1980) studied the function of the cruciate and collateral ligaments, capsule and the popliteus tendon of two cadaveric human knee joints during axial rotation at 0^o and 30^o flexion angle using the method of sequential sectioning. The loads that they applied were relatively high (34 N-m to 47 N-m), near the estimated failure levels of the ligaments of the knee joint. At these load levels, they found out that for both 0^o and 30^o flexion angles of the knee, the medial collateral ligament was more important in resisting internal tibial rotation than external tibial rotation. From these results, they concluded that over this range of flexion the attachment of the medial collateral ligament on the femur was anterior

to its attachment on the tibia. It is important to note that these studies were performed on single specimens, and while they are informative, their results cannot be considered as average values. Although, these studies identified the load-transmitting roles of the ligaments, they were not able to determine the tensions generated in the individual ligaments.

A direct relationship between the stress exerted in the ligaments and the displacement of the tibia relative to the femur has been difficult to determine quantitatively, although many investigators have been trying to do so. To overcome this difficulty several investigators have used the direct stiffness measurements in the ligaments. Buckle transducers were introduced by Salomons (1969) and have been used to measure forces in selected fiber bundles of the anterior cruciate ligament (Ahmed et al., 1986, 1987; Barry and Ahmed, 1986; Lewis and Shybut, 1981; Pauolos et al., 1981). Lewis et al. (1985) studied the biomechanical function of the four major cruciate and collateral ligaments by measuring the *in vitro* ligament forces of seven cadaveric human knees for $\pm$ 3.7 N-m range of external-internal tibial torque at 0^o, 20^o, 45^o, and 90^o flexion angles. In their studies, all soft tissues were removed except the ligaments, capsular structures, and patellar complex, the femur was clamped, and the tibia was free to rotate about its long axis. Their findings concluded that the anteromedial band of the anterior cruciate ligament was highly loaded during internal tibial rotation near extension (85 N at full extension and 77 N at 20^o flexion at 3.7 N-m), the posterior half of the posterior cruciate ligament was only loaded at 90^o flexion at $\pm$ 3.7 N-m, the medial collateral ligament was highly loaded during internal-external rotations throughout the flexion range (27 to 47 N in internal rotation and 80 to 77 N in external rotation), and the lateral collateral ligament was highly loaded during external rotation throughout the flexion range (94 to 77 N). Lewis et al. (1982)

also used the same technique to measure the *in vivo* collateral ligament forces in the stifle (knee) joints of living dogs during functional activities. The main purpose of this study was to demonstrate the close intercation between muscles and ligaments that occurs during *in vivo* function. Direct measurements of ligament strain have been reported using mercury-filled strain gauges that were sutured to selected ligament fibers (Edwards et al., 1970; Kennedy et al., 1977). Fiber strain measurements also have been reported by attaching to the ACL miniature Hall-effect transducers having sharp barbs that penetrate into the ligament (Arms et al., 1984; Renstrom et al., 1986). Arms et al. (1984) measured the strain in the ACL during a series of passive (no muscle contraction) and active (with simulated quadriceps contraction) tests of knee flexion with and without varus, valgus, and axial torques on the tibia. In addition to inherent limitations of the transducers, uncertainties due to ligament preshortening and inability to measure tension in ligaments with nonuniform cross section, the localized measurements of ligament strain cannot be correlated with total ligament force due to the fact that specific bands of the ligament are tensioned at different portions of the loading cycle.

Askew et al. (1988) conducted a study involving 15 fresh cadaveric specimens. The shaft of the femur was placed in a clamp secured to a GENUCOM machine, modified for *in vitro* testing. This machine incorporates a six-degree of freedom spatial linkage to measure the motion of the tibia relative to the femur and a three-dimensional load cell to measure the forces and moments applied to the tibia. Flexibility tests simulating clinical laxity examinations involving internal-external axial rotations and axial torques were carried out at 0^o, 30^o and 90^o of flexion. Again, although this study was able to measure the load-displacement response of the knee joint, it did not determine the tensile forces generated in the individual ligaments and hence their biomechanical role.

Recently, Markolf et al. (1990) used a completely new experimental approach to the direct measurement of the total resultant force within the ACL of seventeen cadaveric knees during internal-external tibial torques of 10 N-m applied manually at different flexion angles of 0, 10, 20, and 45 degrees. The base of the ligament's tibial attachment was mechanically isolated with a coring cutter, and a specially designed load-transducer was fixed to the bone-plug that contained the ligament's tibial insertion so that the forces were directly measured by the load-cell. In their tests, the femur was clamped and the angle of flexion was set in a way that allowed unconstrained rotation of the tibia as torque was applied. These authors concluded that at any level of torque, internal tibial torque always generated greater forces in the ACL than did external torque and that the forces in the ACL that were generated by application of both internal and external tibial torque increased as the knee was extended (ACL force ranged from 80 to 10 N at 0^o to 10^o flexion angles respectively and was less than 10 N for flexion angles greater than 10^o). The *total laxity*, defined as the tibiofemoral rotation between 10 N-m of internal and external tibial torque, averaged 23.6 degrees at full extension and 37.2 at 20 degrees of flexion. More recently, Wascher et al. (1993) used the same technique developed by Markolf et al. (1990) to measure the total resultant force in the posterior cruciate ligament of nine cadaveric knees at 0, 10, 20, 45, 60, 80, and 90 degrees of flexion. Total internal-external rotational laxities were given at $\pm$ 8 N-m of applied tibial torque at each angle of flexion before and after installation of load cells to quantify the effects of the presence of the load cell on laxity of the knee. Wascher et al. (1993) concluded that the mean force generated in the posterior cruciate ligament by application of internal tibial torque was greatest at 90 degrees of flexion and progressively decreased as the knee was extended to 45 degrees; at angles of knee flexion of less than 45 degrees, the mean force in the PCL remained low, with

the exception of a slight elevation at full extension. However, external tibial torque generated measurable force in the PCL in only 8 of the 18 specimens (less than 30 N at 5 N-m), and only at 80 and 90 degrees of flexion of the knee. The major sources of error of this method are related to the cross-talk between the three channels of force components of the load-cell which may cause the calculated resultant forces to vary with the direction of the pull, and to the motion of isolated base of the ligament with respect to the tibial plateau. Non-contacting movements of the plugs of bone, due to cantilievered deflections of the load cell construct, also present a potential source of error.

Bach et al. (1995) measured the strain in the posterolateral bundle (PLB) of the anterior cruciate ligament (ACL) at different flexion angles (-10^o to 120^o) using a liquid metal strain gauge (LMSG) implanted along the posterior fibers of the PLB. Six degree of freedom displacements were monitored along with applied 5 N-m of internal-external axial torque to 5 intact knee specimens (mean age 44.2 years) at 15^o of flexion. These authors also studied the effects of the capsule incision on the internal-external axial rotation of the knee at 15^o of flexion and concluded that the incisions had no significant effect on the axial torque-rotation mechanics of the knee joint. However, one major concern with this method is the fact that the gauge attachment might not be sufficient to accurately measure the strain in the PLB.

1.2.1.2 Contact areas and stresses in the tibiofemoral joint

In light of the emerging evidence regarding the adverse long-term consequences of total meniscectomy, the high incidence of degenerative changes at the tibiofemoral articulation has become a great source of clinical concern. In spite of the existence

of well-accepted values of the resultant force magnitudes in the major weight bearing joints, much remains to be learned concerning the distribution of these forces across the contact surfaces. Solving this distribution problem is of great importance because abnormal intraarticular load transmission is widely implicated in the initiation and progression of osteoarthiritis. Menisci have often been considered worthless, and a meniscal tear has been an indication of a prompt meniscectomy. However, recent clinical evidence has shown that degenerative change of the articular cartilage is more likely to occur after meniscectomy. Hence, quantifying the role of the menisci to load bearing across the joint is crucial for its clinical implication in osteoarthiritis of the tibiofemoral joint.

The first investigations, undertaken specifically to determine the meniscal load-bearing characteristics, considered measurement of the tibiofemoral contact area. It was argued that load transmission across the menisci would be indicated if the measured contact area included the surface normally occupied by the menisci. Walker and Hajeck (1972) were the first to measure the location and size of the contact areas in cadaver knee joints. They considered knee flexion angles from 0^o to 120^o using a casting of bone cement. Average contact areas for lateral and medial condyles were found to be 1.4 and 1.8 cm^2, respectively. Kettelkamp and Jacobs (1972) also measured the tibiofemoral contact area *in vitro* using a roentgenographic method. The method consisted of determining the area of articular-surface contact by measuring the radiolucent area on the roentgenogram of a minimally loaded (30-80 N) knee joint that was surrounded by contrast medium. The measurement was limited to the first 35^o of flexion. The mean lateral and medial contact areas were found to be 2.97 and 4.68 mm^2, respectively, which are more than two times larger than those of walker and Hajeck (1972). Maquet et al. (1975) performed similar experiment but applied a

much greater compressive load (2200 N) across the joint, selecting loads to correspond with estimated peak loads during walking. The measured tibiofemoral contact area ranged from 20 cm^2 at full extension to 11 cm^2 at 90^o flexion. However, when the menisci were removed, the corresponding contact areas decreased to only 12 cm^2 and 6 cm^2, respectively, indicating a substantial load transmission across the menisci.

Walker and Erkman (1975) used a conventional miniature force transducer to measure the relative magnitudes of the local force at various points on the tibial plateau. These authors obtained results corresponding to a sequential increase in joint compressive load up to 1500 N. Although exhibiting considerable variation, their results demonstrated load transmission across the menisci. Fukubayashi and Kurosawa (1980) measured the contact area and pressure distribution of the tibiofemoral joint under various loads and at 0^o flexion using the casting method and pressure sensitive color-forming films (Prescale or Pressensor, Fuji Film Co. Ltd, Japan). At a load of 1000N, the menisci occupied 70 % of the total contact area, and peak pressure magnitudes with and without menisci were 3 and 6 MPa, respectively. The high pressure areas were located on both the meniscus and uncovered cartilage in the lateral compartment and only on the uncovered cartilage in the medial. The contact areas in osteoarthiritic knees were found to be significantly larger than those in normal knees.

Seedhom and Hargreaves (1979) determined the meniscal load-bearing using an approach involving the comparison of the compressive load-deformation properties of the knee joint measured with and without the menisci. They used an analytical model of load transmission across the knee joint to interpret the results. They concluded that an individual meniscus transmits 70 % to 99% of the load acting on the respective knee compartment.

Using a new plastic microindentation transducer, Ahmed and Burke (1983) measured static pressure distribution on the tibial plateau, as well as the fraction of load transmitted through the menisci. The study was carried out at various flexion angles of the knee, with the joint being subjected to various compressive forces, with or without an initial passive relative displacement between the joint members, i.e., an internal-external rotation or anterior-posterior shift. They indicated that a significant fraction of the joint compressive load was transmitted through the menisci (at least 50 % of the total load) and that total meniscectomy causes a drastic alteration in the pressure distribution on the tibial surface. Brown and Shaw (1984) measured contact stress distribution across the tibiofemoral joint by using arrays of miniature piezoresistive transducers inset superficially in the cartilage of the femoral condyles. For the intact joint, the contact stresses rose approximately linearly with the applied loading. The load allocation was higher in the medial compartment, 60.4 % for the intact knee and 61.4 % for the knee following meniscectomy.

More recently, Ateshian et al. (1994) used a stereophotogrammetry (SPG) system for determining contact areas in diarthrodial joints. This method consists of evaluating the proximity of the articular surfaces to determine joint contact areas using precise geometric models of the joint surfaces obtained from the SPG system, and precise kinematic data, also obtained from SPG. In their study, they compared the SPG method to other commonly used methods such as dye staining, silicone rubber casting and Fuji film contact measurement techniques which have often been used and reported by other investigators. These methods yielded consistent contact patterns for the incongruent tibiofemoral articulations.

Bylski-Austrow et al. (1994) studied the displacement of the menisci under joint compression combined with internal-external torques and anterior-posterior forces at

fixed flexion angles (0, 15 and 30 degrees). In their work, nine cadaveric knee joints, in which the capsules, ligaments (except the LCL), articular cartilage, and menisci were intact, were used. Meniscal displacements were measured radiographically. Authors argued that the changes in position of the menisci would directly affect previous estimates of the location and magnitude of high stresses on the menisci and articular surfaces of the tibia and femur. Their results indicated that no radial displacement was observed when increasing joint compression alone from 250 to 1000 N. With the addition of external tibial torque to the compression, the lateral meniscus moved anteriorly with respect to the tibial plateau. With an internal torque, the lateral meniscus moved posteriorly. The medial meniscus moved anteriorly with internal rotation and posteriorly with external rotation. These meniscus displacements are measured with respect to the tibia. These authors also indicated that the relationship between mean anterior-posterior meniscal displacement components and tibial internal-external rotations was highly linear for both menisci. Increasing flexion angle from 0^o to 30^o tended to increase the meniscal displacements. However, this method had a number of limitations. The menisci were treated as rigid bodies while they are actually deformable fibrocartilage tissue. Moreover, removal of the LCL, probably eliminated some restraints to joint motion and therefore influenced meniscal motion.

1.2.2 Analytical model studies

Historically, researchers working on the mechanics of the human knee joint have primarily focused on experimental studies, a trend that continues to persist. More recently, with the development of more powerful computers which have made possible to analyze more complex models, computational tools have been used in order to obtain a better understanding of the complicated biomechanical behavior of the knee

joint. Proper interpretation of experimental results, quantitative investigation of the knee joint mechanisms, evaluation of surgical and diagnostic procedures, and the design of artificial joints are some of the likely areas benefiting from such model studies. Furthermore, parametric alteration of the input data can be used to simulate a wide range of possibilities with clinical relevance.

In 1970, Edwards et al. developed a three-dimensional kinematic model to determine the length of the cruciate and collateral ligaments. In this model, the motion of the femur with respect to the tibia was described only by three degrees of freedom: axial tibial rotation, flexion, and a translation in the proximal-distal direction. All ligaments were assumed to be straight line segments, except for the medial collateral ligament which was divided into two straight line segments to account for wrapping around tibia. Crowninshield et al. (1976) extended Edwards's model by dividing the cruciate, collateral, and capsular ligaments into 13 elements. They added two additional motion components to the three utilized by Edwards et al. (1970); these two degrees of freedom were a varus-valgus rotation and a translation in the anterior-posterior direction. In addition to predicting length changes, the model developed by Crowninshield et al. was also used to determine changes in joint stiffness with flexion and selected ligament cutting. Crowninshield et al. assumed all ligaments had material properties identical to the medial collateral ligament. Furthermore, all ligaments were assumed to be strained to a maximum of 5% during passive flexion.

Wismans et al. (1980) developed a three-dimensional analytical quasistatic model of the knee joint that took into account the ligaments, capsule, and joint surface geometry; however, the menisci were neglected in their model. The tibia was fixed while the orientation of the femur was defined using Euler angles. The model was based on moment and force equilibrium of the femur relative to the tibia. Their model

defines the ligaments and the capsule using seven nonlinear springs and the joint surfaces by polynomials for three-dimensional geometry. In this model, the flexion-extension motion was simulated by prescribing several flexion-extension angles. The dependent variables of the problem, including the ligaments forces, are determined from the equilibrium equations and the geometric compatibility conditions. Contact areas between the femur and tibia were reduced to two contact points, and it was further assumed that both the lateral and the medial articulating surfaces were always in contact with each other. The model was limited since varus-valgus motions that produce separation between a plateau and its opposing femoral condyle could not be analyzed.

Grood and Hefzy (1982) derived analytical expressions describing the nonlinear, coupled stiffness characteristics of the knee at a given joint position using the method of matrix structural analysis. In a later work, Hefzy and Grood (1983) extended their model to introduce two forms of geometric nonlinearities: ligaments wrapping around the surfaces and wrapping of ligaments around each other. The path of the ligament was determined by requiring it to take the shortest distance between insertion sites. The condition of static equilibrium was used to calculate the force acting on the bone at the auxilary nodes. To model the wrapping of ligaments, they used analytic geometry to determine whether wrapping exists or not.

Andriacchi et al. (1983) developed a three-dimensional quasistatic model of the knee joint for the purpose of simulating the effect of ligamentous reconstruction surgery. In this model, the proximal tibia and the distal femur were taken as two rigid bodies. The ligamentous structures were idealized as 21 linear springs using finite element methods. The menisci were modeled as two shear beam elements having shear, bending and axial stiffnesses. Ten hydrostatic elements resisting only forces perpendicular

to their surfaces were selected to represent the contact surfaces. These elements were arranged in two rows along the medial and lateral condyles. Each hydrostatic element was a three-dimensional eight node brick element having four nodes attached to the tibia and four nodes to the femur.

Moeinzadeh et al. (1983) developed a two-dimensional dynamic model considering motion in the sagittal plane only. They described the relative dynamic motions between the femur and tibia and the forces in the joint. The tibia and femur were modeled as rigid bodies with the femur being fixed. Only the two cruciate and the two collateral ligaments, modeled as nonlinear elastic elements, were considered. The profiles of the femoral and tibial articular surfaces were measured from X-rays using a two-dimensional sonic digitizing technique. In their formulation, Moeinzadeh et al. (1983) combined the three equations of motion of the tibia with the contact condition and the geometric compatibility of the problem to obtain a set of six nonlinear differential equations with six unknowns which were solved using Newton-Raphson iterative technique. Wongchaisuwat et al. (1984) presented another two-dimensional anatomical dynamic model to analyze the planar motion between the femoral and tibial contact surfaces in the sagittal plane. In their model, the authors considered the tibia as a pendulum that swings about the femur. Newton-Euler equations were then used to formulate the gliding and rolling motions.

Essinger et al. (1989) developed a three-dimensional mathematical knee model in order to evaluate the mechanical behavior of three commercially available knee prostheses: The Total Condylar (Howmedica Inc., Rutherford), the P.C.A. (Howmedica Inc., Rutherford), and the Freeman-Samuelson (Protek AG, Bern). The model was based on the total energy minimization principle and took into account the articular

surfaces and a simplified patellofemoral joint. Because this model was oriented toward the evaluation of condylar-type knee prostheses, the tibial and femoral surfaces were defined as deformable and rigid, respectively. In this model, the menisci were not considered and friction was neglected. Their model simulated knee prostheses behavior during flexion under physiological loading conditions by applying half of the average body weight (400 N) on the proximal femur. This model generated the kinematics of the joint, the motion of the center of contact, the quadriceps forces, the pressure distribution on the tibial plateau, and ligament lengths and forces between 0^o and 120^o of flexion angle.

Garg and Walker (1990) also performed a model study in order to quantify the effect of tibial surface geometry and component placement of a prosthesis on ligament length change and maximum achievable range of motion. Despite the various computer graphics presented, the bone geometry was described in qualitative way. The tibial surfaces generated were used in the simulation to calculate the ligament length change as a function of knee flexion angle and the maximum achievable range of motion.

Blankevoort et al. (1991) examined the problem of rigid contact in the knee model. They tried to determine how the experimental verification of the knee model was affected by the parameters of the contact and surface descriptions, i.e., the different polynomial approximations of the tibial surfaces, the rigid and deformable contacts, the linear and nonlinear deformable contacts, and the variation of the elastic modulus of the linear deformable surface description. They indicated that the curvature distributions had a second-order effect on the relevant mechanical variables, except for plane approximation; there was no need for a more precise assessment of the cartilage elastic modulus as values between 2.5 and 20 MPa did not dramatically affect the passive motion characteristics; and finally that the introduction of nonlinear

deformable contact did not prove to be of any importance when moderate loading conditions were assumed. Later, Blankevoort and Huiskes (1991) incorporated the model proposed by Hefzy and Grood (1983) for ligament-bone interaction into the above mentioned model and evaluated the effect of the bone intercation with the medial collateral ligament on the axial and valgus rotations of the knee.

Loch et al. (1992) performed a theoretical model analysis to determine the role of the ACL and the cartilage layer in the knee joint stiffness. In their study, the knee was modeled with a generalized stiffness matrix to account for the structure, except the ACL and the contact surfaces; the ACL and cartilage layer were treated separately. The knee stiffness matrix for the specified condition was measured experimentally for the human knee *in vitro*. The model was linear and valid for small motions about the equilibrium position in which the stiffness was measured and a perturbation technique was applied. Only qualitative documentation was given with the results of the simulation.

Recently, Abdel-Rahman and Hefzy (1993) developed a two-dimensional dynamic model of the knee joint to simulate its response under sudden impact. The knee joint is modeled as two rigid bodies, representing a fixed femur and a moving tibia, connected by 10 nonlinear springs representing the different fibers of the cruciate and collateral ligaments and the posterior part of capsule. In this analysis, the joint profiles were presented by polynomials. Model equations include three nonlinear differential equations of motion and three nonlinear algebraic equations representing the geometric constraints. A single point contact was assumed to axist at all times. Numerical solutions were obtained by applying Newmark method and the Newton-Raphson technique. Knee response was determined under sudden rectangular pulsing posterior forces applied to the tibia. Later, Abdel-Rahman and Hefzy

(1993) developed a three-dimensional dynamic model for the tibiofemoral joint. The model consists of two body segments (the femur and the tibia) in contact which are executing a dynamic motion within the constraints of ligamentous forces. Each of the articular surfaces at the tibiofemoral joint were represented by a separate mathematical function. The joint ligaments were modeled as nonlinear elastic springs. The six degrees of freedom joint motions were characterized using six kinematic parameters, and ligamentous forces were expressed in terms of these six parameters. Knee response was studied by considering sudden external pulsing loads applied to the tibia. Model equations consisted of differential equations coupled with nonlinear algebraic constraint conditions. These equations were also solved using the Newmark and then the Newton-Raphson iteration technique. More recently, Tümer and Engin (1993) introduced a two-dimensional three body-segment dynamic model of the human knee. The model includes tibiofemoral and patellofemoral articulations, the cruciate and collateral ligaments and the patellar ligaments. The tibiofemoral and patellofemoral contact forces as well as forces in various ligamentous structures were determined for the extension of the knee under impulsive action of the quadriceps femoris muscle group.

As for the finite element model investigations, to the author's knowledge, the only realistic finite element model of the entire knee joint was recently developed by Bendjaballah et al. (1995) to determine the response of the tibiofemoral joint in full extension under axial forces of up to 1000 N applied to the femur. This model is employed in the current work to study the biomechanics of the tibiofemoral joint under axial rotation and, hence, is described in more details in the subsequent chapter. A few model studies of the menisci have also been performed assuming simplified axisymmetric geometries for the normal condyles, tibial plateau, and menisci with no

consideration of any of the cartilage layers or of ligamentous contribution (Hefzy et al., 1987; Sauren et al., 1984; Spilker and Donzelli, 1992; Tissakht et al., 1989; Tissakht and Ahmed, 1990). More recently, using similar axisymmetric geometries, an analysis has been carried out considering femoral and tibial articular cartilage layers of uniform thickness (Tissakht et al., 1994).

1.3 Shortcomings of the analytical studies

The literature review demonstrates that no realistic three-dimensional anatomical knee model which includes both tibiofemoral and patellofemoral joints has yet been developed. This is a reflection of the fact that the knee is one of the most complex joints in the musculoskeletal system. Furthermore, the previous analytical studies have not taken into account some of the mechanical features essential for a non-linear elastostatic model study of the knee joint. These essential features involve the complex three-dimensional kinematics of both tibiofemoral and patellofemoral joints, the presence of cartilage layers and menisci with accurate articular geometries, the non-linear response including large displacement articulation between cartilage layers of tibia, femur, and patella with each other as well as with the menisci, and the presence of the primary ligaments including the wrapping mechanism of the medial collateral ligament. The results of previous model studies should, hence, be critically evaluated in light of their underlying assumptions. Incorporation of the above features is essential for the accurate prediction of response under various loading conditions. However, such detailed calculation requires the use of advanced computer techniques for both the geometric construction and subsequent stress analysis.

1.4 Objectives

In this research, a realistic three-dimensional model of the entire human knee joint including femur, tibia, patella, cartilage layers, menisci, and joint ligaments developed by Bendjaballah et al. (1995) along with a nonlinear finite element package program (Shirazi-Adl, 1989-a) are used to investigate the response of the tibiofemoral joint, neglecting the patellofemoral joint, at full extension under internal-external femoral torques. The first objective of this study is to attempt to isolate and assess the roles of the major ligaments (cruciates and collaterals) in resisting internal-external torques, with and without axial compression force, at full extension by analyzing and comparing patterns of change in the femoral axial rotation as well as in the total resultant ligament forces upon selective sectioning of particular ligaments. The second objective involves the prediction of regions of contact and the determination of contact forces transmitted through the femur/meniscus, femur/tibia, and meniscus/tibia contact regions at both lateral and medial compartments as internal-external torques are applied on the intact knee joint. In meeting these two objectives, it is expected that the knowledge gained in the course of this research will enhance our understanding of the biomechanics of the tibiofemoral joint, particularly the function of the ligaments in axial rotation, which will then be beneficial in the total knee arthroplasty, prosthetic ligament replacement as well as treatment and prevention of knee ligament injuries.

1.5 Organization of thesis

To help the reader form an idea about the organization of this thesis, a chapter-by-chapter preview follows. Chapter 2 presents the formulation and finite element

modelling of the tibiofemoral joint including details of the finite element meshes, tibiofemoral joint component material properties, loading and boundary conditions and the variables considered in the analysis. Chapter 3 presents the results of the analysis. Chapter 4 is devoted to the discussion of the validation and implications of these results, including the function of the ligaments and the contact regions of the knee joint in axial rotation. Limitations of the model and their likely influence on results are also assessed. Finally, conclusions of this study and recommendations for future work are specified in Chapter 5.

CHAPTER II

METHOD

2.1 Introduction

Knee joint biomechanics are characterized by moving contacts between soft tissue layers separated by a thin layer of synovial fluid. These problems include the multibody contact between the tibial articular cartilage, femoral articular cartilage and menisci, the sliding contact between the retropatellar articular cartilage and the femoral cartilage, and the wrapping mechanism of the medial collateral ligament around the proximal medial bony edge of the tibia. The complexity of such problems requires implementation of sophisticated numerical methods for solutions.

The finite element method is ideally suited for obtaining solutions to knee joint contact problems. This has been facilitated by powerful computers which have made it possible to handle more complex models. However, most finite element analyses have been applied to the study of hard tissue structures, as it relates to prosthetic devices. Finite element formulations involving applications to soft tissues (Hefzy and Grood, 1987; Sauren et al., 1984; Spilker and Donzelli, 1992) have been presented recently; however, a full nonlinear three-dimensional finite element analysis of the entire knee joint of realistic geometry remains a computationally challenging task.

2.2 Formulation

Due to the complex three dimensional kinematics of both tibiofemoral and patellofemoral joints, the presence of cartilage layers and menisci; the nonlinear response including large displacement articulation between cartilage layers of tibia, femur, and patella with each other as well as with the menisci, the nonhomogeneous composite nature of the menisci, and the presence of wrapping mechanism of the medial collateral ligament around the bony edge of the tibia, the problem of knee joint biomechanics is intrinsically nonlinear and hence nonlinear three-dimensional analysis is required. The moving contact problem between different articular surfaces will require that contact conditions be incorporated into the finite element formulation.

Initially, the analysis was carried out using the nonlinear finite element computer program *ADINA* (ADINA, 1992) which has algorithms for nonlinear static and dynamic (frictionless contact only) analysis of large deformation frictional contact problems. These algorithms are based on the the formulations developed by Bathe and Chauhdary (1984). *ADINA* offers two contact solution algorithms:

- Algorithm 1 uses constraint functions to enforce all contact conditions at the contactor nodes. In this algorithm, only the contact conditions of the contactor nodes are considered. The compatibility of the incremental contactor surface displacements and the incremental target surface displacements is only enforced at the discrete locations corresponding to the contactor nodes.
- Algorithm 2 uses Lagrange multiplier approach to enforce that, in the region of contact, the contactor surface displacements are compatible with the target surface displacements. The developed contact forces are calculated directly from

the external loads, inertia forces and the nodal point forces equivalent to the current element stresses. Coulomb's law of friction is enforced by first evaluating the distributed surface tractions from an estimate of the contact forces and then updating the tractions corresponding to the conditions of sticking and sliding contact.

As a first attempt, Algorithm 1, was used to determine the incremental response of the tibiofemoral joint in full extension under axial forces of up to 1000 N applied on the femur. The purpose of this analysis was to compare results obtained by Bendjaballah et al. (1995) and those using *ADINA* program. A Comparison of both results showed a difference in the values of contact forces and displacements. However, since Algorithm 1 does not enforce the frictional conditions (frictionless contact in our case) over the contact surface segments, high tangential stresses (of the same magnitude as normal stresses) were generated causing distortions of the articular contact segments. One way to fix this problem would be to refine the mesh by making the contact surface segments smaller, however this could not be feasible due, at least in part, to the relatively large amount of computational time and memory size required to set up and solve the necessary equations. A second attempt was made using Algorithm 2 which enforced the frictional conditions at the contact segments; however, although the convergence criteria (force and moment) were satisfied, the ADINA program failed to converge during the incremental analysis. This might be due to the inner loop of iterations which Algorithm 2 contains for robustness of the scheme. No information regarding the inner loop iteration is printed out and the user has no control over these iterations.

In view of these fruitless preliminary attempts, an in-house nonlinear finite element package program developed by Shirazi-Adl et al. (1986, 1987, 1989-a, 1989-b) was

used to perform the static nonlinear finite element analysis of the the tibiofemoral joint in axial rotation. Since the details of the formulation of the nonlinear finite element program are available in the literature (Shirazi-Adl, 1984), only a brief review of the analytical formulation is presented in this section.

Since the nonlinear finite element formulation of the in-house package program was extensively used in spinal studies, it is capable of dealing with both geometrical and material nonlinearities and large displacements and strains. The formulation is based on the well-known Updated Lagrangian (U.L.) approach in which the equations of equilibrium for the next increment of deformation are expressed with respect to the continually updated configuration of the structure (Shirazi-Adl et al., 1986). The rate equations of equilibrium expressed with respect to a reference configuration, described by Cartesian coordinates a_i, can be written in the following virtual equation form:

$$\int_V \dot{s}_{ij}\delta v_{j,i}dv = \int_{S_T} \dot{T}_i\delta v_i dS + \int_V \dot{F}_i\delta v_i dV \tag{2.1}$$

where $T_i = s_{ji}n_j$ and $F_i = -s_{ji,j}$ are respectively the traction and body forces and s_{ij} is the unsymmetric nominal stress tensor (Shirazi-Adl et al., 1986). The superimposed dot indicates the partial derivative with respect to the infinitesimal increment of a time-like parameter deformation. δv_i are arbitrary virtual velocity components and S_t refers to the part of the reference surface on which tractions are prescribed. Substitution of $\dot{s}_{ij}$ in Equation 2.1 by the Jaumann invariant stress rate, τ_{ij}^{∇} of the Kirchhoff stress τ_{ij} , and taking the current configuration as the reference for the following increment, $a_i = x_i$, results in the following:

$$\int_v E^{\tau}_{ijkl}D_{kL}\delta D_{ij}dV + \int_V [-\sigma_{ik}D_{kj} - D_{ik}\sigma_{kj} + \sigma_{ik}v_{j,k}] \tag{2.2}$$
$$\delta v_{j,i}dV = \int_{S_T} \dot{T}_i\delta v_i dS + \int_V \dot{F}_i\delta v_i dV.$$

For the bulk elements, E^{τ}_{ijkl} can be expressed as follows:

$$E^{\tau}_{ijkl} = \frac{E}{1+\nu}[\delta_{ik}\delta_{jl} + \frac{\nu}{1-2\nu}\delta_{ij}\delta_{kl}] \tag{2.3}$$

where E and ν are the Young's modulus and Poisson's ratio of the material, respectively. This constitutive relation defines a hypoelastic material with no dependence on the current state of stress and the deformation history. To account for the large relative displacements at the articulating surfaces, Shirazi-Adl et al. (1986) developed a method for employing continuous examination of the possibility of contact between the contacting surfaces. After each increment of the load, the perpendicular distance is computed between a set of points on the contactor surfaces and triangular plane elements on the target surfaces. If the perpendicular distance of a point is found to be smaller than a specified gap-limit and furthermore if its projection on the plane of the same lower triangle is found to be inside the boundary, then it is assumed that contact has occurred at the point examined. The frictionless contact constraint is modeled by generating an element for the next increment of the load. This link element is assumed to possess nonlinear stress-strain characteristics which yield high stiffness in compression but none in tension. The stiffness in compression increases as the perpendicular distance between two surfaces decreases. As for the problem of nonlinear wrapping mechanism of the MCL around the proximal medial bony edge of the tibia and its peripheral attachments to the medial meniscus, a nonlinear finite element technique that analyzes the wrapping of uniaxial elements around general solid body edges developed by Shirazi-Adl (1989-a) was used. In this formulation, The body edges may be fixed or allowed to deform during the course of loading. This formulation accounts for both large displacements and large strains. Shirazi-Adl (1989-a) approached the problem of wrapping uniaxial elements by developing an incremental stiffness matrix for the whole wrapping element which accounts for the change in the

direction of the element caused by the contact with the rest of the structure. In this manner, the degrees of freedom of all the nodes (end and contact nodal points) are coupled assuring identical axial force in the sub-elements. A detailed description of this formulation is readily available in the literature (Shirazi-Adl, 1989-a).

2.3 Geometry and mesh

Merging computer-assisted tomography, direct digitization and measurements, Bendjaballah et al. (1995) reconstructed the detailed geometry of an entire human knee joint specimen of a 27-year-old woman. The finite element model is briefly outlined for the sake of completeness.

A rigid body representation was considered for each bony structure: tibia, femur and patella. This is time-efficient in a non-linear analysis and accurate owing to their much larger stiffness compared to that of soft tissues. Each bony structure was represented by a primary node located at its centre and by a set of local convective coordinates system that rotates with the rigid body. The finite element mesh generation was then automatically performed leading to 81 8-node solid elements for both medial and lateral tibial articular cartilages, 244 8-node solid elements for femoral cartilage, and 49 8-node solid elements for patellar articular cartilage. For meniscal tissues, a non-homogeneous composite model of a matrix of ground substance reinforced by a network of radial and circumferential collageneous fibres was considered. Due to their shapes, the meniscal tissues were modeled by solid elements in the radial, circumferential, and axial directions resulting in a total of 424 8-node solid elements for both menisci. A total of 1212 truss elements reinforcing these solid elements was also used to model the collagen network throughout the meniscal material in radial and

circumferential directions. Moreover, 39 uniaxial elements modeled various ligaments of the knee joint, the anterior and posterior bundles of the anterior cruciate ligaments by three elements each; the anterior and posterior bundles of the posterior cruciate ligaments by three elements each; the anterior, posterior and superior bundles of the lateral collateral ligament by three elements; and finally, the patellar ligament by nine elements. Special attention was focused on the medial collateral ligament that wraps around the proximal medial bony edge of the tibia in addition to its peripheral attachments to the medial meniscus. This ligament was modeled in its proximal part by 15 trusses in the anterior, posterior and inferior bundles, each bundle starting from the femoral bony insertion to the distal outer surface of the medial meniscus and connected to a wrapping element to give a total of five wrapping elements for the distal part of the medial collateral ligament. The overall finite element mesh is shown in Figures 2.1 and 2.2. In Figure 2.2, each ligament bundle is represented by a 2-node truss element; also shown is the attachment of the medial collateral ligament to the periphery of the medial meniscus: ACL, anterior cruciate ligament; PCL, posterior cruciate ligament; LCL, lateral collateral ligament; MCL, medial collateral ligament.

For the frictionless non-linear contact problem modeling articulation at the tibiofemoral and the patellofemoral joints, seven potential contact areas were identified. These are, first, the medial femoral condyle against medial tibial cartilage and proximal medial meniscus; distal medial meniscus against medial tibial cartilage. Second, three similar contact regions on the lateral side of the tibiofemoral joint were also determined. Finally contacting regions were defined at the patellofemoral joint between the femoral cartilage and the retropatellar articular cartilage. In the non-linear finite element model, the femoral articular cartilage surface and the distal meniscal surfaces were considered to be the contactor surfaces represented by nodal

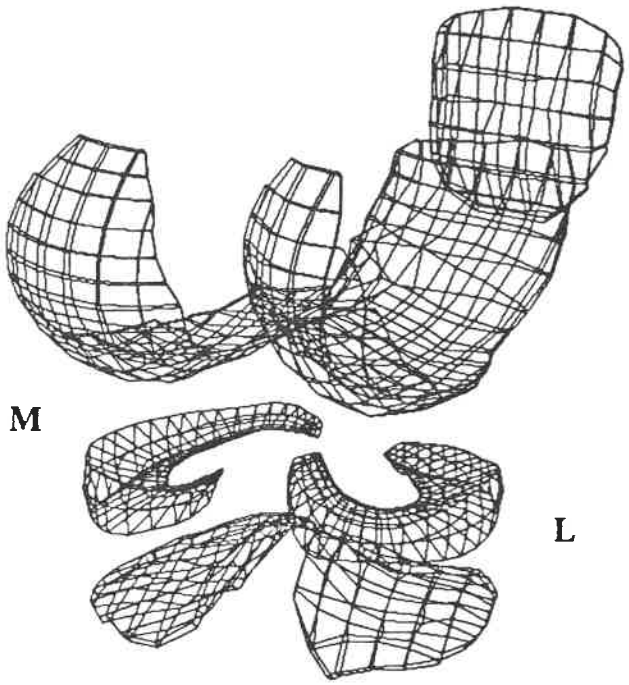

Figure 2.1: A typical posterolateral view of the finite element mesh representation of cartilage layers and menisci using 8-node solid elements: M, medial; L, lateral. The ligaments as well as rigid bodies representing tibia, femur, and patella are not shown.

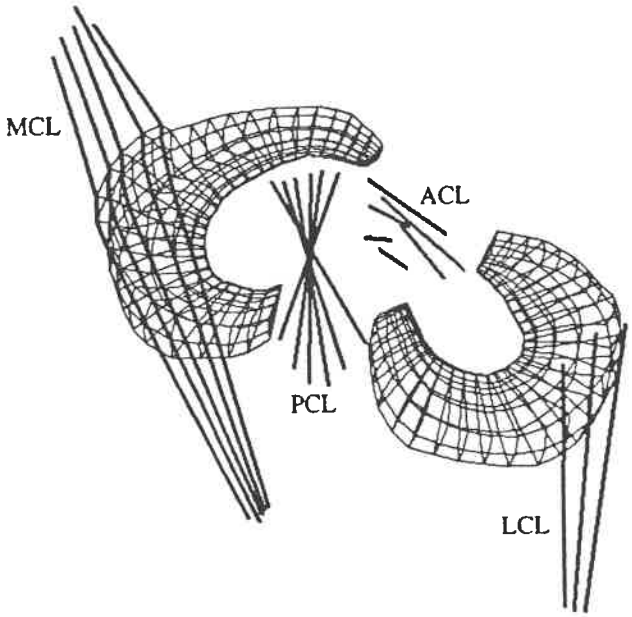

Figure 2.2: Finite element model of menisci and ligaments. The bony structures and articular cartilage layers are not shown.

points while tibial and patellar cartilage surfaces and proximal meniscal surfaces were, on the other hand, taken as target areas modeled by triangular patches. For this representation of the contact problem, a total number of 758 contactor nodal points and 740 target triangular facets were used.

2.4 Material properties

For the present finite element analysis of the model taking into account only the tibiofemoral joint at a fully extended position, the material properties were derived from the data available in the literature. As discussed earlier, the bony structures were modeled by rigid bodies. The articular cartilage layers were assumed to be isotropic with an elastic modulus of $E = 12$ MPa and Poisson's ratio of $\nu = 0.45$ (Brown et al, 1983; Hayes and Mockros, 1971; Hayes et al., 1972). Similar values for elastic moduli have been used in previous finite element analyses (Galbraith and Bryant, 1989; Little et al., 1986). For the representation of the menisci; a composite of isotropic matrix reinforced by collagen fibres was considered. The elastic modulus of the matrix was chosen as $E = 8$ MPa which is close to values obtained from measurements on specimens cut in the radial direction at the deep parts of the menisci (Tissakht and Ahmed, 1993; Whipple et al., 1984). This value is in accordance with the observation that meniscal tissue is roughly one-half as stiff in compression as articular cartilage (Fithian et al., 1990). The Poisson ratio was taken as $\nu = 0.45$. These moduli were used in the hypoelastic constitutive relations employed in the finite element program.

The non-linear material properties for collagen fibres were chosen to be similar to those for disc collagen fibres used in the spinal model studies of Shirazi-Adl et al. (1986) and Shirazi-Adl (1989-b)(Figure 2.3). In the 30 μm to 150 μm thick membrane on the

proximal surface as reported by Fithian et al. (1990) or in the 200 μm thick membrane as suggested by Whipple et al. (1984), the fibres are randomly oriented resulting in nearly equal properties for meniscal specimens in the radial and circumferential directions yielding elastic moduli of 70 MPa and 50 MPa, respectively (Whipple et al., 1984). A mean value of 60 MPa was assumed in this work for the purpose of the following calculations. In the deep region of menisci, the collagen fibres are reported to be predominant in the circumferential direction (Bullough et al., 1970) with a mean tensile elastic modulus of about 170 MPa (Fithian et al., 1989). The equivalent collagen fibre content in each direction was then evaluated based on the equilibrium equation of a meniscal specimen under tension, developed to relate a homogeneous orthotropic material to a non-homogeneous composite one as that used in the model:

$$E_T^{SEC} = \alpha E_F^{SEC} + E_M \tag{2.4}$$

Where α is the collagen fibre volume fraction content, $E_M = 8$ MPa is the estimated elastic modulus of the matrix, E_T^{SEC} and E_F^{SEC} are the strain-dependent non-linear elastic secant moduli of the meniscus as a homogeneous orthotropic material and collagen fibres, respectively. Equation 2.4 was employed for several strain magnitudes yielding an averaged fibre volume fraction content of 14 % in the circumferential direction in the deep parts of menisci and 7 % in both directions in the superficial regions.

Material properties for different ligaments were derived from data available in the literature. some specific parameters most commonly reported for ligaments are the ligament stiffness K, linear elastic modulus E, initial or reference strain, non-linear strain level parameter ϵ_1, ultimate stresses and strains, and energy density at failure (Butler et al., 1986; Race and Amis, 1994). From these data, the stress-strain curves

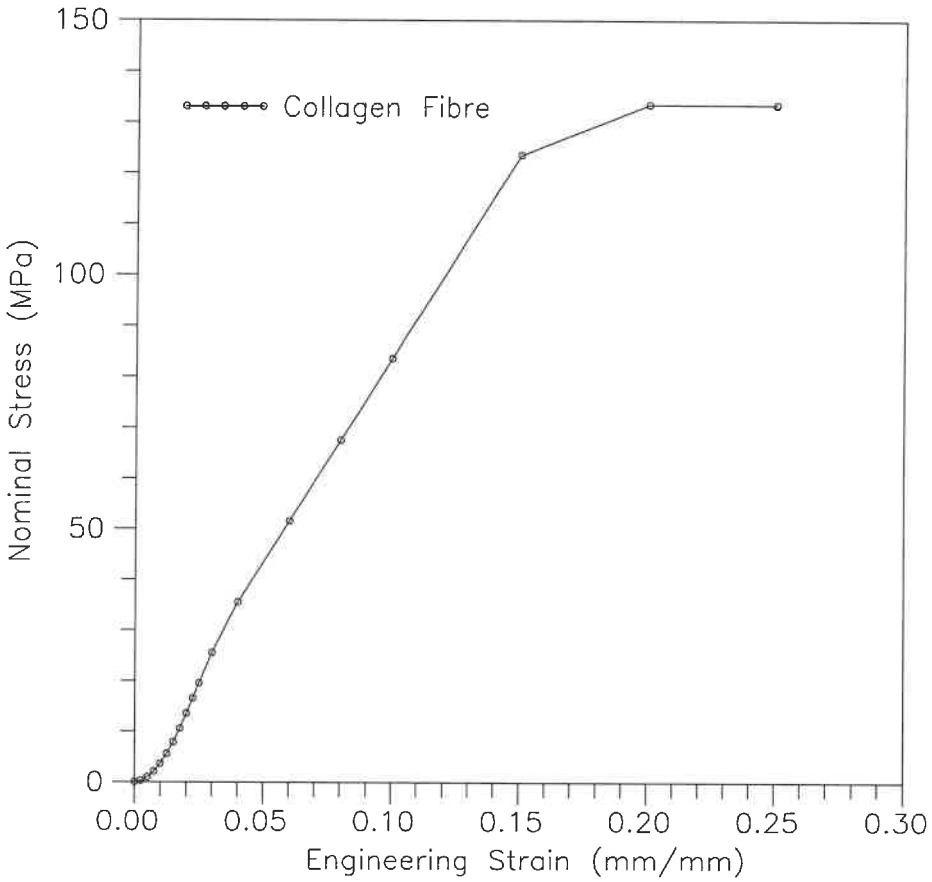

Figure 2.3: Stress-strain curve of collagen fibre.

relating nominal stress to engineering strain were reproduced assuming a non-linear quadratic stress-strain behavior for low strains and a linear behavior for strains higher than $2\epsilon_1$ as suggested by Wismans et al. (1980):

$$\begin{array}{lll} \sigma = 0 & \text{for} & \epsilon \leq 0 \\ \sigma = E\epsilon^2/4\epsilon_1 & \text{for} & 2\epsilon_1 \geq \epsilon \geq 0 \\ \sigma = E(\epsilon - \epsilon_1) & \text{for} & \epsilon \geq 2\epsilon_1 \end{array} \tag{2.5}$$

The linear elastic moduli of the anterior cruciate ligament, ACL, and lateral collateral ligament, LCL, have been reported by Butler et al. (1986). The linear elastic modulus for the medial collateral ligament, MCL, was obtained from the stiffness values used in a previous model study (Andriacchi et al., 1983) accounting for the ligament's cross sectional area measured directly on the specimen. The elastic modulus of the patellar tendon was based on the ligament stiffness values reported by Hirokawa (1991) while data for the anterior and posterior bundles of the posterior cruciate ligaments, aPCL and pPCL, were derived from recent measurements performed by Race and Amis (1994). The nonlinear strain level parameter known also as the linear strain limit parameter was set at about $\epsilon_1 = 0.03$ for all ligaments (Butler et al., 1986), while the reference strain for each ligamentous bundle defined as the strain at no external load was derived from earlier studies (Blankevoort et al., 1991; Grood and Hefzy, 1982; Wismans et al., 1980) and is listed in Table 2.1. The stress-strain curves for the ACL, LCL, PCL and MCL are shown in Figure 2.4.

In the event of contact between a contactor point and a target facet, a two-node contact gap element is automatically generated by the contact algorithm in the program which is assumed to have a modulus of 100 MPa in compression and nil in tension. The contact between adjacent bodies is assumed to initiate at distances below 0.15

Table 2.1: Areas and reference strains for ligament bundles.

Ligament	Bundle	Area (mm^2)	Reference strain (%)	Reference
ACL	anterior (aACL) posterior (pACL)	21 21	3.1 2	Grood and Hefzy (1982)
PCL	anterior (aPCL) posterior (pPCL)	45 15	-2 -2	Wismans et al. (1980)
LCL	anterior (aLCL) superior (sLCL) posterior (pLCL)	6 6 6	3 3 3	Wismans et al. (1980)
MCL	anterior (aMCL) inferior (iMCL) posterior (pMCL)	14 7 14	3 3 3	Blankevoort et al. (1991)

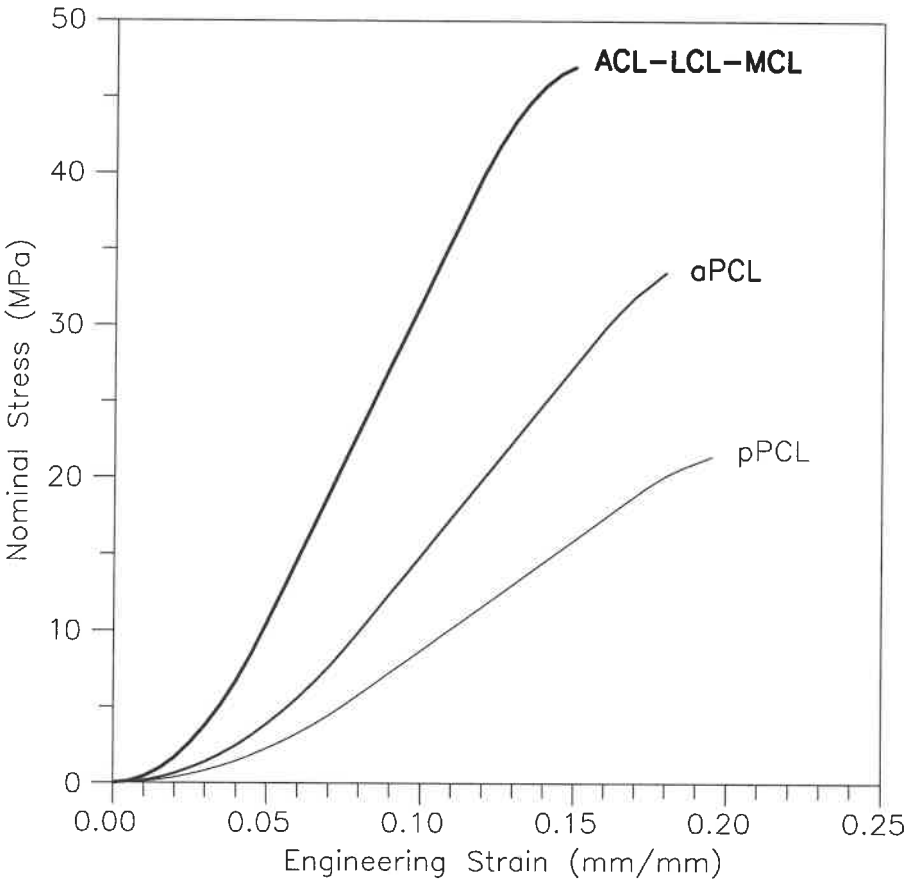

Figure 2.4: Stress-strain curves of the ligaments.

mm (i.e. gap limit). These values were chosen based on a number of preliminary studies on the effect of contact parameters on predicted results (Bendjaballah et al., 1995).

2.5 Loadings, boundary conditions and parameters

The present nonlinear stress analysis is performed considering the tibiofemoral joint only in full extension. For the sake of validation of the model predictions, the load applications and boundary conditions are set to be as close as possible to those in experimental studies. The tibia is fixed while the femur is free to translate in the proximal-distal, medial-lateral, and anterior-posterior directions; the varus-valgus rotation is first fixed and then left free while flexion-extension rotation is maintained fixed throughout the analyses. This allows to apply an axial torque at the primary node positioned approximately at the centre of mass of the femur instead of attempting to locate the joint mechanical balanced point, the position of which varies with load. The reconstructed joint has an initial varus-valgus alignment of 6^o and flexion of 5^o. In the presence of initially prestressed ligaments, the axial torque is incrementally applied to reach the maximum value of $\pm$ 10 N-m while the tibia is completely fixed. Additional analyses are also carried out in which the femoral varus-valgus rotation is restrained while the ligamentous structures are selectively sectioned to simulate a ligament-deficient knee for the purpose to isolate and assess the role of ligaments. Moreover, to study the effect of compressive preload on the axial rotational laxity of the tibiofemoral joint, a preload of 1000 N was applied on the femur, while the axial torque was varied from 0 N-m to $\pm$ 10 N-m.

In this work, neglecting the patella, the response of the tibiofemoral joint in the fully extended position is predicted under internal-external torques applied to the femur in increments of 0.5 N-m up to 10 N-m. For each increment, two iterations are executed to obtain a satisfactory convergence on the overall equilibrium, contact forces, strains and stresses in uniaxial and solid elements. Also, due to the presence of initial strains in the ligaments, in every case, six iterations are executed to obtain a satisfactory convergence on these parameters.

CHAPTER III

RESULTS

3.1 Introduction

In this chapter, the results are presented only for the tibiofemoral joint at full extension under internal-external torques applied to the femur. The predicted load-displacement data of the femoral shaft for intact and ligament-deficient tibiofemoral joints under internal-external torques are first presented. The total ligament forces of intact and ligament-deficient tibiofemoral joints are then investigated. The forces transferred through the femur-meniscus, femur-tibia, and meniscus-tibia contact regions along with the contact areas within the intact tibiofemoral joint are subsequently presented. Finally, special attention is given to the load-bearing of both lateral and medial menisci during internal-external femoral axial rotations. It is important to note that in this study, the terms *internal rotation* and *external rotation* refer to *femoral internal axial rotation* and *femoral external axial rotation*, respectively; however in the literature, they often refer to *tibial internal axial rotation* and *tibial external axial rotation*, respectively. A discussion of the results of the proposed method and those available in the literature is given in a later chapter.

3.2 Load-displacement results

The predicted axial torque-axial rotation curves of the femoral shaft for the intact tibiofemoral joint when the varus-valgus rotation is left free (TY$\neq$0) or fixed (TY=0)

exhibit, as shown in Figure 3.1, an increasing stiffness with increasing internal-external torques. In Figure 3.1, the computed axial rotations represent the change in femoral axial rotations relative to the configuration with initial ligamentous pre-stress forces. Figure 3.1 indicates that the constraint on the varus-valgus rotation has negligible effects on the femoral internal axial rotations whereas it substantially decreases the femoral external axial rotations. Indeed, an internal torque of 10 N-m applied at full extension results in internal rotations of 22^o and 22.5^o for the cases in which the femoral varus-valgus rotation is fixed or left free, respectively; however, an external torque of 10 N-m applied at full extension results in external rotations of 21.6^o and 28.3^o for the cases in which TY=0 and TY$\neq$0, respectively. Along with primary axial rotation, coupled femoral displacements are also computed that are shown in Figures 3.2-3.5. Similar to the axial rotations, the coupled displacements are evaluated at the femoral primary node relative to their magnitudes in intact cases following the application of initial ligamentous forces. Letting the varus-valgus rotation free results in larger coupled displacements of the femur particularly during external rotation. Hence, the restraint of the varus-valgus rotation diminishes the laxity of the knee joint. The coupled axial translation is shown in Figure 3.4 and is noted to be upward in both directions. In the case where both varus/valgus and flexion/extension rotations are restrained, this translation remains the same everywhere on the femur. However, in the case where the varus-valgus rotation is free, these coupled displacements depend on the location of the primary node chosen to represent the femur and, hence, they cannot be classified as the coupled translations of the femur as a whole. Figure 3.5 shows that a minimal coupled varus rotation of 0.6^o accompanies 10 N-m of internal torque at full extension, whereas approximately 4.5^o of coupled valgus rotation is seen at 10N-m of external torque.

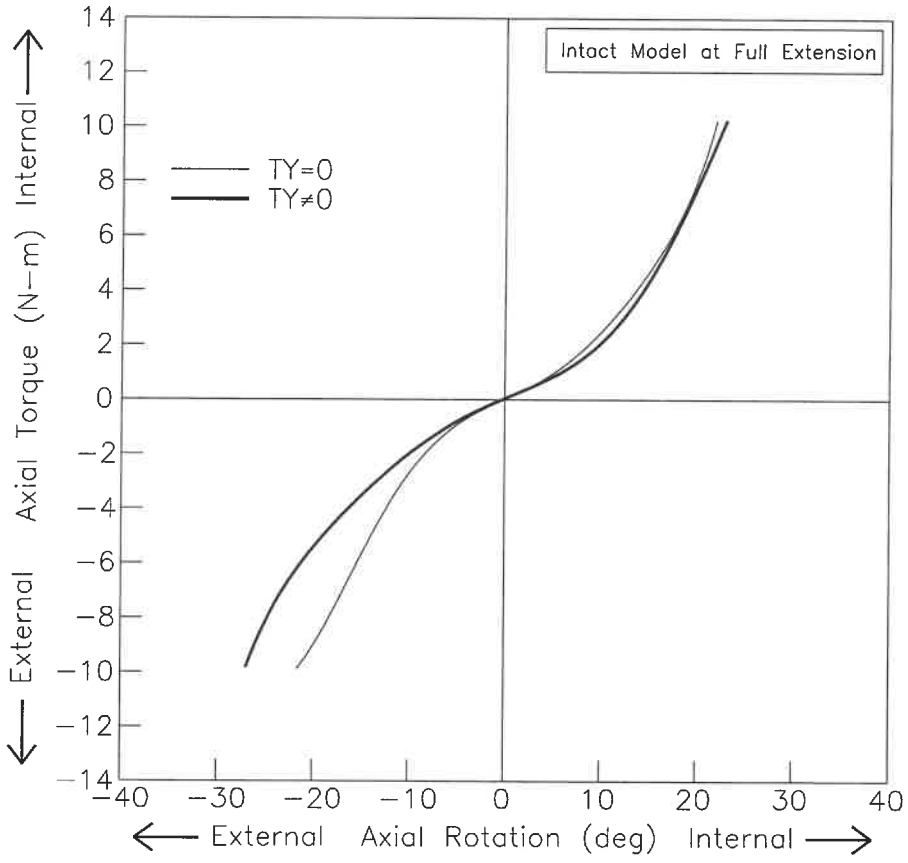

Figure 3.1: The predicted internal-external rotations of the femur for applied internal-external torques with the tibiofemoral joint in full extension with the varus-valgus rotations fixed (TY=0) or free (TY≠0).

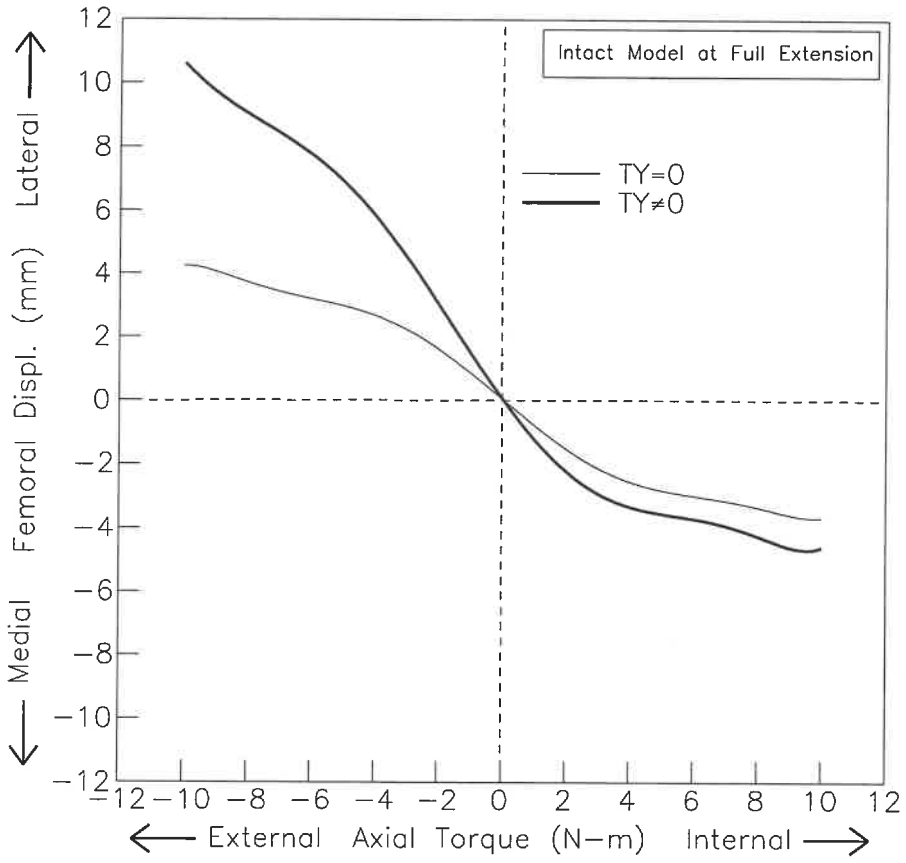

Figure 3.2: Coupled femoral medial-lateral translations for the tibiofemoral joint at full extension under internal-external torques with the varus-valgus rotations fixed (TY=0) or free (TY≠0).

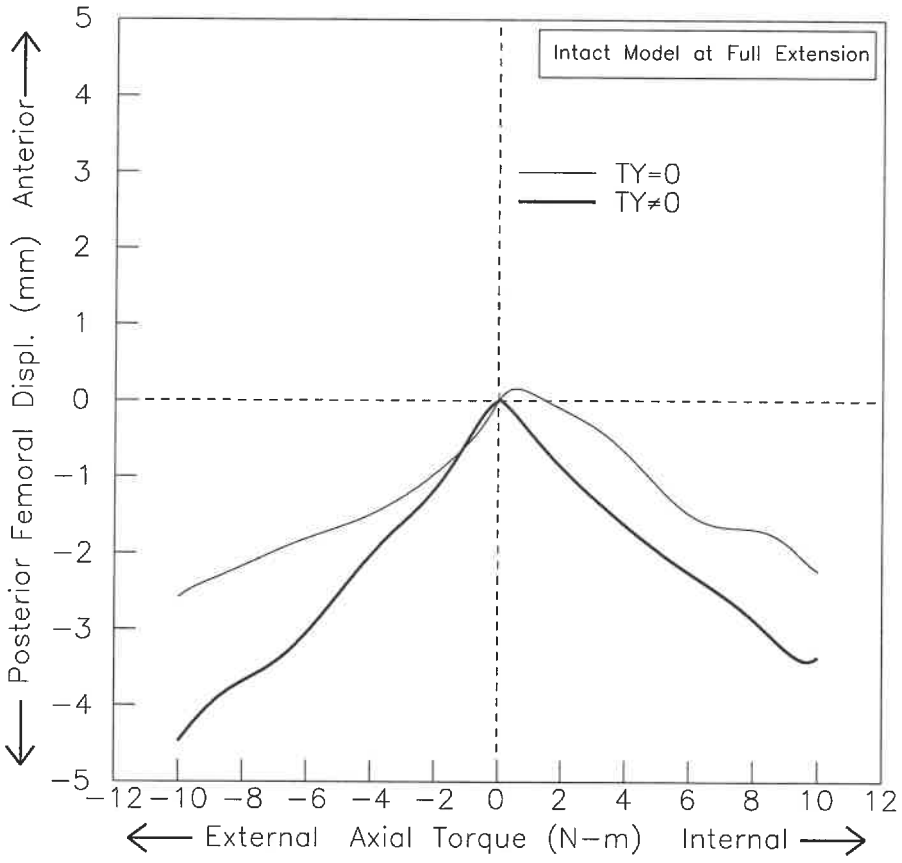

Figure 3.3: Coupled femoral posterior-anterior translations for the tibiofemoral joint at full extension under internal-external torques with the varus-valgus rotations fixed (TY=0) or free (TY≠0).

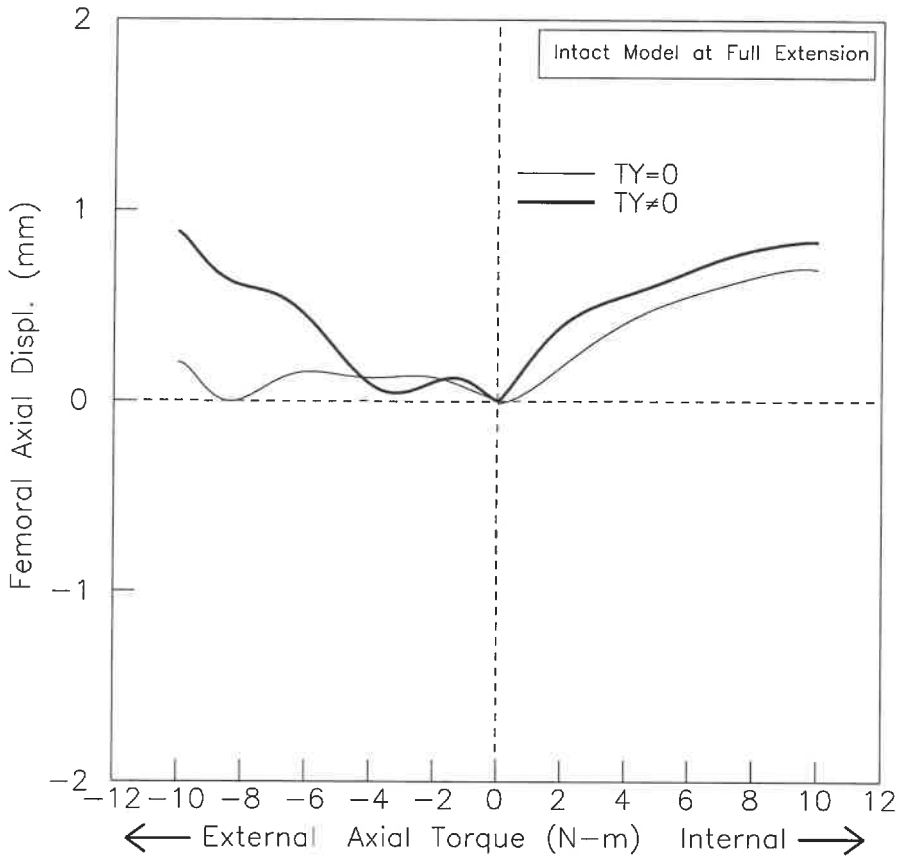

Figure 3.4: Coupled femoral proximal-distal translations for the tibiofemoral joint at full extension under internal-external torques with the varus-valgus rotations fixed (TY=0) or free (TY≠0). (Positive: upward in the distal-proximal direction).

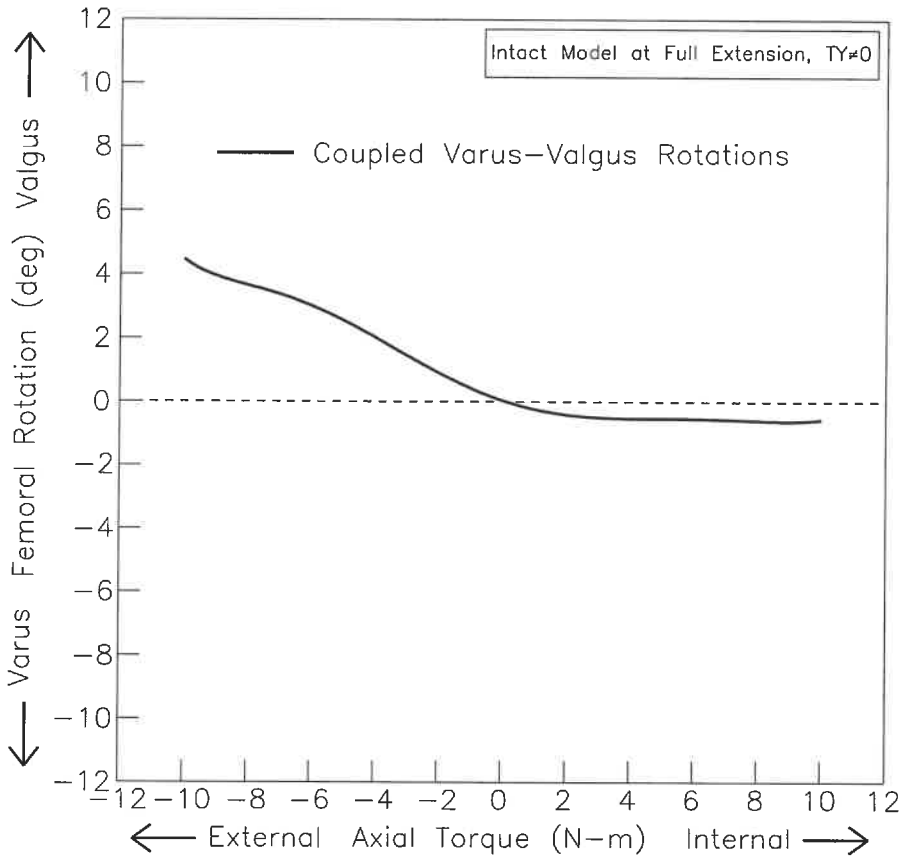

Figure 3.5: Coupled femoral varus-valgus rotations for the tibiofemoral joint at full extension under internal-external torques.

In order to assess the role of the major ligaments in resisting internal-external torques at full extension, a selective sectioning of particular ligaments is performed. Both varus-valgus and flexion-extension rotations are fixed throughout the analyses. Again, it is important to note that the computed axial rotations of the ligament-deficient joint represent the change in femoral axial rotation relative to the configuration of the ligament-deficient joint with initial ligamentous prestress forces. Isolated or combined sectioning of the ACL and the PCL produces only minor increases in torsional laxity with the tibiofemoral joint in full extension (Figures 3.6, 3.7 and 3.8). However, isolated sectioning of the MCL caused a significant increase in the internal torsional laxity but only minor changes in the external torsional laxity (Figure 3.9). On the other hand, isolated sectioning of the LCL produced significant increases in both internal and external torsional laxities (Figure 3.9). Thus, the MCL can be considered an important restraint to the femoral internal axial rotation. Moreover, the LCL ligament seems to be the major restraint in both internal and external rotation. Indeed, as shown in Figure 3.9, sectioning of the LCL brings the internal and external laxities to approximately 32^o at only 6 N-m torque and 37^o at 9 N-m torque, respectively.

Figure 3.10 shows the effect of a 1000 N compressive preload on the axial rotation of the femur under internal-external torques. In this figure, the absolute axial rotations represent the relative increase in femoral axial rotations from their initial ligamentous prestress forces; however, the relative rotations represent the relative increase in femoral rotations from the compressive preload condition. The compressive preload caused a significant decrease in the primary laxity, defined by Markolf et al. (1976) to be the total angular rotation for a torque of $\pm$ 0.5 N-m. Moreover, the compressive preload produced a decrease of the relative axial rotations during any level of internal torque up to 10 N-m and during external torque of magnitude under 5 N-m. Thus,

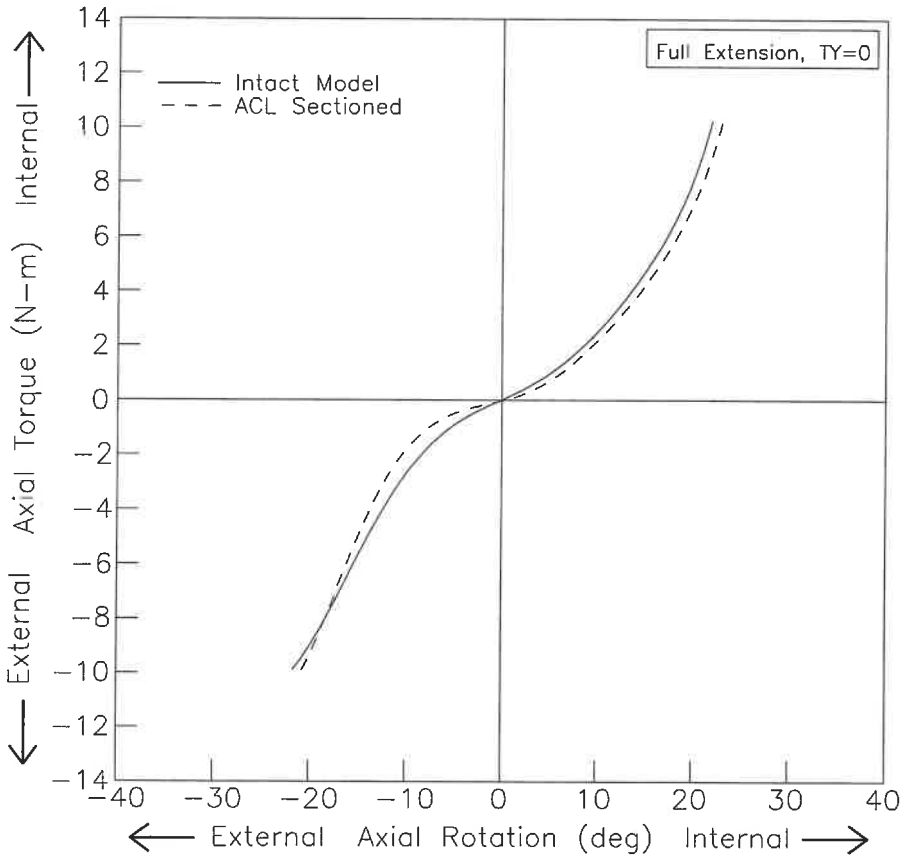

Figure 3.6: Effect of ACL sectioning on internal-external rotations of the femur for applied internal-external torques with the tibiofemoral joint in full extension and the varus-valgus rotations fixed.

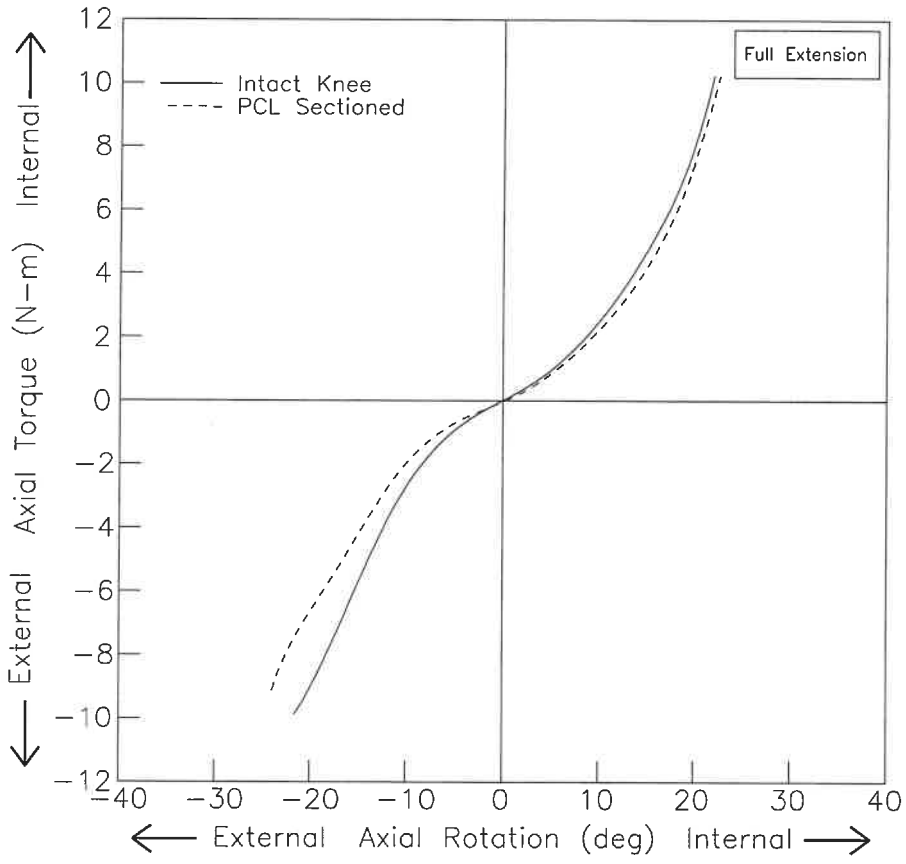

Figure 3.7: Effect of PCL sectioning on internal-external rotations of the femur for applied internal-external torques with the tibiofemoral joint in full flexion and the varus-valgus rotations fixed.

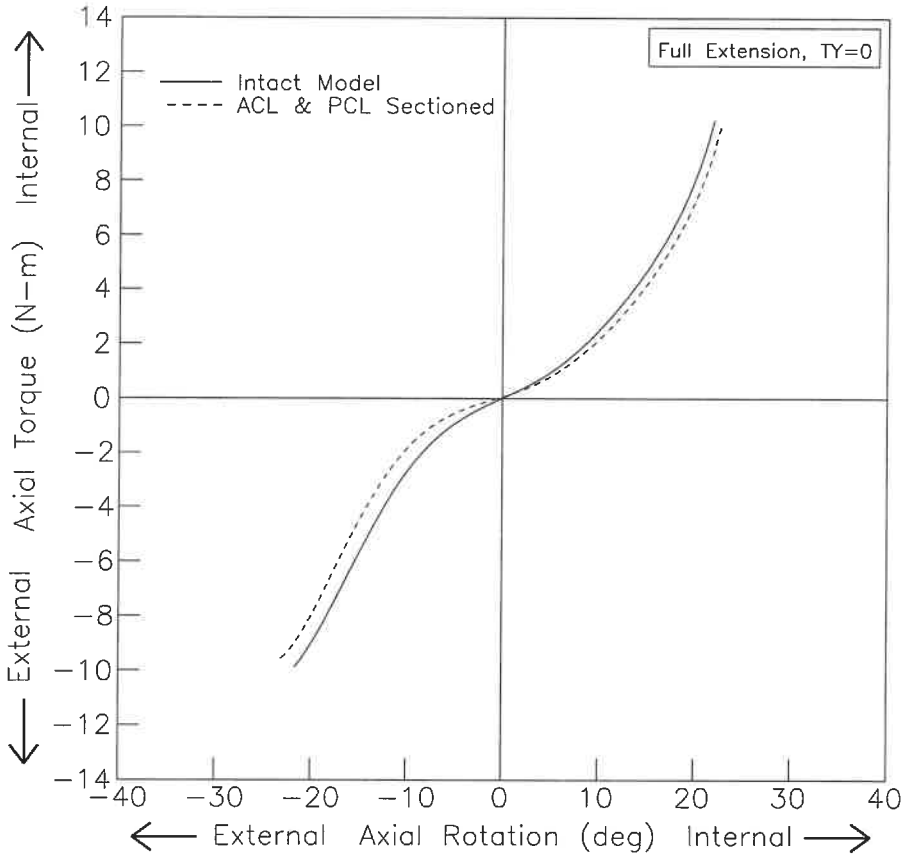

Figure 3.8: Effect of sectioning of both ACL and PCL on internal-external rotations of the femur for applied internal-external torques with the tibiofemoral joint in full extension and the varus-valgus rotations fixed.

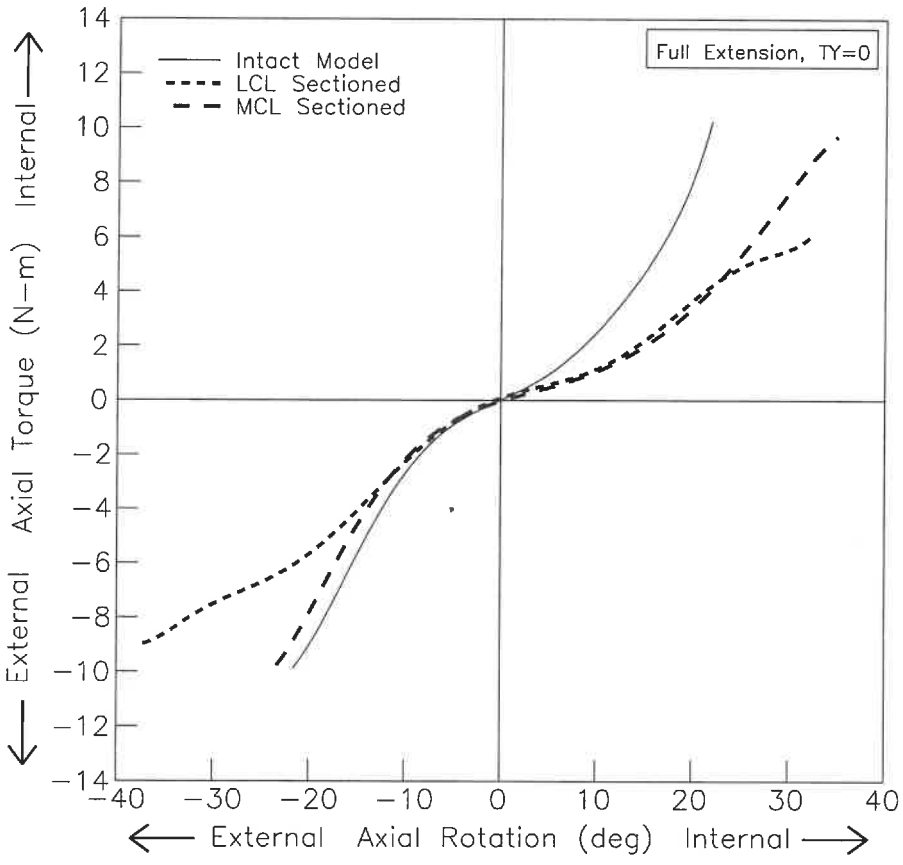

Figure 3.9: Effect of isolated sectioning of LCL and MCL on internal-external rotations of the femur for applied internal-external torques with the tibiofemoral joint in full flexion and the varus-valgus rotations fixed.

the effect of the compressive preload is predominately a marked increase in the joint stiffness near the neutral position (0 N-m).

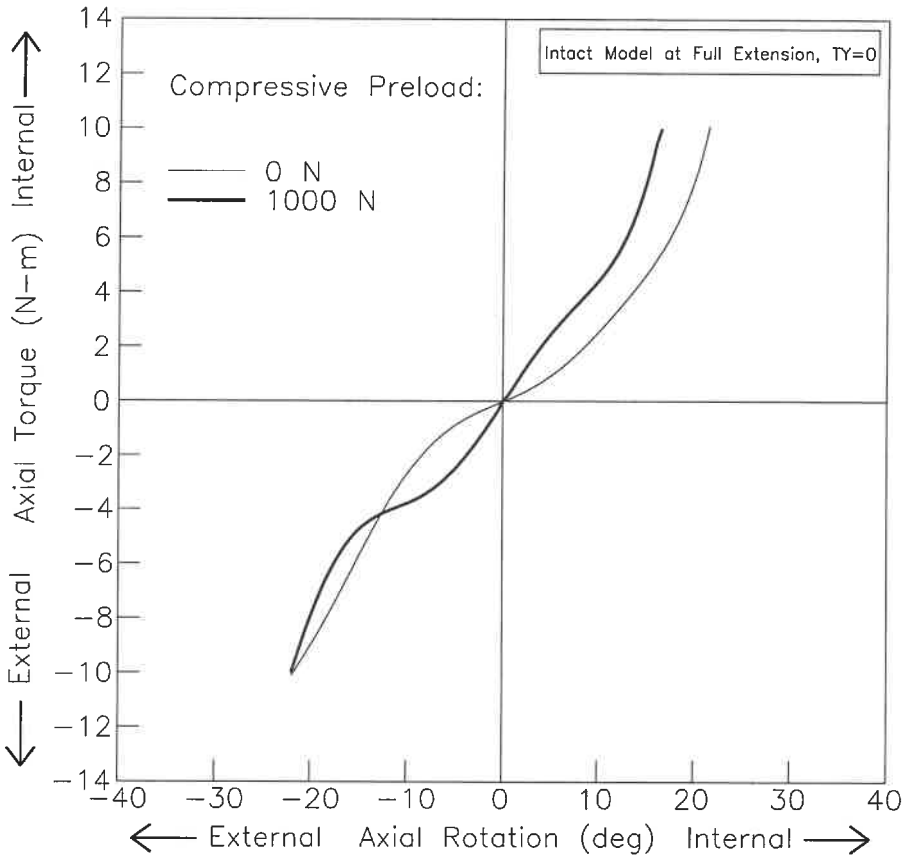

Figure 3.10: Femoral axial rotation at full extension as a function of the applied torque with and without the compressive preload (TY=0).

3.3 Ligament forces

Under no external load, the joint is initially compressed due to the prestress in some ligaments (Table 2.1). With the varus-valgus rotation being constrained, the total initial tensile forces of the intact model are respectively, 17 N in the ACL, 12 N in the PCL, 20 N in the LCL and 24 N in the MCL (see Figure 3.11), whereas, when the varus-valgus rotation is set free, these tensile forces become, 13 N in the ACL, 5 N in the PCL, 30 N in the LCL 14 N in the MCL (see Figure 3.12). By comparing results in Figures 3.11 and 3.12, it is interesting to note that the ligament tension response varies with changes in the boundary conditions on the varus-valgus rotation of the joint. Indeed, the results corresponding to a restrained varus-valgus rotation indicate that the application of external torque generates relatively high forces in the ACL, LCL and PCL. The total tensile forces carried by these ligaments at 10 N-m of external torque are respectively, 268 N in the ACL, 287 N in the PCL and 292 N in the LCL, however, the force resisted by the MCL is less than 50 N during any level of external torque up to 10 N-m. These results also show that during internal rotation, only the LCL and MCL are relatively loaded. At 10 N-m of internal torque, the total tensile forces in the LCL and MCL are 271 N and 242 N, respectively. The PCL does not carry any load during any level of internal torque beyond 1 N-m. The ACL does not play a major role in the restraint of internal rotation and its total force is less than 40 N at 10 N-m of internal torque. On the other hand, representative results of ligament tensile forces computed when the varus-valgus rotation is left free clearly show that the cruciate ligaments, particularly the ACL, are under relatively high tension during external torque. The total tensile forces carried by these ligaments at 10 N-m of external torque are respectively, 335 N in the ACL (although the tensile force reached 348 N at 9 N-m of external torque), 267 N in the PCL, 186 N in the

LCL and 210 N in the MCL. At 10 N-m of internal torque the total tensile forces in the LCL and MCL reach 310 N and 215 N, respectively. The PCL does not carry any load during any level of internal torque beyond 0.5 N-m. The ACL plays a relatively major role in resisting internal rotation and its total tensile force is less than 75 N at 10 N-m of internal torque.

With the varus-valgus rotation being restrained, isolated sectioning of the ACL results in an increase in the the total forces of the LCL and the MCL and a significant decrease in the total force of the PCL during external rotation; however, it produces only minor changes in the total tensile forces of the LCL and MCL during internal rotation (Figures 3.13-3.15). Similarly, sectioning of the PCL causes an increase in the total LCL and MCL forces and a significant decrease in the total force of ACL during external rotation; in contrast, only minor changes are produced during internal rotation (Figures 3.13, 3.14 and 3.16). The combined sectioning of both the ACL and PCL seems to have the same effects as the isolated sectioning of the ACL or the PCL.

Figure 3.16 indicates that sectioning of the LCL results in a large increase in the ACL forces during external torque. Indeed, at 9 N-m of external torque, the ACL tension force computed in response to the sectioning of the LCL exhibits the greatest variation in terms of tension magnitude and is evaluated to be approximately 577 N. The PCL exhibits the second highest variation in terms of tension magnitude and its tensile force reaches 501 N at 9 N-m of external torque (Figure 3.15). However, the MCL tensions computed in response to LCL sectioning exhibits relatively minor variations with the largest tensile force being 112 N evaluated at 9 N-m of external torque (Figure 3.14). On the other hand, the sectioning of the LCL during internal rotation causes the ACL to become completely slack while relatively a high increase in the tensile forces of the PCL and the MCL is produced.

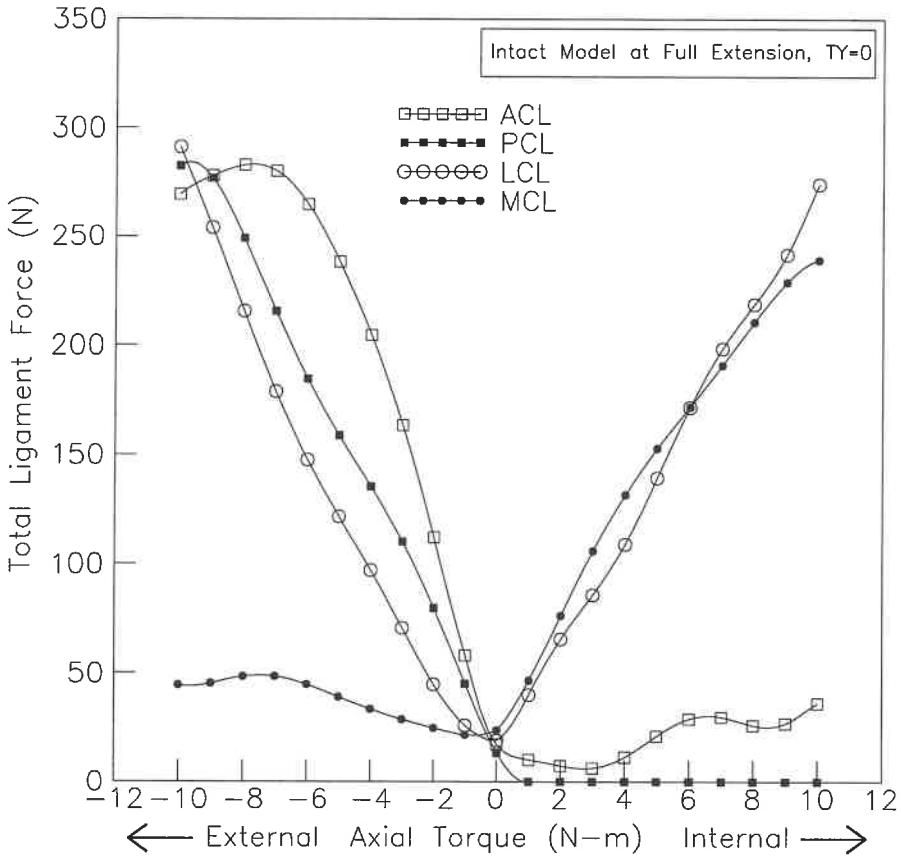

Figure 3.11: Total forces in the four primary ligaments under internal and external torques applied at full extension (TY=0).

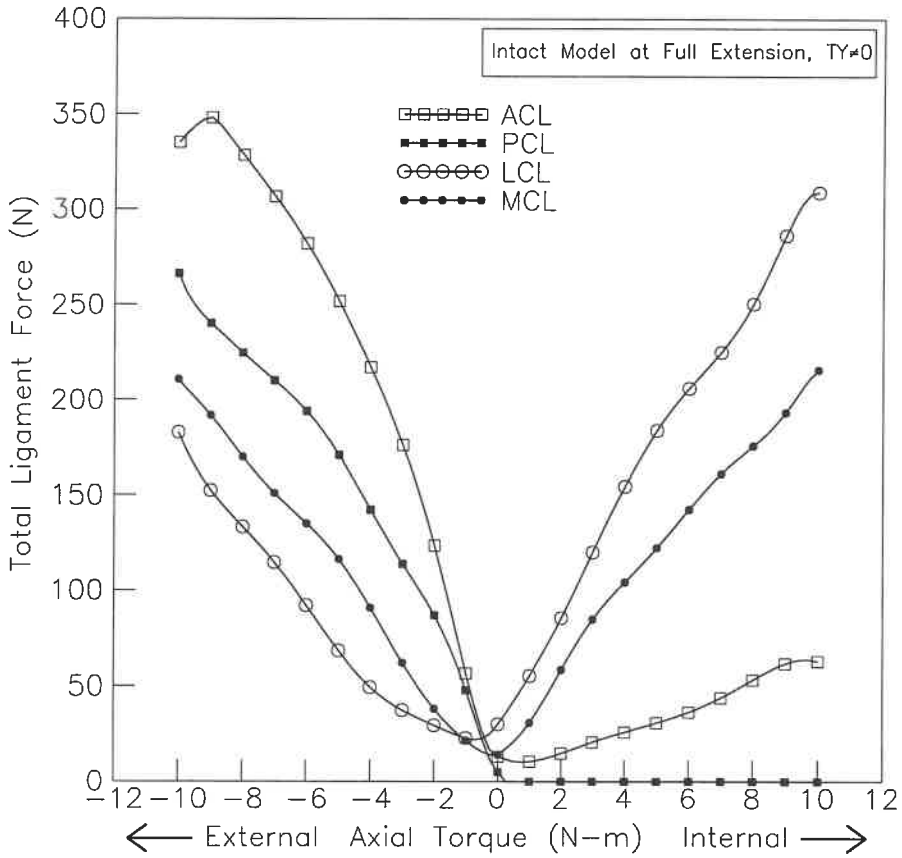

Figure 3.12: Total forces in the four primary ligaments under internal and external torques applied at full extension (TY≠0).

The isolated sectioning of the MCL seems to produce a substantial increase in the total tensile forces of the ACL and LCL during internal rotation. At 10 N-m of internal torque, the LCL tensile force computed in response to the sectioning of the MCL yields the highest variation in terms of tension magnitude and is evaluated to be approximately 580 N. The ACL exhibits the second highest variation in terms of tension magnitude and its tensile force reaches 389 N at 10 N-m of internal torque. On the other hand, isolated sectioning of the MCL does not produce any changes in the tensile force of the PCL which remains completely slack during internal rotation. As shown in Figures 3.16, 3.13 and 3.15, the selective sectioning of the MCL in external torque causes only minor increases in the tensile forces of the ACL, LCL and PCL.

Figures 3.17 and 3.18 indicate that, under the compressive preload of 1000 N, the PCL remains slack and does not carry any load during the internal rotation and during applied external torques of up to 4.5 N-m. This means that it requires higher values of external torque (> 4N-m) to generate tensile forces in the PCL. Similarly, under the compressive preload, the LCL remains completely slack within the range of 0 to 4 N-m of internal-external torques and it requires higher values of internal-external torques (> 4 N-m) to produce tensile forces in the LCL. On the other hand, in the range of 0 to 5 N-m of internal-external torques, the compressive preload seems to cause an increase in the total forces of the ACL with only minor changes in the range of 5 to 10 N-m (Figure 3.19). The MCL exhibits some decreases in the total forces showing less resistance to the internal-external torques due to the effect of the compressive load (Figure 3.20).

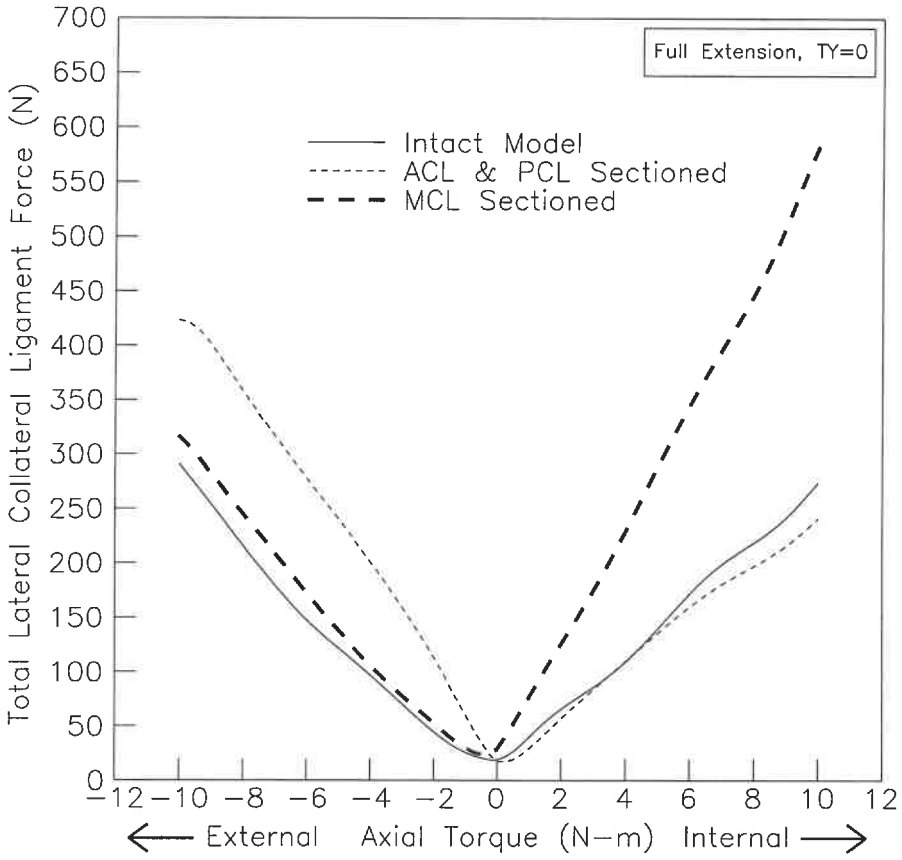

Figure 3.13: Total forces in the LCL under internal and external torques applied at full extension (TY=0).

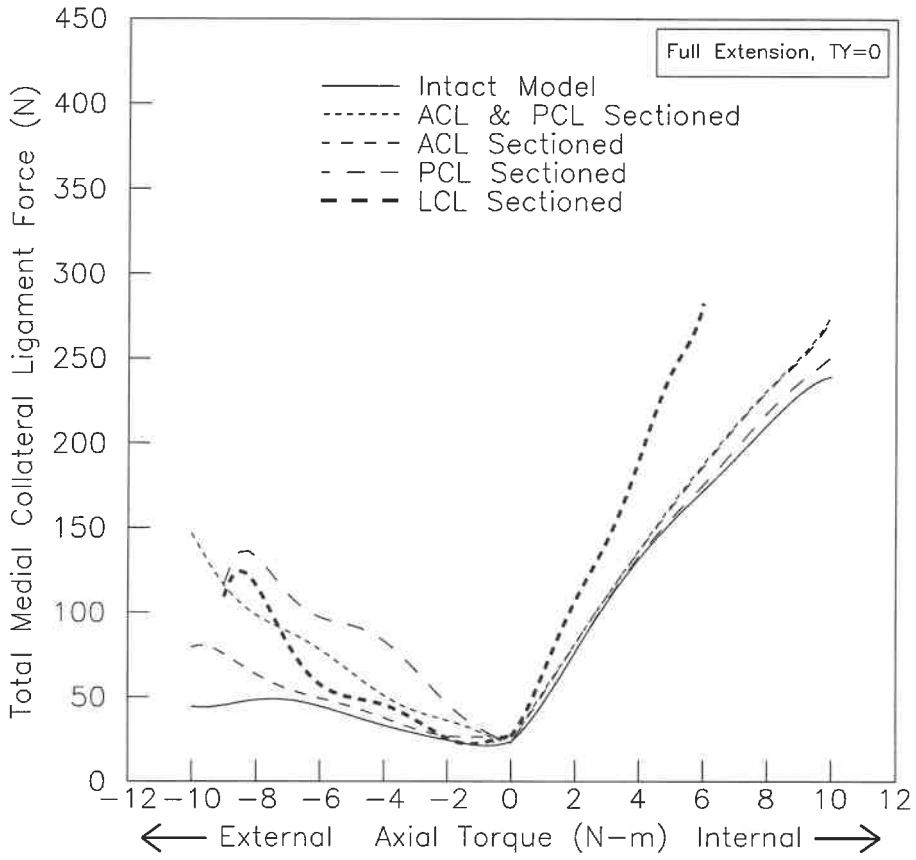

Figure 3.14: Total forces in the MCL under internal and external torques applied at full extension (TY=0).

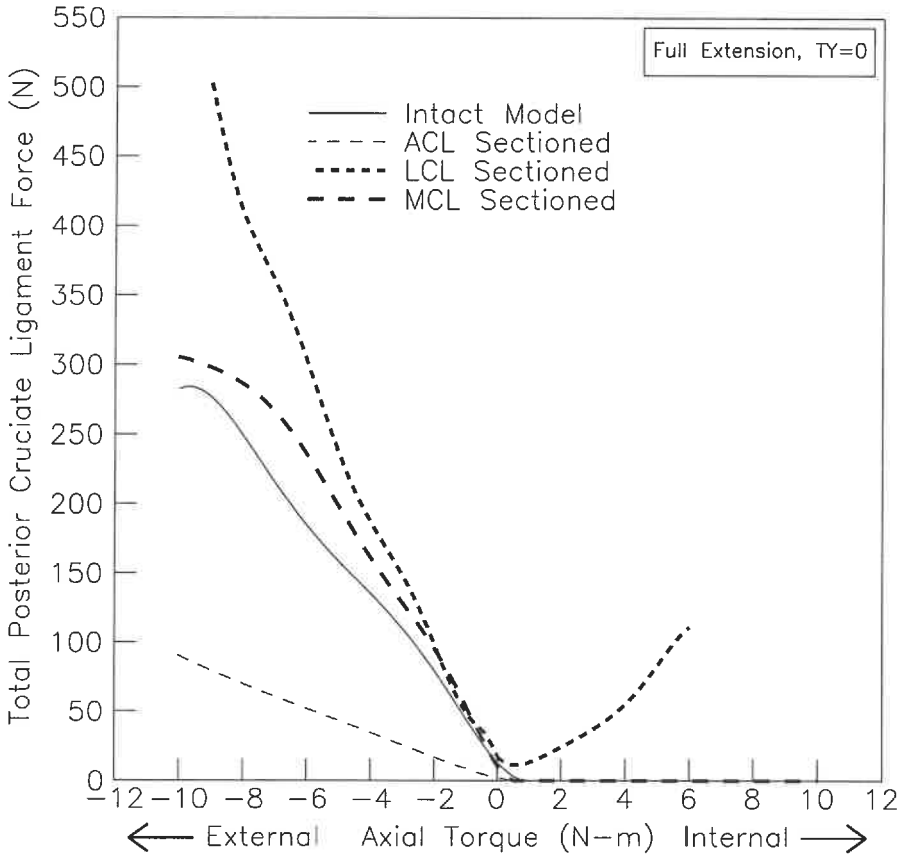

Figure 3.15: Total forces in the PCL under internal and external torques applied at full extension (TY=0).

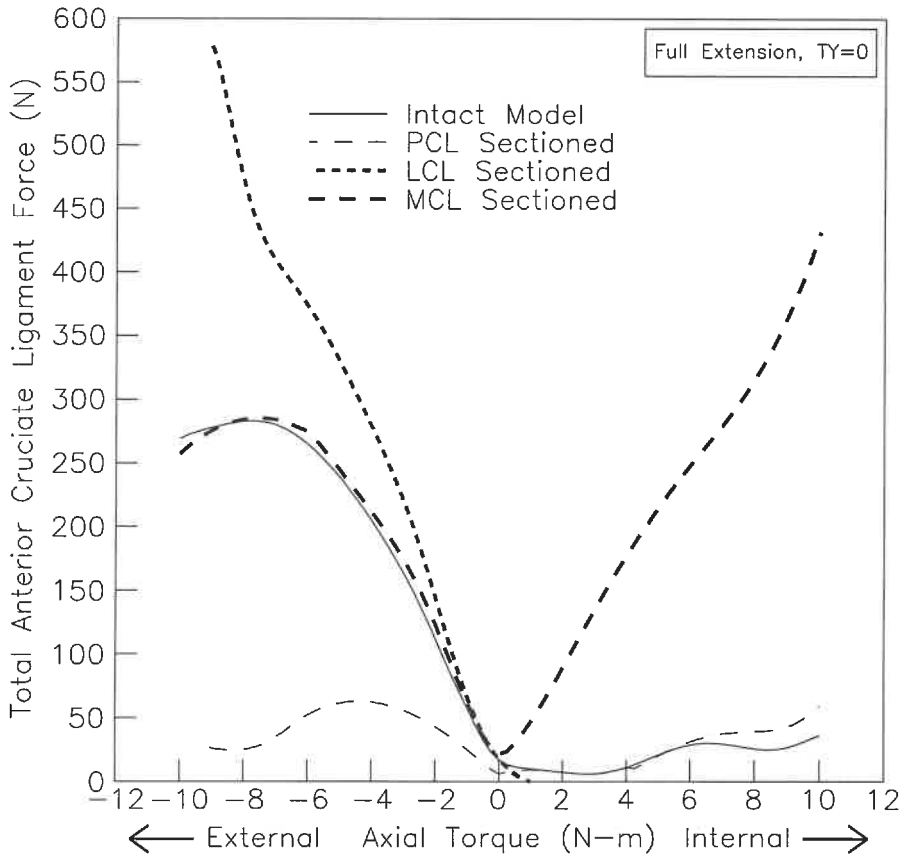

Figure 3.16: Total forces in the ACL under internal and external torques applied at full extension (TY=0).

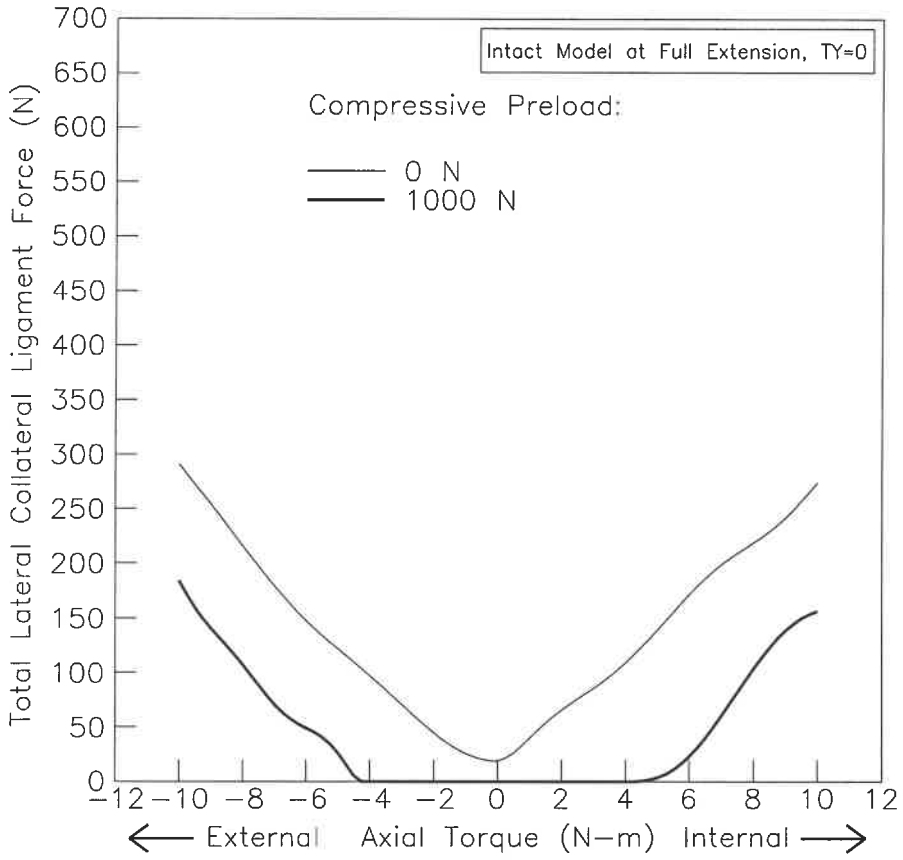

Figure 3.17: LCL total tensile force at full extension as a function of the applied axial torque with and without the compressive preload (TY=0).

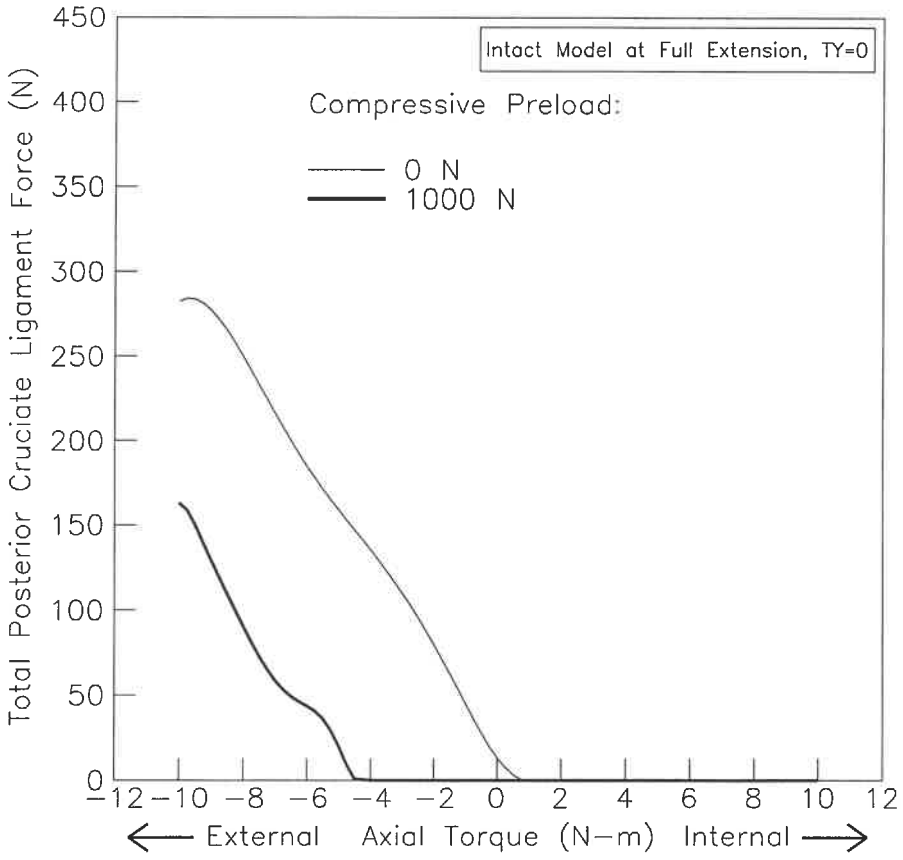

Figure 3.18: PCL total tensile force at full extension as a function of the applied axial torque with and without the compressive preload (TY=0).

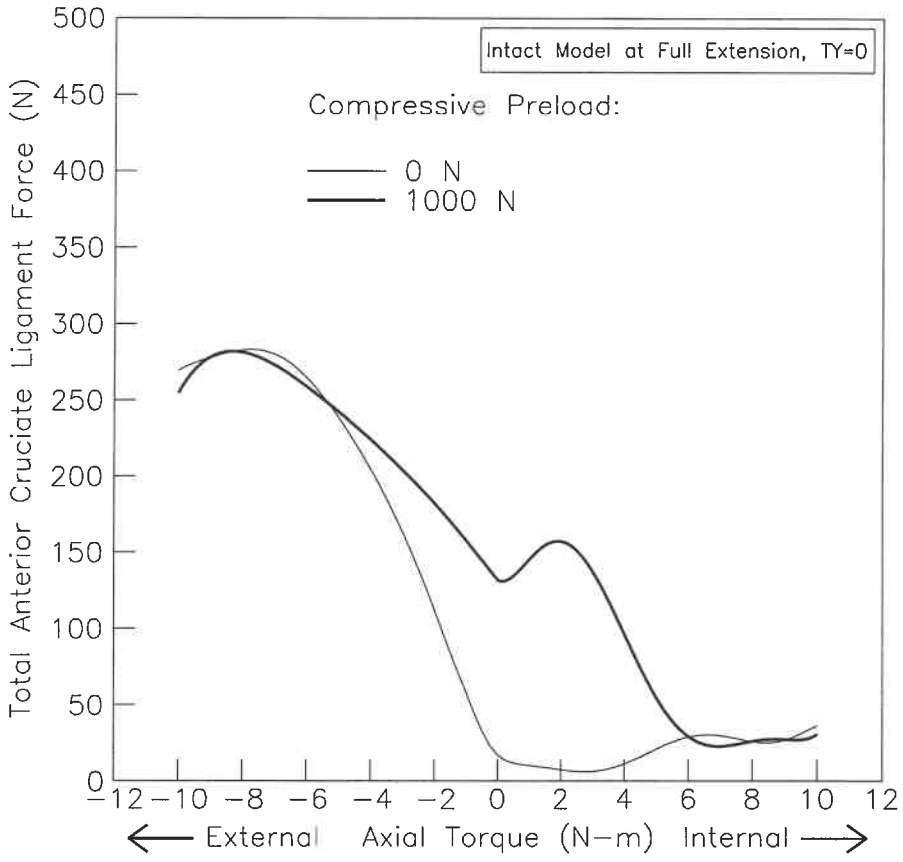

Figure 3.19: ACL total tensile force at full extension as a function of the applied axial torque with and without the compressive preload (TY=0).

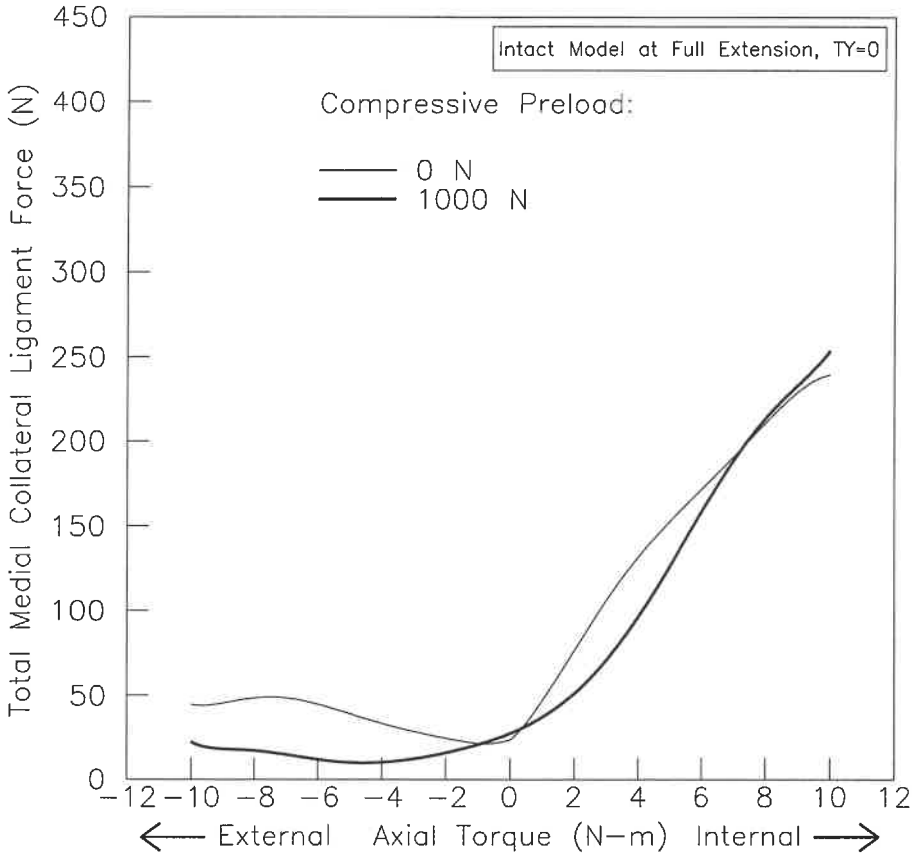

Figure 3.20: MCL total tensile force at full extension as a function of the applied axial torque with and without the compressive preload (TY=0).

3.4 Contact forces and areas

The forces transferred through the femur-meniscus, femur-tibia, and meniscus-tibia contact regions for both lateral and medial compartments are computed for each incremental internal-external torque and verified to almost completely equilibrate the total load in the joint. Analysis of contact forces indicates that in the intact tibiofemoral joint, the medial compartment carries more load during external rotation than does the lateral compartment; however, the reverse holds during internal rotation (see Figure 3.21). At 10 N-m of external torque, the medial and lateral compartments share the generated axial load of 689 N at ratios of 88% and 12%, respectively. However, at 10 N-m of internal torque, the medial and lateral compartments share the generated axial load of 437 N at ratios of 25% and 75%, respectively. The contribution of the menisci in the load bearing is demonstrated by evaluating the portion of axial compartmental load transmitted through menisci as compared with the whole axial compartmental load (see Table 3.1).

Analysis of the stresses in the tibial cartilage layers, at the centroid of solid elements, indicates that the maximum principal stresses are oriented approximately normal to the contact surfaces which are almost completely in compression (Figure 3.22). In Figure 3.22, tibial cartilage elements with no stress bar are in low tension (less than 0.1 MPa), however tension stress values of 0.4 MPa and 0.8 MPa are computed at 10 N-m of external torque in two small medial tibial covered cartilage elements located respectively, in the anterior third and close to the outer boundaries and in the posterior third and close to the inner boundaries. At 10 N-m of internal torque, these normal stresses are greater in lateral plateau as compared to those in the medial one (Figure 3.22-a). A maximum compressive stress of 2.2 MPa in the lateral plateau is

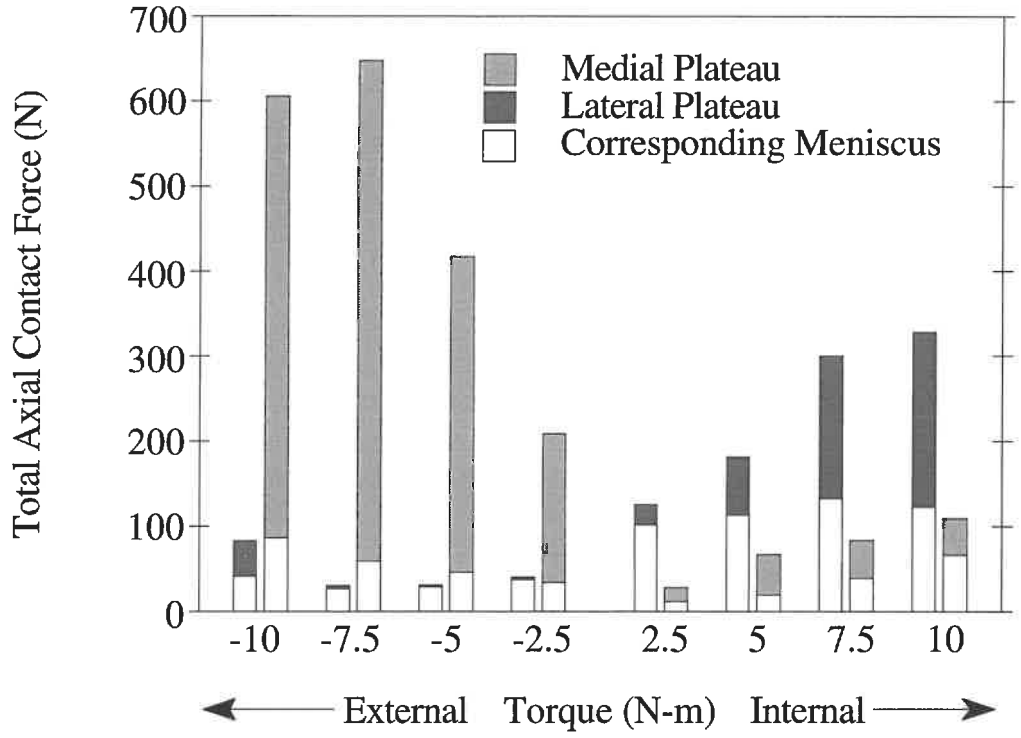

Figure 3.21: Distribution of the axial forces in medial and lateral plateaus of the tibiofemoral joint at full extension under internal-external torques (TY=0).

Table 3.1: Loads transmitted by menisci as a ratio of total compartmental load for the intact tibiofemoral joint at full extension.

Torque (N-m)		Ratio of compartmental load (%)	
		Lateral	Medial
External Torque (N-m)	2.5	93	16
	5	92	11
	7.5	88	9
	10	50	14
Internal Torque (N-m)	2.5	81	41
	5	62	29
	7.5	44	49
	10	37	62

computed in the covered cartilage located centrally and laterally. As for the medial plateau, a maximum compressive stress of 0.8 MPa at 10 N-m of internal torque is obtained in the uncovered cartilage located posteriorly and laterally. However, at 10 N-m of external torque, the normal stresses are much larger in medial plateau than those in the lateral plateau (Figure 3.22-b). A maximum compressive stress of 3.2 MPa in the medial plateau is computed in the uncovered cartilage located close to the tibial spine (Figure 3.22-b). As for the lateral plateau, a maximum compressive stress of 1.3 MPa at 10 N-m of external torque is obtained in the covered cartilage located posteriorly and medially.

At 10 N-m of internal torque, tensile strains in collagen fibres are found to be higher in medial meniscus than in lateral meniscus. In medial meniscus, the tensile strains of circumferential and radial fibres are mainly between 0.5% and 3.5% with some circumferential and radial fibres exhibiting 4% to 7.2% strains in the inner boundaries of the anterior and the posterior third and 4% to 8.3% strains in the distal surface of the central third of the medial meniscus, respectively. In lateral meniscus, most of the tensile strains of circumferential and radial fibres range from 0.5% to 2.5%, however, some radial fibres, in the distal layer of the meniscus, exhibit 3% to 4.5% strains.

At 10 N-m of external torque, the tensile strains of circumferential and radial fibres of both menisci are mainly between 0.5% and 3%. However, some radial fibres show higher strain values of 3% to 8.5% and 4% to 6% in the anterior third of the medial meniscus and in the proximal inner boundaries of the posterior third of the lateral meniscus, respectively. Yet, an isolated radial fibre element, located in the proximal inner boundaries of the anterior third of the medial meniscus, undergoes a high strain value of 15.4%. The strains in the matrix element of this radial fibre are also high with

the largest normal strain computed to be 10.5% in the posterior-anterior direction. As for the circumferential fibres, some exhibited higher strain values of 3% to 7% and 3% to 6% in the proximal inner boundaries of the anterior third of the medial meniscus and in the proximal inner boundaries of the posterior third of the lateral meniscus, respectively. Nevertheless, an isolated circumferential fibre element, located in the distal layer of the posterior third of the lateral meniscus, undergoes a high strain of 14.7%. Besides, the strains in the matrix element of this circumferential fibre are also high and the largest one is computed to be 7% in the medial-lateral direction. As predicted, both isolated radial and circumferential fibres, which exhibit large strain values, are located in the cartilage contact areas where high stresses are present.

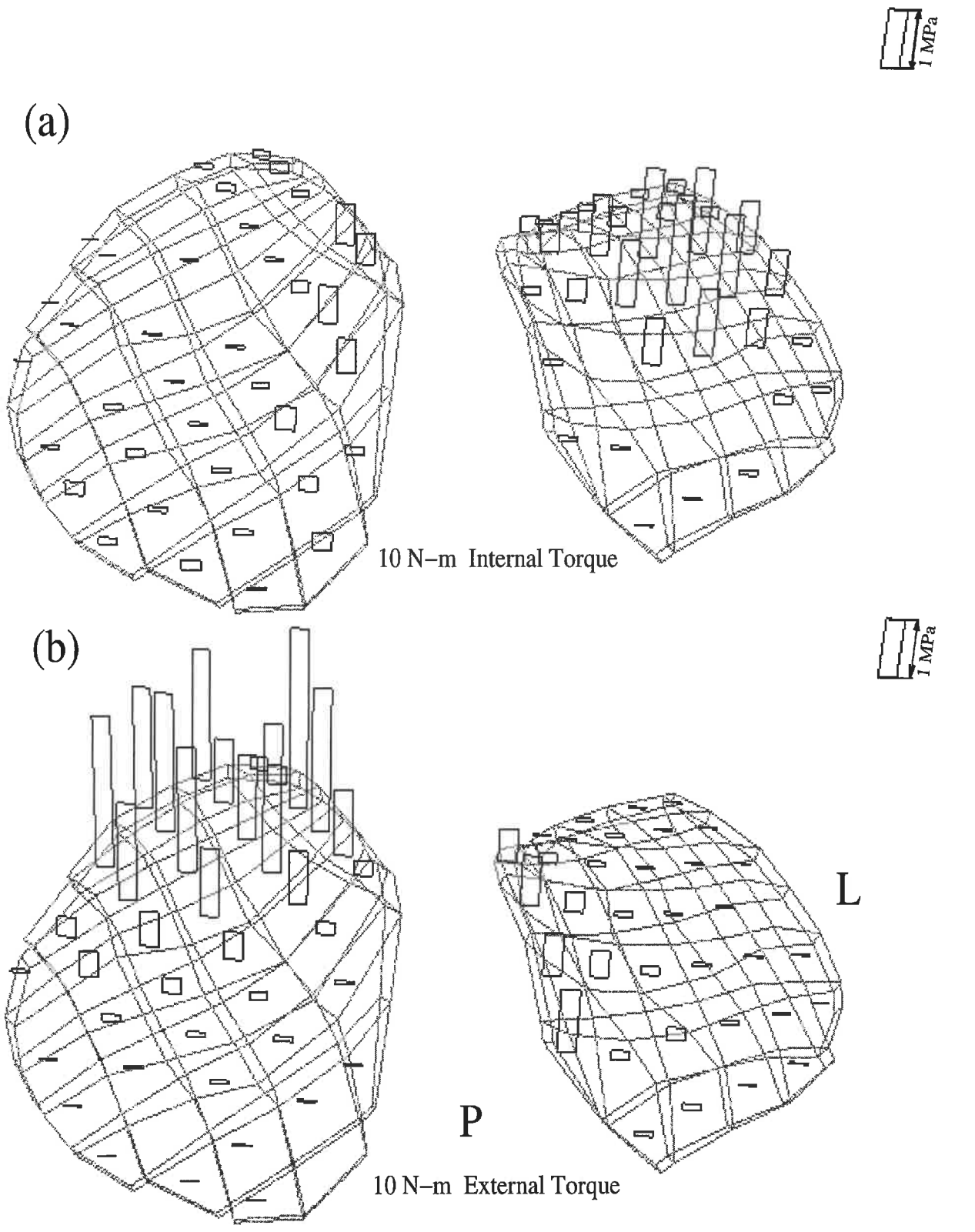

Figure 3.22: Principal compressive stresses in centroid of tibial cartilage elements for the intact joint with varus-valgus rotation fixed (TY=0), (a) 10 N-m Internal torque, (b) 10 N-m External torque. Elements with no stress bar are in low tension.

CHAPTER IV

DISCUSSION

4.1 Introduction

In this study, a realistic three-dimensional model of the entire human knee joint including femur, tibia, patella, cartilage layers, menisci, and joint ligaments developed by Bendjaballah et al. (1995) along with a nonlinear finite element package program (Shirazi-Adl et al., 1986, 1989-b) were used to investigate the response of tibiofemoral joint, neglecting the patellofemoral joint, at full extension under internal-external torques. To the author's best knowledge, such a model describing interactions between femur, tibia, menisci and ligaments is the only one available in the literature. In the finite element modeling of the joint, Bendjaballah et al. (1995) gave special attention to the precise reconstruction and discretization of the menisci and articular cartilage surfaces, knowing their relative importance in joint biomechanics. The finite element discretization of the knee joint model accounted for the articular surfaces needed for the nonlinear contact analysis, the composite (non-homogeneous) nature of the menisci, the wrapping of the medial collateral ligament around proximal tibia and various other ligaments. In this study, the level of mesh refinement appears to be adequate, nevertheless a more refined discretization of the cartilage articular surfaces could improve the contact modeling as well the prediction of stresses in the cartilage layers. Although, the articular cartilage, the meniscal tissue and ligaments exhibit a time-dependent, viscoelastic behavior under an applied load, the present study considered the elastostatic response only in which the transient response, the viscoelasticity and fluid movements of these tissues are neglected. Thus, the model

is best suited for short term quasi-static loadings. The author would like to emphasize the fact that the material properties were taken from the literature, hence, changes in these properties as well as joint geometry may affect the predictions but the conclusions of the work are not expected to be influenced. Moreover, the ligament initial strains were estimated from the literature. Although the variability of these parameters between individual knee joints is expected to be fairly high, such variations might influence the predicted results but not the general conclusions of this work. Furthermore, it is important to note that the absence of the joint capsule in the present model could affect the predicted laxities and ligament forces. As for the boundary conditions, it is important to emphasize that in this work, the femur was loaded while the tibia was left fixed which is the contrary to what often is taken in experimental studies. These different boundary conditions might have some effects on the predicted results, the extent of which is not yet determined. Besides, in the literature except for Askew et al. (1988) and Blankevoort et al. (1988), the experimental studies of the response of the knee joint in axial torque have often overlooked the coupled varus-valgus rotations. Because of the multi-compliant articulation of the knee joint, a more convergent contact algorithm was used to perform the present nonlinear finite element analysis which allowed some penetrations of contacting bodies into each other.

4.2 Analysis and comparison of predictions with previous works

It needs to be noted that all of the experimental studies on the biomechanics of the knee joint in axial rotation considered the femur fixed and applied the torque on the tibia, which is the opposite of what was performed in this study. Thus, in the literature, *internal* or *external* rotation refers to *internal tibial* or *external tibial*

rotation, respectively. However, in this study, *internal* or *external* rotation refers to *femoral internal* or *femoral external* rotation, respectively.

4.2.1 Kinematics of the tibiofemoral joint in axial rotation

Figure 4.1 shows that internal torques of 10 N-m applied to the intact tibiofemoral joint with varus-valgus rotation fixed, result in internal rotations of 22^o at full extension. With the varus-valgus rotation fixed, the same load of 10 N-m of external tibial torque has been reported to result in external rotations of the tibia of about 10^o to 15^o at full extension (Lipke et al., 1981; Markolf et al., 1976). Similarly, external torques of 10 N-m result in external rotations of 22^o at full extension, while rotations of 10^o (Markolf et al., 1976; Piziali et al., 1980) and up to 25^o (Lipke et al., 1981; Shoemaker and Markolf, 1985) have been reported by others (see Figure 4.1). With the varus-valgus rotation left free, the total axial rotary laxity at $\pm$ 3 N-m, i.e. the total amount of axial rotation between the limits of 3 N-m of internal torque and 3 N-m of external torque, is computed to be 26^o which is although higher than the average value for four specimens (18.5^o) reported by Blankevoort et al. (1988), it is very close to their largest value of 25^o. Figures 4.2 and 4.3 compare the internal-external rotations and the coupled varus-valgus rotations, respectively, with those reported by Askew et al. (1988) for the intact knee at full flexion with the varus-valgus rotation free under applied internal-external torques. Taking in consideration that the present tibiofemoral joint model has an initial flexion angle of approximately 5^o, the predictions, hence, show a reasonable agreement between our results and the ones obtained by Markolf et al. (1976) and Askew et al. (1988). Although the results obtained by Bach et al. (1995) (shown in Figure 4.1) are for the case where the flexion angle is 15^o, they give an idea about the scatter in the axial rotary laxity values published in

the literature due to smallness of samples studied, the variations in the specimens, and the lack of precision in the measurements.

During internal rotation with the varus-valgus rotation fixed, of all the primary ligaments (ACL, LCL, MCL and PCL), isolated sectioning of only the LCL or the MCL yields a significant increase in internal rotary laxity. At full extension, the anterior cruciate ligament plays a minor role in the restraint of internal rotation while the posterior ligament is completely ineffective. These predictions are in accordance with the results of the ligament forces in which the PCL does not carry any load during any level of internal torque higher than 0.5 N-m and the tensile force in the ACL is less than 40 N during the whole loading (see Figure 3.11). The literature agrees with our results in that the MCL is a major restraint to the external rotation of the tibia (Ahmed et al., 1987; Lewis et al., 1985; Markolf et al., 1976; Seering et al., 1980) and that the external rotational laxity of the tibia is significantly increased only when the posterolateral structures and/or the lateral collateral ligaments are cut (Grood et al., 1988; Lipke et al., 1981; Shoemaker and Markolf, 1976).

During external rotation and with the varus-valgus rotation fixed, our study shows that sectioning of only the LCL results in a significant increase in the external rotary laxity. This is in contrast with experimental results reported in the literature (Lipke et al., 1981; Markolf et al., 1976; Piziali et al., 1980; Shoemaker and Markolf, 1985). These authors reported that only the sectioning of the MCL or the ACL that causes increases in internal laxity of the tibia.

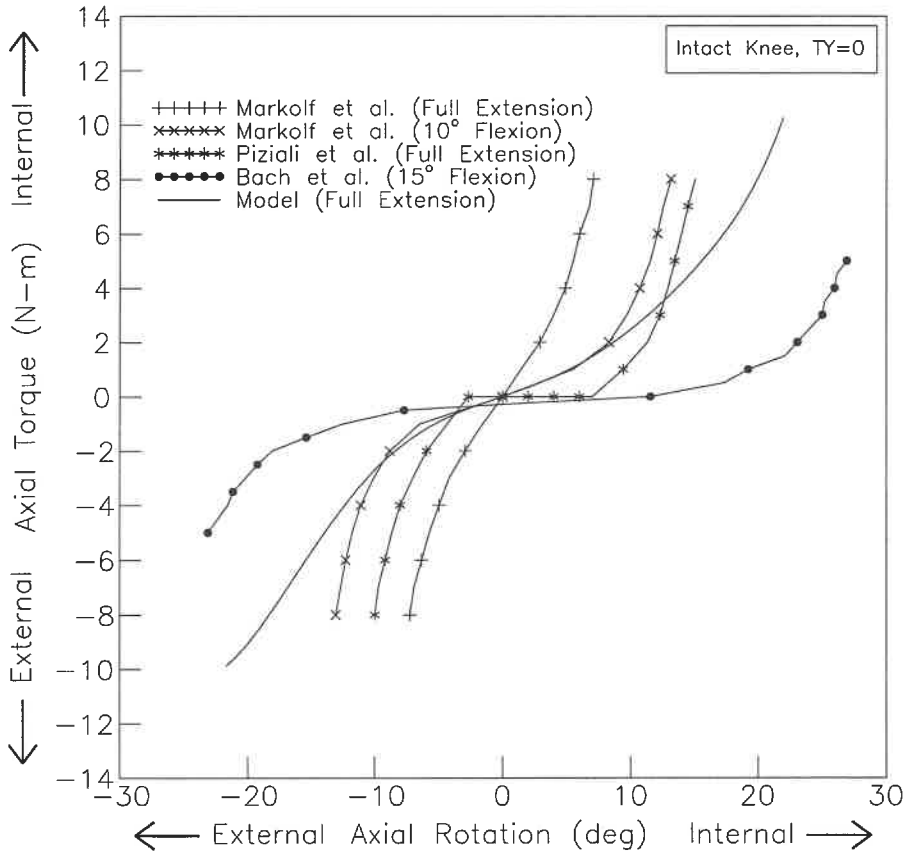

Figure 4.1: Comparison of the internal-external torque-rotation of the knee at full extension with the varus-valgus rotation fixed (TY=0).

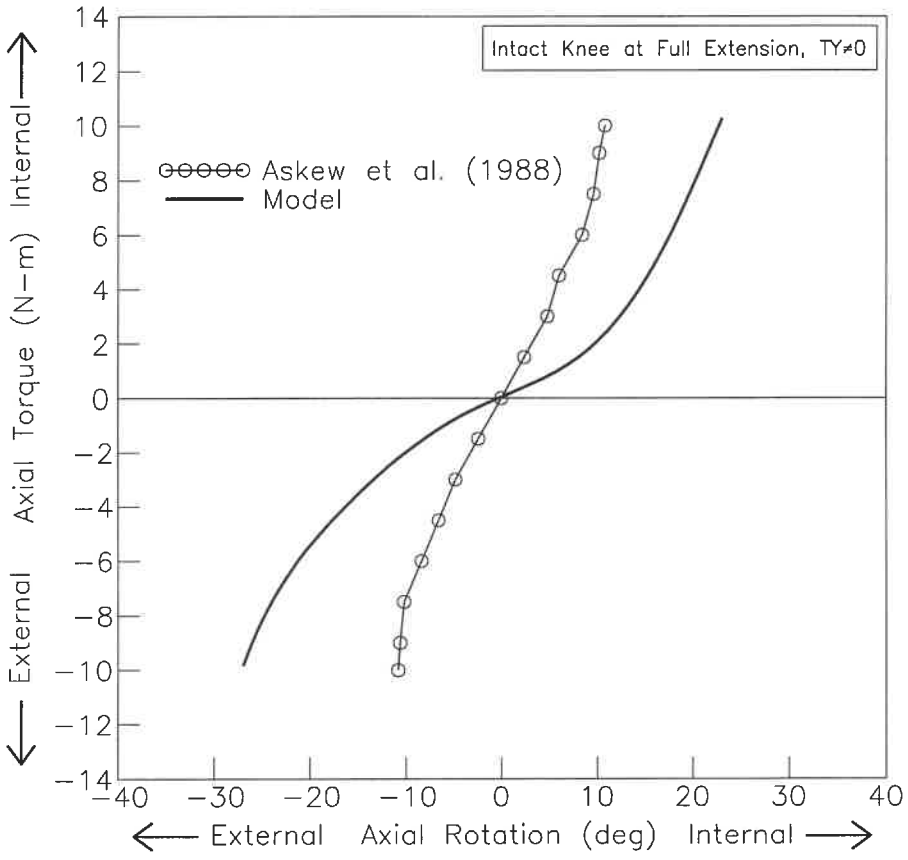

Figure 4.2: Comparison of the internal-external torque-rotation of the knee at full extension with the varus-valgus rotation free (TY≠0).

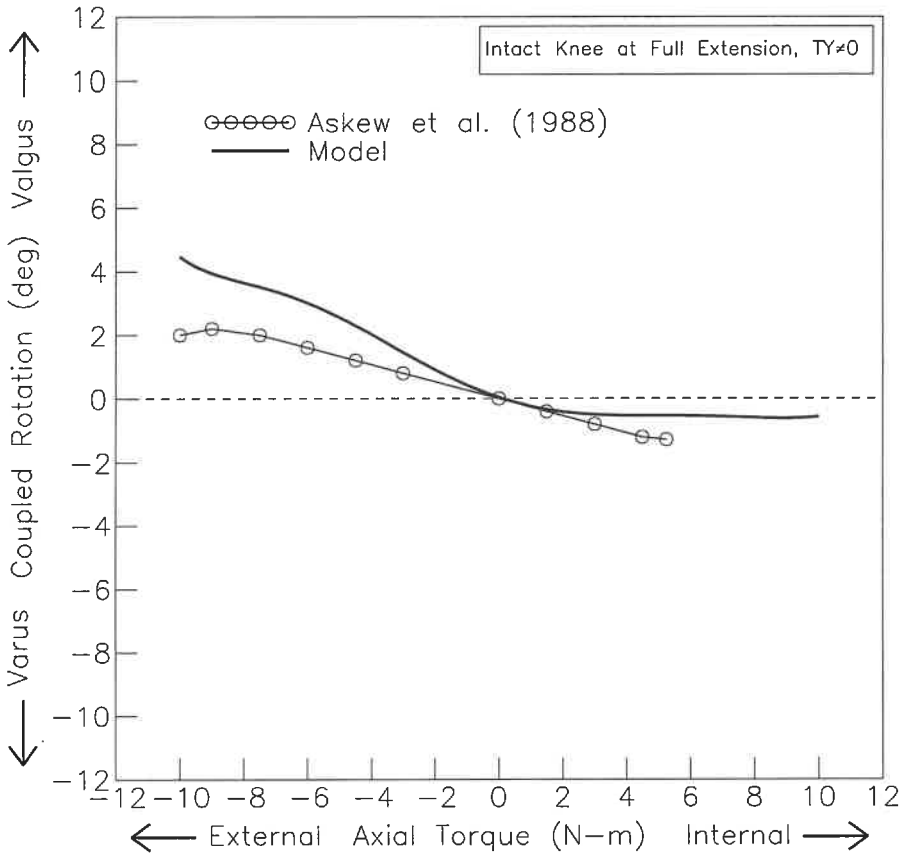

Figure 4.3: Comparison of the coupled varus-valgus rotation of the knee at full extension under internal-external torques.

4.2.2 Role of the primary ligaments in axial rotation

Although, the above mentioned authors were able to determine the relative load-transmitting roles of the ligaments under the applied load, the tensions generated in the individual ligaments, and hence their specific mechanical responses, could not often be determined. Our results for the forces in the ACL during internal-external torques with the varus-valgus rotation fixed are in general agreement with the results reported by Markolf et al. (1990) (see Figure 4.4).

It is interesting to note that the ACL and the PCL are interdependent during external rotation since the sectioning of one causes a large drop in the tensile force of the other (Figures 3.16 and 3.15). Hence, the effects of one ligament cannot be determined in the absence of the other. Figure 3.11 shows that the ACL and PCL are both loaded in external rotation and not in internal rotation, a behavior that is primarily due to the orientation of these ligaments. In comparison with collaterals in the joint under axial torque, the cruciates are at a disadvantage due to smaller lever arms whereas at an advantage due to their more inclined orientation.

This is the first study that determines the ligament forces with the varus-valgus rotation left free. Hence, no published data are available for comparison. However, it is interesting to note that during internal torque, setting the varus-valgus rotation free generates only minor changes in the distribution of tensile forces in the ligaments. Nevertheless, during external torque, some major changes were produced due to the unrestraint of the varus-valgus rotation. Indeed, these results underline the important effects of the coupled varus-valgus rotation parameter on the ligament tension response. Additional tests, in which the individual sectioning of the ligaments during internal-external torques with varus-valgus rotation left free, are planned to be

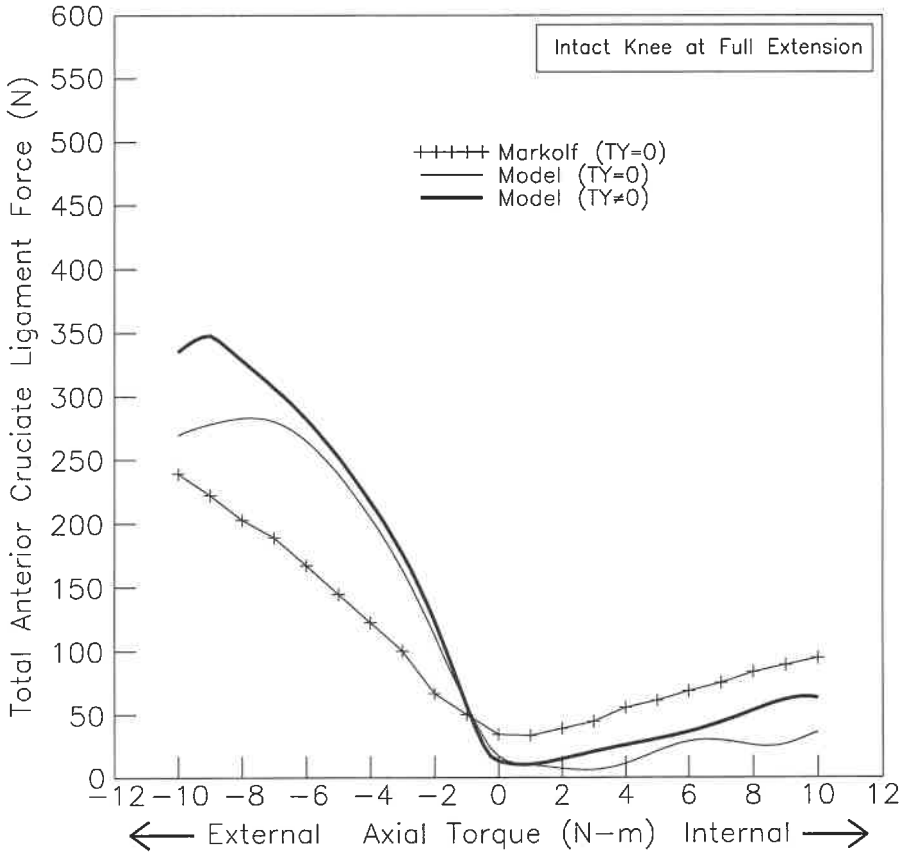

Figure 4.4: Comparison of the total force in the ACL under internal and external torques applied at full extension.

performed in the near future. The tensile forces in collaterals are directly influenced by the presence or absence of coupled varus-valgus (TY) rotations. This is evident when comparing Figures 3.11 and 3.12 accounting for the coupled rotations given in Figure 3.5.

The compressive preload of 1000 N causes a sharp decrease in the primary laxity. This is in agreement with the results of Wang et al. (1974) who reported that a compressive preload of 1000 N applied to the knee joint at 25^o of flexion caused the reduction of the primary laxity, defined as the rotation for a low torque of $\pm$ 0.5 N-m, to 20 % of that at zero axial Load. In our case, the compressive preload of 1000 N causes a reduction of the primary laxity to 25 % of that at zero axial load. Moreover, the total torsional laxity (between $\pm$ 10 N-m) was decreased approximately by 12% in presence of a compressive preload of 1000 N which is in agreement with the results of Shoemaker and Markolf (1985) who reported that an application of 925 N of axial joint load caused a 16% decrease in the total torsional laxity (between $\pm$ 10 N-m). Our results also show that the compressive preload causes a decrease in all ligament forces with the exception of the tensile force in the ACL which is in agreement with the findings of Markolf et al. (1990) who reported that the joint load did not act to protect the ACL from high forces that are generated by applied internal or external tibial torque. This might be due to the fact that the compressive preload causes the femur to translate posteriorly (about 3 mm coupled posterior translation at 0 N-m and 1000 N compressive force) generating higher tensile forces in the ACL.

4.2.3 Mechanics of load transmission in axial rotation

In the present complex multibody contact problem, the analysis predicts the regions of contact as well as the transmitted contact force at each node with its target element

on the opposing surface. The orientation of the contact surface varies from one region to another depending on the spatial geometry of proximal articulating surfaces of tibial cartilage and menisci. Analysis of predicted results at each load step verifies the equilibrium of external and internal loads, accounting for the ligamentous forces as well.

To the author's best knowledge, this is the first study that determines the contact regions and computes the forces transferred through the various contact areas of the tibiofemoral joint under internal-external torques. At 10 N-m of internal torque, the medial and lateral compartments share the generated axial load of 437 N at ratios of 25 % and 75 %, respectively. On the other hand, during external torque, the medial and lateral compartments share the generated axial load of 689 N at ratios of 88% and 12%, respectively. During internal rotation, the lateral meniscus carries a larger portion generated axial load (122 N) than does its counterpart (67 N); on the other hand, during external rotation the medial meniscus carries a larger axial load (87 N) than does the lateral one (41 N).

Analysis of the contact forces and regions on tibial plateaus and stresses at the centroid of tibial cartilage layers (Figure 3.22) indicates that during internal rotation, the covered cartilage is loaded primarily in the region located centrally and laterally at the lateral plateau; however, the uncovered cartilage is primarily loaded in the region located posteriorly and laterally at the medial plateau. On the other hand, during external rotation, the uncovered cartilage is mainly loaded in the region located near the medial tibial spine; however, the covered cartilage is mainly loaded in the region located posteriorly and medially at the lateral plateau.

4.3 Clinical implications

In this study, the determination of the axial rotary laxity and the tensile forces in the primary ligaments of the tibiofemoral joint provides a quantitative basis for the evaluation of the changes likely to be found during the examination of knees with ligament disruption. It is very important to determine the magnitude of change in the femoral axial rotation as well as in the total resultant ligament forces because it is these magnitudes that are often the basis of the clinical diagnosis.

Our results show that when any primary ligament is sectioned, the tibiofemoral joint becomes more lax during internal-external torques. Furthermore, these results do delineate the expected magnitude of change in either rotary laxity or ligament forces due to a ligament disruption. Indeed, sectioning of one or both cruciate ligaments in full extension without coupled varus-valgus rotation produces only minor changes in torsional laxity which would most likely not be detectable in a clinical examination. On the other hand, our findings after sectioning of the LCL during internal-external torques with the varus-valgus rotation of the femur fixed, indicate that the LCL is the most important ligament in resisting axial rotation. When the LCL is sectioned, axial rotary laxity increases by 15 degrees and 10 degrees in full extension at 9 N-m and 6 N-m of external and internal torques, respectively. However, after sectioning of the MCL during internal-external torques with varus-valgus rotation fixed, our results indicate that the MCL is important in limiting only the internal rotation since axial rotary laxity increases by 14 degrees and only 1.6 degrees in full extension at 10 N-m of internal and external torques, respectively.

As far as the change in the magnitude of the tensile forces in the ligaments upon selective sectioning of particular ligaments, our findings indicate that sectioning of

the LCL results in large increases in the ACL and PCL forces during external torque. Indeed, at 9 N-m of external torque, the ACL and PCL tension forces computed in response to the sectioning of the LCL are evaluated to be approximately 577 N and 501 N, respectively. The high loads in both cruciate ligaments are generated to account for the loss of the LCL. Although, knowing that the ACL fails at an average load of 1730 N for the younger humans and only 734 N for the older group (Noyes and Grood, 1976), this appears to leave some reserve for the ACL protection in the younger humans but external torques higher than 10 N-m, may cause serious damage to the ACL of the older population (older than 47 years). Similarly, the sectioning of the MCL generated a high tensile force of 580 N in the LCL under 10 N-m of internal torque. Therefore, the risk of failure of the ACL in axial torque is substantially increased when either of the collateral ligaments are damaged. It is important to note that such high forces are obtained during only one type of loading (axial torque in this case) and hence, combined loading conditions (e.g., combined anterior-posterior translations and axial torque) are expected to generate a much complex ligamentous response pattern yielding much higher tensile forces in the ACL. Moreover, our results suggest that near extension, the forces that are generated in the four primary ligaments, particularly in the cruciates, are relatively high during external torque which might explain some of the ligamentous injuries during skiing. Indeed, external femoral torque when knee is near extension can be produced when a skier crosses the tips of the skis and the upper part of the body is thrust forward over an extended knee (Markolf et al., 1990).

CHAPTER V

CONCLUSIONS

In this work, a realistic three-dimensional model of the entire human knee joint including femur, tibia, patella, cartilage layers, menisci, and joint ligaments along with a nonlinear finite element package program were used to investigate the response of the tibiofemoral joint, neglecting the patellofemoral joint, at full extension under internal-external torques of up to 10 N-m applied to the femur. For the sake of validation of the model predictions, the load applications and boundary conditions were set to be as close as possible to those in experimental studies. The tibia was fixed while the femur was free to translate in the proximal-distal, medial-lateral, and anterior-posterior directions; the internal-external rotation was left free, the varus-valgus rotation was first fixed and then left free while flexion-extension rotation was maintained fixed throughout the analyses.

The model was used to isolate and assess the role of the major ligaments (cruciates and collaterals) in resisting internal-external torques, with and without axial compression force, at full extension by analyzing and comparing changes in the femoral axial rotation as well as in the total resultant ligament forces upon selective sectioning of particular ligaments. Our results have shown at full flexion with the varus-rotation fixed, the collateral ligaments (LCL and MCL) were the major restraints to internal rotation; however, only the LCL played a major role in resisting external torque. Moreover, our findings suggested that the ACL and the PCL are interdependent (sectioning of one caused a large drop in the tensile force of the other) during external rotation and that the PCL is completely lax during internal rotation. Setting the

varus-valgus free was shown to generate some major changes in the distribution of the ligaments tensile forces only during external rotation. Although, no tests, in which the individual sectioning of the ligaments during internal-external torques with the varus-valgus rotation left free, were performed in this study but it is expected that the results could yield somewhat different conclusions as far as the role of the ligaments, particularly during external torque, are concerned. Furthermore, the compressive preload of 1000 N caused a major reduction in the axial rotary laxity during applied torques of ± 0.5 N-m and some decreases in all ligaments tensile forces with the exception of the tensile force in the ACL.

The model was also used to predict the regions of contact and to determine the contact forces transmitted through the femur/meniscus, femur/tibia, and meniscus/tibia contact regions at both lateral and medial compartments as internal-external torques were applied to the intact tibiofemoral joint. The results obtained implied that during internal rotation, the lateral meniscus carried a larger axial load than did its counterpart; on the other hand, during external rotation the medial meniscus carried a larger axial load than did the lateral one. Analysis of the contact forces and regions on the tibial plateaus and stresses at the centroid of tibial cartilage layers suggested that during internal rotation, the covered cartilage was loaded primarily in the region located centrally and laterally at the lateral plateau; however, the uncovered cartilage was primarily loaded in the region located posteriorly and laterally at the medial plateau. On the other hand, during external rotation, the uncovered cartilage was mainly loaded in the region located near the medial tibial spine; however, the covered cartilage was mainly loaded in the region located posteriorly and medially at the lateral plateau.

In general, the predictions of the present study were found to be in a reasonable agreement with the experimental results available in the literature describing the kinematics and role of the ligaments in axial rotation. Moreover, it is important to emphasize the fact that the present model describing interactions between femur, tibia, menisci and ligaments is the only one available in the literature. The previous analytical studies have not taken into account some of the mechanical features essential for a realistic non-linear elastostatic model study of the knee joint. Hence, the present model offers a number of advantages over existing analytical models in that its finite element discretization accounted for the articular surfaces needed for the non-linear contact analysis, the composite (non-homogeneous) nature of the menisci, the wrapping of the medial collateral ligament around proximal tibia and various other ligaments. Moreover, the level of mesh refinement of the present model appeared to be adequate, nevertheless a more refined discretization of the cartilage articular surfaces could improve the contact modeling as well as the prediction of stresses in the cartilage layers. However, the present model is best suited for short term quasi-loadings since it considered only the elastostatic response of the knee in which the transient response, the viscoelasticity and fluid movements of these tissues were neglected. Furthermore, the material properties and the ligament initial strains were taken from the literature, hence, changes in these parameters as well as joint geometry may affect the predictions but the conclusions of the work are not expected to be influenced. In addition, the absence of the joint capsule in the present model and the different boundary conditions (the tibia was fixed while the femur was loaded) could affect the predicted results. Due to the multi-compliant articulation of the knee joint, a more convergent contact algorithm was used to perform the present nonlinear finite element analysis which allowed some penetrations (less than 1,6 mm).

The knowledge gained in the course of this research is expected to enhance our understanding of the biomechanics of the tibiofemoral joint, particularly the function of the ligaments in axial rotation, which will then be beneficial in the total knee arthroplasty, prosthetic ligament replacement as well as knee ligament injuries treatment and prevention.

Furthermore, the relative accuracy of the present model under the single load conditions considered so far suggests future studies to explore the role of the ligaments and the mechanics of load transmission of the joint including the patellofemoral articulation at different flexion angles and under combined loading conditions to establish the functional mechanism of the knee joint in general and to clarify the criteria for the clinical assessment of complex ligamentous and meniscus injuries in particular.

REFERENCES

ABDEL-RAHMAN, E. and HEFZY, M.S. (1993). Three-dimensional dynamic modeling of the tibio-femoral joint. *ASME Advances in Bioengineering*, 26, 315-318.

ADINA. (1992). A finite element program for automatic dynamic incremental nonlinear analysis. Report ARD 92-8, ADINA Engineering, Watertown, MA 02172.

AHMED, A.M. and BURKE, D.L. (1983). In-vitro measurement of static pressure distribution in synovial joints - Part I: Tibial surface of the knee. *Journal of Biomechanical Engineering*, 105, 216-225.

AHMED, A.M., BURKE, D.L. and HYDER, A. (1986). Effect of tibial prerotation on the ligamentous response of the flexed knee to passive anterior shear. *Trans. Orthoped. Res. Soc.*, 1, 127.

AHMED, A.M., HYDER, A., BURKE, D.L. and CHAN, K.H. (1987). In-vitro Ligament tension pattern in the flexed knee in passive loading. *Journal of Orthopeadic Research*, 5, 217-230.

ANDRIACCHI, T.P., MICKOSZ, R.P., HAMPTON, S.J. and GALANTE, J.O. (1983). Model studies of the stiffness characteristics of the human knee joint. *Journal of Biomechanics*, 16, 23-29.

ARMS, S.W., POPE, M.H., JOHNSON, R.J., FISCHER, R.A., ARVIDSSON, I. and ERIKSSON, E. (1984). The biomechanics of anterior cruciate ligament rehabilitation and reconstruction. *American Journal of Sports Medicine*, 12, 8-18.

ASKEW, M.J., MELBY III, A. and BROWER, R.S. (1988). Knee Mechanics: A review of *in vitro* simulations of clinical laxity tests. In: Articular cartilage and knee

joint function: Basic science and arthroscopy, edited by J.W. Ewing. Raven Press, Ltd., New York, 249-266.

ATESHIAN, G.A., KWAK, S.D., SOSLOWSKY, L.J. and MOW, V.C. (1994). A stereophotogrammetric method for determining *in situ* contact areas in diarthrodial joints, and a comparison with other methods. *Journal of Biomechanics*, 27, 111-124.

BACH, J.M., PATTERSON, H.A. and HULL, M.L. (1995). Direct measurement of strain in the posterolateral bundle of the ACL. *BED Advances in Bioengineering*, 31, 215-216.

BARRY, D. and AHMED, A.M. (1986). Design and performance of a modified buckle transducer for the measurement of ligament tension. *Journal of Biomechanical Engineering*, 108, 149-152.

BATHE, K.J. and CHAUHDARY, A. (1984). On Finite element analysis of large deformation frictional contact problems. In: *Unification of finite element methods, finite differences, and calculus of variations*, edited by Kardestuncer, H., North-Holland, Amsterdam.

BENDJABALLAH, M.Z., SHIRAZI-ADL, A. and ZUKOR, D. (1995). Biomechanics of the human knee joint in compression: reconstruction, mesh generation and finite element analysis. *The Knee*, 2, 66-79.

BLACK, J. (1988). Orthopeadic biomaterials in research and practice. Churchill Livingstone, New York.

BLANKEVOORT, L., HUISKES and De LANGE, A. (1988). The envelope of passive knee joint motion. *Journal of Biomechanics*, 21, 705-720.

BLANKEVOORT, L., KUIPER, J.H., HUISKES, R. and GROOTENBOER, H.J. (1991). Articular contact in a three-dimensional model of the knee. *Journal of Biomechanics*, 24, 1019-1031.

BLANKEVOORT, L. and HUISKES, R. (1991). Ligament-bone interaction in a three-dimensional model of the knee. *ASME Journal of Biomechanical Engineering*, 113, 263-269.

BRANTIGAN, O.C. and VOSHELL, A.F. (1941). The mechanics of ligaments and menisci of the knee joint. *Journal of Bone and Joint Surgery (Am)*, 23, 44-66.

BROWN ,T.D. DIGIOIA, A.M. and MEARS, D.C. (1983). A contact coupled non-linear finite element analysis of the hip joint. *Trans.* 29^{th} *Ann. Meeting ORS*, 8, 66.

BROWN, T.D. and SHAW, D.T. (1984). In vitro contact stress distribution of the femoral condyles. *Journal of Orthopeadic Research*, 1, 190-199.

BULLOUGH, P.G., MUNUERA, L., MURPHY, J. and WEINSTEIN, A.M. (19970). The strength of the menisci of the knee as it relates to their fine structure. *Journal of Bone and Joint Surgery (Br)*, 52, 564-570.

BUTLER, D.L., KAY, M.D. and STOUFFER, D.C. (1986). Comparison of material properties in fascil-bone units from human patellar tendon and knee ligaments. *Journal of Biomechanics*, 19, 425-432.

BYLSKI-AUSTROW, D., CIARELLI, M.J. and KAYNER, D.C (1994). Displacements of the menisci under joint load: an in vitro study in human knees. *Journal of Biomechanics*, 27, 421-431.

CHEN, E.H. and BLACK, J. (1980). Materials design analysis of the prosthetic anterior cruciate ligament. *Journal of Biomedical Materials Research*, 14, 567-586.

CROWNINSHIELD R., POPE, M.H and JOHNSON, R.J. (1976). An analytical model of the knee. *Journal of Biomechanics*, 9, 397-405.

DANIEL

DOWSON, D. (1981). Basic tribology. In: Dowson, D., Wright, V., eds. *Introduction to the biomechanics of joints and joint motion.* London: Institute of Mechanical Engineering, 49-60.

DUVAL, P. (1989). Cractérisation des propriétés mécaniques des ménisques du genou à l'état normal et irradié. Mater Thesis, École Polytechnique de Montéal.

EDIXHOVEN, Ph., HUISKES, R., de GRAAFF, R., van RENS, Th.J.G. and SLOOFF, T.J. (1987). Accuracy and reproductibility of instrumented knee-drawer tests. *J. Orthop. Res.*, 5, 378-387.

EDWARDS, R.G., LAFFERTY, J.F. and LANGE, K.O. (1970). Ligament strain in the human knee joint. *Journal of Basic Engineering*, 92, 131-136.

ESSINGER, J.R., LEYVRAZ, P.F., HEEGARD, J.H. and ROBERTSON, D.D. (1989). A mathematical model for the evaluation of the behaviour during flexion of condylar-type knee prostheses. *Journal of Biomechanics*, 22, 1229-1241.

EWING, J.W. (1989). Articular cartilage and knee joint function. In: *Basic science and arthroscopy*, New York, Raven Press.

FITHIAN , D.C., SCHMIDT, M.B., RATCALFE, A. and MOW, V.C. (1989). Human meniscus tensile properties: Regional variation and biomechanical correlation. *Trans. 35^{th} Ann. Meeting ORS*, 14, 205.

FITHIAN, D.C., KELLY, M.A. and MOW, V.C. (1990). Material properties and structure-function relationships in the menisci. *Clin. Orthop. Rel. Res.*, 252, 19-31.

FRANKEL, V.H., BURSTEIN, A.H., and BROOKS, D.B. (1971). Biomechanics of internal derangement of the knee. *Journal of Bone and Joint Surgery (Am)*, 53, 53, 945-962.

FRANKEL, V.H and NORDIN, M. (1980). Biomechanics of the knee, in *Basic Biomechanics of the Skeletal System*, Frankel, V.H. and Nordin, M., Eds., Lea & Febiger, Philadelphia, 113-148.

FUKUBAYASHI, T. and KUROSAWA, H. (1980). The contact area and pressure distribution pattern of the knee. *Acta Orthoped. Scand.*, 51, 871-879.

GALBRAITH, PC. and BRYANT, J.T. (1989). Effects of grid dimensions on finite element models of an articular surface. *Journal of Biomechanics*, 22, 385-393.

GARG, A. and WALKER, P.S. (1989). Prediction of total knee motion using a three-dimensional computer-graphics model. *Journal of Biomechanics*, 23, 45.

GIRGIS, F.G., MARSHALL, J.L., and AL MONAJEM, A.R.S. (1975). The cruciate ligaments of the knee joint: anatomical, functional and experimental analysis. *Clin. Orthop.*, 106, 216-231.

GOODFELLOW, J.W. and O'CONNOR, J.J. (1978). The mechanics of the knee and prosthesis design. *Journal of Bone and Joint Surgery (Br)*, 60, 358.

GRAY, H. (1973). Anatomy of the human body. Lea & Febiger, Philadelphia.

GROOD, E.S. and HEFZY, M.S. (1982). An analytical technique for modeling knee joint stiffness. Part I: Ligamentous forces. *Journal of Biomechanical Engineering*, 104, 330-337.

GROOD, E.S., SUNTAY, W.J., NOYES, F.R. and BUTLER. (1984). Biomechanics of the knee extension exercise. *Journal of Bone and Joint Surgery (Am)*, 66, 5.

GROOD, E.S., STOWERS, S.F. and NOYES, F.R. (1988). Limits of movement in the human knee. *Journal of Bone and Joint Surgery (Am)*,70, 88-97.

HAINAULT, K. (1974). *Intoduction à la biomécanique*, Librairie Maloine.

HAYES, W.C. and MOCKROS, L.F. (1971). Viscoelastic properties of human articular cartilage. *Journal of Applied Physiology*, 31, 562-568.

HAYES, W.C., KEER, L.M. and MOCKROS, L.F. (1972). A mathematical analysis for indentation tests of articular cartilage. *Journal of Biomechanics*, 5, 541-551.

HEFZY, M.S. and GROOD, E.S. (1983). An analytical technique for modeling knee joint stiffness. Part II: Ligamentous geometric nonlinearities. *Journal of Biomechanical Engineering*, 105, 145-153.

HEFZY, M.S., GROOD, E.S. and ZOGHI, M. (1987). An axisymmetric finite element model of the menisci. *ASME Advances in Bioengineering*, 57-62.

HEFZY, M.S. and YANG, H. (1993). Three-dimensional anatomical model of the patello-femoral joint. *ASME Advances in Bioengineering*, 26, 329-332.

HIROKAWA, S. (1991). Three-dimensional mathematical model analysis of the patellofemoral joint. *Journal of Biomechanics*, 24, 659-671.

INSALL, J.N. (1984). Disorders of the patella. In: Insall J.N., ed. *Surgery of the knee*. New York. Churchill Livingstone, 191-303.

KAPANDJI, I.A. (1970). *The physiology of the joints.* Vol. 2. Lower Limb. Edinburgh, London, and New York, Churchill livingstone, from the French, Phisiologie Articulaire, Librane Malone, Paris.

KENNEDY, J.C. and FOWLER, P.J. (1971). Medial and anterior instability of the knee: an anatomical and clinical study using stress machines. *Journal of Bone and Joint Surgery (Am)*, 53, 1257.

KENNEDY, J.C., HAWKINS, R.J. and WILLIS, R.B. (1977). Strain gauge analysis of knee ligaments. *Clin. Orthop.*, 129, 225-229.

KETTELKAMP, D.B. and JACOBS, A.W. (1972). Tibiofemral contact area determination and implications. *Journal of Bone and Joint Surgery (Am)*, 54, 349-356.

LEWIS, J.L. and SHYBUT, G.T. (1981). In vivo forces in the collateral ligaments of canine knees. *Trans. Orthop. Res. Soc.*, Las Vegas. 6, 4.

LEWIS, J.L., LEW, W.D. and SCHMIDT, J. (1982). A note on the application and evaluation of the buckle transducer for knee ligament force measurement. *ASME Journal of Biomechanical Engineering*, 104, 125.

LEWIS, J.L., LEW, W.D., SHYBUT, G.T., JASTY, M. and HILL, J.A. (1985). Biomechanical function of the knee ligaments. In: Finerman, G., ed. *AAOS Symposium on sports medicine-the knee.* St. Louis: C.V. Mosby, 152-168.

LIN, H-C. KWAN, M.K-W. and WOO, S.L-Y. (1987). On the stress relaxation properties of anterior cruciate ligament (ACL). *Advances in Bioengineering*, 3, 5-6.

LIPKE, J.M., JANECKI, C.J., NELSON, C.L. et al. (1981). The role of incompetence of the anterior cruciate and lateral ligaments in anterolateral and anteromedial instability. *Journal of Bone and Joint Surgery (Am)*, 63, 954-960.

LIPSHITZ, H. and GLIMCHER, M.J. (1979). In vitro studies of the wear of articular cartilage. *Wear*, 52, 297-339.

LITTLE, E.B., WEVERS, H.W., SIU, D. and COOKE, T.D.V. (1986). A three dimensional finite element analysis of the upper tibia. *ASME Journal of Biomechanical Engineering*, 108, 111-119.

LOCH, D.A., LUO, Z., LEWIS, J.L. and STEWART, N.J. (1992). A theoretical model of the knee and ACL: theory and experimental verification. *Journal of Biomechanics*, 25, 81.

MALCOLM, L.L. (1976). An experimental investigation of the frictional and deformational responses of articular cartilage interface and dynamic loading. Ph.D. Thesis, University of California, San Diego.

MAQUET, P.G., VAN De BERG, A.J. and SIMONET, J.C. (1975). Femorotibial weight-bearing areas. *Journal of Bone and Joint Surgery (Am)*, 57, 766-771.

MAQUET, P.G. and PELZER, G.A. (1977). Evolution of the maximum stress in osteo-arthritis of the knee. *Journal of Biomechanics*, 10, 107-117.

MARKOLF, K.L., MENSCH, J.S. and AMSTUTZ, H.C. (1976). Stiffness and laxity of the knee-the contributions of the supporting structures. *Journal of Bone and Joint Surgery (Am)*, 58, 583-594.

MARKOLF, K.L., GRAFF-RADFORD, A. and AMSTUTZ, H.C. (1978). In vivo Knee stability. *The Journal of Bone and Joint Surgery (Am)*, 60, 664.

MARKOLF, K.L. (1985). A summary of of knee stability measurements. In : Finerman G., ed. *AAOS Symposium on sports medicine-the knee.* St Louis: CV Mosby, 87-93.

MARKOLF, K.L., GOREK, J. and KABAO, J.M. (1990). Direct measurement of resultant forces in the anterior cruciate ligament. *The Journal of Bone and Joint Surgery (Am)*, 72, 557-567.

MOEINZADEH, M.H., ENGIN, A.E. and AKKAS, N. (1983). Two-dimensional dynamic modeling of human knee joint. *Journal of Biomechanics*, 16, 253-264.

MOW, V.C. and MAK, A.F. (1986). Lubrication of diarthrodial joints. In: Shalak R., Chien S., eds. *Handbook of Bioengineering*, New York, McGraw-Hill, 5.1-5.34.

MOW, V.C., RATCALFE, A. and WOO, S. L-Y. (1990). *Biomechanics of diarthrodial joints*, vols. I & II. New York: Springer-Verlag.

MOW, V.C., RATCALFE, A., CHERN, K.Y., and KELLY, M.A. (1992). Structure and function relationships of the menisci of the knee. In: *Knee Meniscus: Basic and Clinical Foundations*, edited by Mow, V.C., Arnoczky, S.P., and Jackson, D.W. New York, Raven Press, Ltd., 37-57.

MÜLLER, W. (1983). The knee: form, function and ligament reconstruction. New York: Springer-Verlag.

NEWTON, P.O., McKENNA, D.A., KITABAYASHI, L.R., AKESON, W.H. and WOO, S.L-Y. (1990). Improved methodologies to differentiate the mechanical properties of the rabbit anterior cruciate ligament (ACL) and medial collateral ligament (MCL). *TRANS. of* 36^{th} *annual ORS*, 15, 509.

NEWTON, P.O., McKENNA, D.A., KITABAYASHI, L.R., AKESON, W.H. and WOO, S.L-Y. (1990). Biomechanical and ultrastructural changes in the rabbit anterior cruciate ligament (ACL) following immobilization. *TRANS. of* 36^{th} *annual ORS*, 15, 35.

NETTER, N.H. (1991). Atlas of human anatomy. CIBA-GEIGY Corporation, Summit, New Jersey.

NIWA, S., PERREN, S.M. and HATTORI, T. (1992). *Biomechanics in orthopedics*, Springer-Verlag, Tokyo.

NOYES, F.D. and GROOD, E.S. (1976). The strength of the anterior cruciate ligament in humans and rhesus monkeys. Age related and species changes. *Journal of Bone and Joint Surgery (Am)*, 58, 1074-1082.

NOYES, F.R., MOOAR, P.A., MATTHEWS, D.S and BUTLER, D.L. (1983). The symptomatic anterior cruciate deficient knee - Part I: The long term functional disability in athletically active individuals. *Journal of Bone and Joint Surgery (Am)*, 65, 154-162.

OLIVER J. and COUGHLIN L. (1987). Objective knee evaluation using the GENUCOM knee analysis system: clinical applications. *American Journal of Sports Medicine*, 15, 671-578.

PAUL, J.P. (1976). Force actions transmitted by joints in the human body. *Proc. Roy. Soc. (Br)*, 192, 163-172.

PIZIALI, R.L., RASTEGAR, J. and NAGEL, D.A. (1977). Measurement of the nonlinear, coupled stiffness characteristics of the human knee. *Journal of Biomechanics*, 10, 45.

PIZIALI, R.L., RASTEGAR, J., NAGEL, D.A. and SCHURMAN, D.J. (1980). The contribution of the cruciate ligaments to the load-displacement characteristics of the human knee joint. *Journal of Biomechanical Engineering*, 102, 277-283.

PAUOLOS, L.E., NOYES, F.R., GROOD, E.S. and BUTLER, D.L. (1981). Knee rehabilitation after anterior cruciate ligament reconstruction and repair. *American Journal of Sports Medicine*, 9, 140.

POSTAK, P.D., BLAKE, T. and GREENWALD, A.S. (1992). Performance characteristics of primary modular total knee systems. Technical report of the MT. Sïnai Mediacl Center, Cleveland, Ohio.

RACE, A. and AMIS, A.A. (1994). The mechanical properties of the two bundles of the human posterior cruciate ligament. *Journal of Biomechanics*, 27, 13-24.

RASTEGAR, J., PIZIALI, R.L., NAGEL, D.A. and SCHURMAN, D.J. (1979). Effects of fixed axes of rotation on the varus-valgus and torsional load-displacement characteristics of the in-vitro human knee. *ASME Journal of Biomechanical Engineering*, 101, 134-140.

REIDER, B., MARSHLAA, J.L. and KOSLIN, B. (1981) The anterior aspect of the knee joint. An anatomical study. *Journal of Bone and Joint Surgery (Am)*, 463, 351.

RENSTROM, P., ARMS, S.W., STANWYCK, T.S., JOHNSON, R.J. and POPE, M.H. (1986). Strain within the anterior cruciate ligament during hamstring and quadriceps activity. *American Journal of Sports Medicine*, 14, 83-87.

SAUREN, A.A., HUSON, A. and SCHOUTEN, R.Y. (1984). Axisymmetric finite element analysis of the mathematical function of the meniscus. *International Journal of Sports Medicine*, 5, 93-95.

SEEDHOM, B.B. and HARGREAVES, D.J. (1979). Transmission of the load in the knee joint with special reference to the role of the menisci - Part II: experimental results, discussion and conclusions. *Eng. Med.*, 8, 220-228.

SEERING, W.P., PIZIALI, R.L., NAGEL, D.A. and SCHURMAN, D.J. (1980). The function of the primary ligaments of the knee in varus-valgus and axial rotation. *Journal of Biomechanics*, 13, 785-794.

SHIAVI, R., LIMBIRD, T., FRAZER, M., STIVERS, K., STRAUSS, A. and ABRAMVITZ, J. (1987). Helical motion analysis of the knee-I. Methodology for studying kinematics during locomotion. *Journal of Biomechanics*,20, 459-469.

SHIAVI, R., LIMBIRD, T., FRAZER, M., STIVERS, K., STRAUSS, A. and ABRAMVITZ, J. (1987). Helical motion analysis of the knee-II. Kinematics of uninjured knees during walking and pivoting. *Journal of Biomechanics*, 20,653-665.

SHIRAZI-ADL, A. (1984). Three dimensional nonlinear finite element stress analysis of a lumbar intervertebral joint. Ph.D. Thesis, McGill University.

SHIRAZI-ADL, A., AHMED, A.M. and SHRIVASTAVA, S.C. (1986). A finite element study of lumbar motion segment subjected to pure sagittal plane moments. *Journal of Biomechanics*, 19, 331-350.

SHIRAZI-ADL, A. and DROUIN, G. (1987). Load-bearing role of facets in a lumbar motion segment under sagittal plane loadings. *Journal of Biomechanics*, 20, 601-613.

SHIRAZI-ADL, A. (1989-a). Nonlinear finite element analysis of wrapping uniaxial elements. *Computers and Structures*, 32, 119-123.

SHIRAZI-ADL, A. (1989-b). Strain in fibres of a lumbar disc - Analysis of the role of lifting in producing disc prolapse. *Spine*, 14, 96-103.

SHOEMAKER, S.C. and MARKOLF, K.L. (1985). Effects of joint load on the stiffness and laxity of ligament deficient knees. *Journal of Bone and Joint Surgery (Am)*, 67, 136-146.

SHOEMAKER, S.C., and MARKOLF, K.L. (1986). The role of the meniscus in the anterior-posterior stability of the loaded anterior cruciate deficient knee. *Journal of Bone and Joint Surgery (Am).* 68, 71-79.

SALOMONS, S. (1969). Meeting report: the Eighth International Conference on Medial and Biological Engineering. *J. Biomed. Eng.*, 4, 467.

SPILKER, R.L. and DONZELLI, P.S. (1992). A biphasic finite element model of the meniscus for stress-strain analysis. In: *Knee Meniscus: Basic and Clinical Foundations*, edited by Mow, V.C., Arnoczky, S.P. and Jackson, D.W., New York, Raven Press, Ltd.

SYDNEY, S.V., HAYNES, D.W., HUNGERFORD, D.S. and CONNOR, K.M. (1987). The functional anatomy of the iliotibial tract. *Trans* 33^{rd} *ORS*, 12, 244.

TISSAKHT, M., FARINACCIO, A. and AHMED, A.M. (1989). Effects of ligament attachments on the response of the knee menisci in compression and torsion: a finite element study. *Trans. Orthop. Res. Soc.*, 14, 203.

TISSAKHT, M. and AHMED, A.M. (1990). Effect of tibial axial rotation on the knee meniscal stress: finite element study. *Trans. Orthop. Res. Soc.*, 15, 243.

TISSAKHT, M., AHMED, A.M., TANZER, M. and MISRA, A.K. (1994). The thickness of the articular cartilage affects the load-bearing characteristics of the menisci. *Trans.* 40^{th} *Ann. Meeting ORS*, 19, 414.

TORZILLI, P.A, GREENBERG, R.L., and INSALL, J. (1981). An in vivo biomechanical evaluation of anterior-posterior motion of the knee. Roentgenographic measurement technique, stress machine, and stable population. *Journal of Joint Bone and Surgery (Am)*, 63, 960-968.

TÜMER, S.T. and ENGIN, A.E. (1993). Three-body segment dynamic model of the human knee. *ASME Journal of Biomechanical Engineering*, 115, 350-356.

UNSWORTH, A., DOWSON, D. and WRIGHT, V., eds. (1975). Some new evidence on human joint lubrication. *Ann. Rheum. Dis.*, 34, 277-285.

WALKER, P.S. and HAJECK, J.V. (1972). The load-bearing area in the knee joint. *Journal of Biomechanics*, 5, 581.

WALKER, P.S. and ERKMAN, M.J. (1975). The role of the menisci in force transmission across the knee. *Clin. Orthop. Rel. Res.*, 109, 184-192.

WANG, C.J.W., WALKER, P.S. and WOLF, B. (1973). The effects of flexion and rotation on the length patterns of the ligaments of the knee. *Journal of Biomechanics*, 6, 587-596.

WANG, C.J.W. and WALKER, P.S. (1974). Rotary laxity of the human knee joint. *Journal of Joint Bone and Surgery (Am)*, 56, 161-170.

WASCHER, D.C, MARKOLF, K.L. and SHAPIRO, M.S. (1993). Direct in vitro measurement of forces in the cruciate ligaments. *The Journal of Bone and Joint Surgery (Am)*, 75, 377-386.

WISMANS, J., VELDPAUS, F., JANSEN, J., HUSON, A. and STRUBEN, P. (1980). A three-dimensional mathematical model of the knee joint. *Journal of Biomechanics*, 13, 677-685.

WHIPPLE, R., WIRTH, C.R. and MOW, V.C. (1984). Mechanical properties of the meniscus. *ASME Advances in Bioengineering*, 32-33.

WONGCHAISUWAT, C., HEMAMI, H. and BUCHNER, H.J. (1984). Control of sliding and rolling at natural joints. *Journal of Biomechanical Engineering*, 106, 368-375.

WOO, S.L-Y., GOMEZ, M.A. and AKESON, W.H. (1981). The time and history dependent viscoelastic properties of the canine medial collateral ligament. *Journal of Biomechanical Engineering*, 103, 293-298.

WOO, S.L-Y., GOMEZ, M.A., WOO, Y.K. and AKESON, W.H. (1982). Mechanical properties of tendons and ligaments. *Biorheology*, 19, 397-308.